



Programa de Doctorado “Matemáticas”

PHD DISSERTATION

STUDY OF PDE-ODE
GLIOBLASTOMA MODEL WITH
NONLINEAR DIFFUSION AND
CHEMOTAXIS

Author

Antonio Fernández Romero

Supervisor

*Prof. Dr. Francisco
Guillén González*

Supervisor

*Prof. Dr. Antonio
Suárez Fernández*

September 24, 2021

*A todos los que me habéis ayudado a alcanzar una de mis metas.
En especial, a mis padres.*

This thesis has been supported by under the Project MTM2015-69875-P of Plan Estatal 2013-2016 Excelencia - Proyectos I+D, Ministerio de Economía y Competitividad.

Agradecimientos

Debo empezar estos agradecimientos pidiendo disculpas si me olvido de alguien ya que he tenido la gran fortuna de contar con la ayuda de maravillosas personas en este camino y no me gustaría dejarme a nadie fuera. Por ello, aunque no encuentres tu nombre aquí, quiero que sepas que has formado parte de uno de los logros más importante de mi vida. Esto no habría podido llevarse a cabo sin ti, gracias.

El primer agradecimiento es para mis padres, Antonio y María. Sé que la inconmensurable ayuda y el apoyo incondicional en estos más de 29 años no se devuelven ni con un párrafo ni con mil, pero debéis estar presente aquí porque en gran medida, este trabajo también es vuestro. Ha sido un camino muy largo, con muchos impedimentos que oscurecían y alejaban la luz al final del túnel y, sin embargo, siempre habéis estado ahí, para avanzar juntos y llegar hasta el día de hoy. De todas las enseñanzas y vivencias que me habéis aportado, me gustaría destacar los valores tan bonitos y profundos que tenéis y me habéis transferido. Sin estos, no habríamos podido alcanzar ningún objetivo de los que me he propuesto porque los objetivos pueden ser míos pero los logros son nuestros. Añadir que sois los mejores padres que se pueda tener, los mejores amigos, los mejores pilares y referentes se me hace corto ya que merecéis todos los halagos posibles y nunca os estaré suficientemente agradecido por todo lo que habéis hecho por mí. Gracias por estar siempre cuando volvía a casa, ya fuera derrotado por algún problema o victorioso por un logro más conseguido, por apoyarme en cada decisión que tomaba, muchas de ellas desafortunadas y otras acertadas, por dejarme vivir experiencias que me hacían feliz a costa de la vuestra, por todo, GRACIAS.

Gema, no sabes cuánto has cambiado mi vida y por mucho que pueda decírtelo, siempre serán pocas. Nunca pensé que conocería a alguien con tu luz, tu bondad y tu todo. Y mucho menos que decidiera embarcarse como mi acompañante en el viaje de mi vida. Me has hecho mejor día a día, me has enseñado, me has escuchado, me has ayudado, me has apoyado y,

en definitiva, me has acompañado. No quisiera pensar como habría sido este camino sin ti y espero que sientas este logro que hemos conseguido tan tuyo como mío porque si no estuvieras, esto no existiría. Casi 6 años después de conocerte, puedo decir con la mayor alegría y el máximo orgullo que he sido testigo de que logras todo lo que te propones, que luchas como nadie, que eres admirable y que has querido compartir todo eso conmigo. No sabes lo feliz que me haces y lo mucho que me motivas para seguir adelante, no solo eres mi compañera, eres mi musa. GRACIAS. A los protagonistas de esta parte les debo una vida entera porque es lo que me aportan cada vez que los veo y comparto tiempo con ellos. Podría enumeraros uno a uno y decir mil maravillas individuales, pero en conjunto sois incluso más increíbles. En todos estos años me habéis demostrado el valor de la amistad de la mejor manera y me habéis hecho disfrutar de las mejores vivencias que he tenido. Recuerdo mil días de playa, noches, viajes, aventuras de las que no reímos con solo recordar una palabra, situaciones difíciles y momentos de felicidad absoluta. Sin que lo supierais me dabais fuerza para seguir adelante con cada quedada, cada charla, cada whatsapp y gracias a vosotros he conseguido llegar hasta aquí. Me habéis motivado con vuestros logros, me habéis hecho feliz con vuestra felicidad y en definitiva me habéis hecho mejor con vuestra continua mejoría. Por todo esto, no os considero solo mis amigos/as, porque lo que me habéis demostrado es mucho más que eso, sois la familia que elegí tener y no pude hacer mejor elección. Seguiré agradeciándoos todo lo que me dais eternamente porque no merecéis menos y sé que, aun así, me quedaría corto. De verdad, GRACIAS.

Ahora me toca agradecer a una persona que seguramente sea más propietaria de este trabajo que yo mismo, Ana, mi psicóloga. Has estado prácticamente desde el primer día que empecé la tesis ayudándome a tener mejor salud mental y por ende a estar lo más sano posible. Puedo decir que me has salvado la vida ya que cuando llegué a ti, estaba en el peor momento que recuerdo, todo lo veía oscuro y nada valía la pena. A ti no te debo una vida, te debo mi vida, la cual he podido recuperar gracias a ti y la cual ordenas cuando me tratas. Me has enseñado a entender mis pensamientos, mis temores, mis impulsos, a reflexionar, a ser más asertivo y por supuesto, a mejorar día a día. No sabes todo lo que te debo. Te deseo todo lo mejor en la vida porque menos de eso no te mereces. GRACIAS.

Para acabar, me gustaría ser un poco egocéntrico y agradecerme a mí mismo. Antonio, tú sabes mejor que nadie todo lo que has pasado hasta llegar aquí y el por qué has acabado.

Eres consciente que esta etapa te ha cambiado en muchísimos aspectos de tu día a día y que probablemente nunca volverás a ser como antes, pero, en cierta medida puedes decir que ahora eres mejor y debes recordarlo. Espero que cada vez que leas esto, recuerdes los buenos momentos, porque los ha habido y han sido muy buenos, y cuando se te vengan a la mente de los malos, levanta la cabeza con orgullo y sonríe porque los has superado todos y lo seguirás haciendo, yo confío en ti.

Y si aun así no lo ves claro, recuerda lo que gritamos a viva voz en cada concierto de Los Chikos del Maíz:

“No nacimos para resistir, nacimos para VENCER”

Antonio Fernández Romero

September 2021

Resumen

Esta tesis está dedicada a modelar y analizar matemáticamente el desarrollo del Glioblastoma. Gracias a considerar la vasculatura como una variable adicional, es posible obtener modelos matemáticos más realistas desde el punto de vista biológico y, además, introducir la posibilidad de diferentes tipos de movimiento de las células tumorales como la difusión no lineal o la quimiotaxis relacionadas con la vasculatura.

En la Introducción (Capítulo 1), presentamos el problema que se estudiará a lo largo de la tesis. Comenzaremos explicando las características biológicas del Glioblastoma y mencionaremos algunos estudios realizados a través de datos reales y usando modelos matemáticos. Posteriormente, diseñaremos un modelo general PDE-ODE con difusión no lineal y quimiotaxis detallando en la modelización, los efectos del Glioblastoma. Además, presentaremos tres modelos obtenidos a partir del modelo general, que estudiaremos en los diferentes Capítulos, con sus principales resultados. Por último, comentaremos las diferencias entre los modelos con difusión no lineal y con quimiotaxis y mostraremos algunos problemas abiertos.

En el Capítulo 2, estudiamos el sistema PDE-ODE con difusión lineal (y sin quimiotaxis) obtenido como una simplificación del modelo general de Glioblastoma introducido en el Capítulo 1. Principalmente, probamos la existencia y unicidad de la solución clásica global en el tiempo utilizando un argumento de punto fijo. Además, mostramos algunos resultados de comportamiento a largo plazo de la solución dependiendo de algunas condiciones sobre los parámetros que aparecen en el modelo.

En el Capítulo 3, analizamos un modelo PDE-ODE obtenido del general, que incluye un término de difusión anisotrópica no lineal con una velocidad de difusión que aumenta con respecto a la vasculatura y no presenta quimiotaxis. Primero, probamos la existencia de

soluciones débiles-fuertes globales en el tiempo utilizando una técnica de regularización a través de una difusión artificial en el sistema ODE y un argumento de punto fijo. Además, los resultados de comportamiento a largo plazo de los puntos críticos se dan bajo algunas restricciones en los parámetros. Finalmente, diseñamos un esquema numérico completamente discreto de elementos finitos para el modelo que conserva las estimaciones puntuales y de energía del problema continuo.

En el Capítulo 4, probamos mediante simulaciones numéricas, que el modelo considerado en el Capítulo 3 captura diferentes tipos de crecimiento del tumor cambiando adecuadamente los parámetros del modelo. En primer lugar, realizamos un estudio adimensional para reducir el número de parámetros. Posteriormente, detectamos los principales parámetros que determinan los diferentes anchos del anillo formado por células proliferativas y necróticas y los diferentes comportamientos regular/irregular de la superficie tumoral; aspectos que determinan en muchos casos la agresividad del tumor.

En el Capítulo 5, consideramos el tercer modelo PDE-ODE obtenido del general presentado en el Capítulo 1, que incluye un término de quimiotaxis dirigido a la vasculatura y difusión lineal. Primero, obtenemos algunas estimaciones a priori para las (posibles) soluciones del modelo. En particular, bajo algunas condiciones sobre los parámetros, obtenemos que el sistema no puede producir explosión en tiempo finito. A continuación, diseñamos un esquema de elementos finitos totalmente discreto para el modelo que conserva algunas estimaciones puntuales del problema continuo.

Finalmente, en el Capítulo 6 realizamos un estudio similar al realizado en el Capítulo 4, si bien ahora el modelo utilizado es el que incluye el término de quimiotaxis.

Abstract

This thesis is dedicated to modeling and analyzing mathematically the development of Glioblastoma. Thanks to considering the vasculature as an additional variable, it is possible to obtain more realistic mathematical models from the biological point of view and, in addition, to introduce the possibility of different types of tumor cell movement such as non-linear diffusion or chemotaxis related to the vasculature.

In the Introduction (Chapter 1), we present the problem that we will study in this thesis. We begin explaining the biological characteristics of Glioblastoma and we mention some studies made with real data and using mathematical models. Later, we design a general PDE-ODE model with nonlinear diffusion and chemotaxis detailing the modeling of the Glioblastoma effects. In addition, we present three models obtained from the general model, which we study in the different Chapters, with their main results. Finally, we will discuss the differences between the nonlinear diffusion and chemotaxis models and show some open problems.

In Chapter 2, we study the PDE-ODE system with linear diffusion (and without chemotaxis) obtained as a simplification of the general Glioblastoma model introduced in Chapter 1. Mainly, we prove the existence and uniqueness of the global classical solution in time using a fixed point argument. Furthermore, we show some long-term behaviour results of the solution depending on some conditions in the parameters which appear in the model.

In Chapter 3, we analyse a PDE-ODE model derived from the general one, which includes a nonlinear anisotropic diffusion term with a diffusion rate that increases relative to the vasculature and without chemotaxis. First, we prove the existence of global strong-weak solutions in time using a regularization technique through artificial diffusion in the ODE system and a fixed point argument. Furthermore, the long-term behaviour results of the critical points are

given under some constraints on the parameters. Finally, we design a completely discrete finite element numerical scheme for the model that preserves the point and energy estimates of the continuous problem.

In Chapter 4, we prove through numerical simulations that the model considered in Chapter 3 captures different types of tumor growth by suitably changing the parameters of the model. First, we make a dimensionless study in order to reduce the number of parameters. Later, we detect the main parameters that determine the different widths of the ring formed by proliferative and necrotic cells and the different regular/irregular behaviour of the tumor surface; aspects that define in many cases the aggressiveness of tumor.

In Chapter 5, we consider the third PDE-ODE model obtained from the general one presented Chapter 1, including a chemotaxis term directed to vasculature and linear diffusion. First, we obtain some a priori estimates for the (possible) solutions of the model. In particular, under some constraints on the parameters, we obtain that the system can not produce blow-up in finite time. Next, we design a totally discrete finite element scheme for the model that preserves some point estimates of the continuous problem.

Finally, in Chapter 6, we make a similar study to the Chapter 4, although now the model used is the one that includes the chemotaxis term.

Contents

1	Introduction	11
1.1	Model with nonlinear diffusion and chemotaxis	4
1.2	Linear Diffusion Model without chemotaxis	6
1.3	Nonlinear Diffusion Model without chemotaxis	8
1.4	Chemotaxis model with linear diffusion	12
1.5	Comparison between two models	15
1.6	Current and future research lines	18
2	Theoretical analysis for a PDE-ODE system with linear diffusion related to a Glioblastoma tumor with vasculature	21
2.1	Preliminaries	22
2.2	Existence and uniqueness of Classical Solution of Problem (2.1)-(2.3)	24
2.2.1	Step 1. Define the fixed-point map	28
2.2.2	Step 2. The map is well-defined and continuous	29
2.2.3	Step 3. The map is compact	34
2.2.4	Step 4. A priori estimates of possible fixed-points and conclusion	34
2.3	Asymptotic behaviour	34
2.3.1	Stability of the (non-diffusion) ODE system	34
2.3.2	Stability of the Diffusion Model (2.1)-(2.3)	37
2.3.3	Numerical Simulations	46
2.4	Conclusions	48

3	Theoretical and numerical analysis for a hybrid tumor model with nonlinear diffusion depending on vasculature	49
3.1	Preliminaries	50
3.2	Existence of Solution of Problem (3.1)-(3.3)	51
3.2.1	Truncated problem	52
3.2.2	Existence of Weak-Strong Solution of Problem (3.8)	54
3.2.2.1	Proof of Theorem 3.3	55
3.3	Asymptotic behaviour	62
3.4	A FE numerical scheme	67
3.4.1	A priori energy estimates	69
3.4.2	Numerical Simulations	76
4	Determining parameters giving different growths of a new Glioblastoma differential model	81
4.1	The model	82
4.2	Adimensionalization	83
4.3	Ring width	85
4.3.1	Tumor Ring quotient	86
4.3.2	Density tumor growth	87
4.4	Regularity surface	89
4.4.1	Regularity Surface quotient	90
4.4.2	Area	92
4.4.3	Tumor growth	93
4.5	Discussion	94
5	A priori estimates for a tumor chemotaxis model and for a numerical scheme	97
5.1	A priori estimates of the solutions of (5.1)-(5.3)	100
5.1.1	Proof of Theorem 5.1 a)	100
5.1.2	Proof of Theorem 5.1 b)	102
5.1.3	Proof of Theorem 5.1 c)	105
5.2	A FE numerical scheme	107
5.2.1	Proof of Theorem 5.2	109
5.3	Appendix	113

6 Numerical Simulations of a Glioblastoma PDE-ODE system with chemotaxis	115
6.1 Model	115
6.2 Adimensionalization	117
6.3 Numerical Simulations	119
6.3.1 Ring width	119
6.3.1.1 Tumor Ring quotient	121
6.3.1.2 Density tumor growth	121
6.3.2 Regularity surface	122
6.3.2.1 Regularity Surface quotient	123
6.3.2.2 Area	125
6.3.2.3 Tumor growth	125
6.3.3 Discussion	126
Bibliography	127

Introduction

Glioblastoma (GBM) is one of the most lethal malignant brain tumor with a medium survival of 14.6 months [43]. These include the presence of necrosis and high proliferation of cells. The magnetic resonance imaging (MRI) shows a necrotic area in the center surrounded by a white ring as we see in Figure 1.1. This ring is an indicator of areas with poor vasculature.

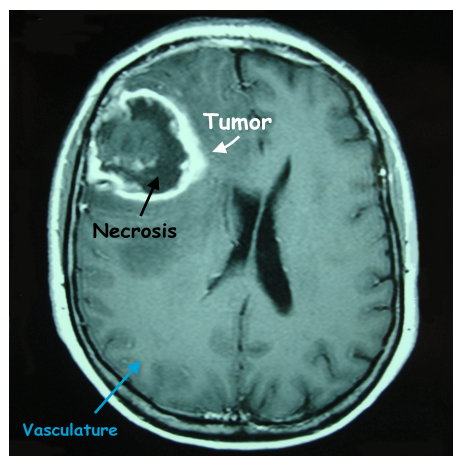


Figure 1.1: MRIs of a GBM areas showing contrast enhancement².

Moreover, it is well-known that GBM presents pathologically important differences with respect to other brain tumors of lesser malignancy. Clinical, molecular and imaging parameters have been used to

²<https://pdfs.semanticscholar.org/7d7b/2f5f038cf961be42c789db6a8dfafa8637733.pdf>

1. Introduction

build mathematical models able to classify GBM patients in terms of survival, identify GBM subtypes, predict response to treatment, prediction the outcome and different therapies or classify patients according to prognosis [1, 18, 28, 40].

Some studies about the morphology of GBM are based in the magnetic resonance images (MRI) in order to obtain results related to prognosis and survival (see [39, 48]). Even recently, Molab³ group classifies the GBM depending on the width of the tumor ring and/or the tumor surface regularity (see [47, 49] respectively) using image treatment.

With respect the width of the tumor ring, necrosis plays a relevant role in the GBM since the amount of necrosis can change and hence the volume of GBM and its prognosis in relation to mortality. According to that, an experimental study relating the ring width of proliferative tumor with respect to necrosis and its mortality is shown in [47] (see Figure 1.2).

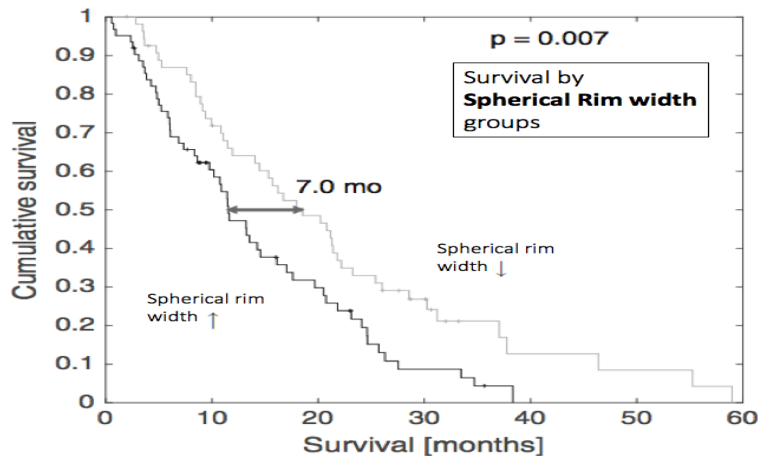


Figure 1.2: Survival vs the spherical rim width of GBM, [47].

The study of [47] concludes that tumors with slim ring have better prognostic, specifically 7 months of more survival than tumors with thick ring. Other way to understand this study is based on the amount of necrosis, since tumors with slim ring have more amount of necrosis than tumor with thick ring.

The another relevant aspect of a GBM observed in the MRIs is the regularity surface of the tumor. In [49], and the references therein, the authors made an experimental study about the survival of patients in relation to the surface growth, regular or irregular, of the GBM. Indeed, Figure 1.3 shows that tumors

³<http://matematicas.uclm.es/molab/>

with a regular surface have better prognostic, more than 5 months of survival, than tumor with irregular surface.

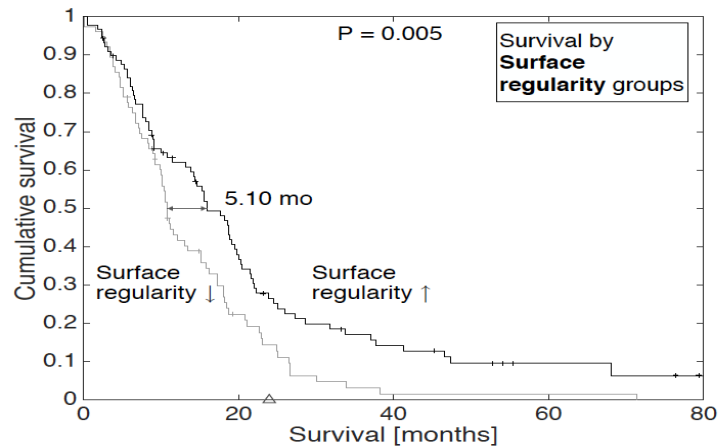


Figure 1.3: Survival vs the regularity surface of GBM, [49].

Therefore, given the great difficulties presented by the treatment of GBM, the mathematical modeling of GBM has been a relatively broad topic in the applied mathematics community (see [2, 7, 8, 36, 38, 45, 47] and references therein). However, the applicability of the results has been very reduced. One of the reasons that could explain this limitation is that either the key biological variables have not been included or real data of sufficient quality have not been used.

In [61], the authors use the Fisher-Kolmogorov equation to reproduce the infiltrative characteristic of the GBM. However, the use of more complex mathematical models, in order to simulate the phenomena such that the tumor ring and the regularity surface of the GBM, is essential. Molab group has contributed to solve this problem, working with a PDE-ODE system recently, see [46], in order to explain the correlation between magnetic resonance images and tumor growth speed. For that, two variables are considered in [46]: tumor and necrosis, and they quantify the tumor ring and obtain a relation with the survival.

In this thesis, we propose some models including an essential variable: the vasculature, since it is well-known that vasculature plays a relevant role on the tumor growth. Moreover, our models including vasculature are able to capture some phenomena about GBM such as the ring width in [46, 47] and the regularity surface of the tumor in [49].

1.1 Model with nonlinear diffusion and chemotaxis

Thus, we present the following general PDE-ODE system in which we consider different possibilities according to that we want to study in every case:

$$\left\{ \begin{array}{l} \frac{\partial T}{\partial t} - \underbrace{\nabla \cdot ((\kappa_1 P(\Phi, T) + \kappa_0) \nabla T)}_{\text{Nonlinear diffusion}} + \underbrace{\kappa \nabla \cdot (T \nabla \Phi)}_{\text{Chemotaxis}} = f_1(T, N, \Phi) \\ \frac{\partial N}{\partial t} = f_2(T, N, \Phi) \\ \frac{\partial \Phi}{\partial t} = f_3(T, N, \Phi) \end{array} \right. \quad (1.1)$$

endowed with non-flux boundary condition

$$(-(\kappa_1 P(\Phi, T) + \kappa_0) \nabla T + \kappa T \nabla \Phi) \cdot n = 0 \quad (1.2)$$

where n is the outward unit normal vector to $\partial\Omega$ and initial conditions

$$T(0, x) = T_0(x), \quad N(0, x) = N_0(x), \quad \Phi(0, x) = \Phi_0(x), \quad x \in \Omega. \quad (1.3)$$

Here $\kappa, \kappa_0, \kappa_1 \geq 0$ are the chemotaxis and diffusion parameters, respectively and $T(t, x) \geq 0$, $N(t, x) \geq 0$ and $\Phi(t, x) \geq 0$ represent the tumor density, necrotic density and vasculature concentration, respectively, at the point $x \in \Omega \subseteq \mathbb{R}^3$ at the time $t \in (0, T_f)$ where $\Omega \subseteq \mathbb{R}^3$ is a smooth bounded domain and $T_f > 0$ the final time.

According to the model (1.1)-(1.3), we can comment that it has been observed that tumor cells show a random movement when there is no nutrient limitation (which is modelled by a linear diffusion term). Moreover, we introduce an anisotropic diffusion speed increasing with respect to the vasculature given by $\kappa_1 P(\Phi, T)$ and a chemotactic movement of the tumor directed to the gradient of vasculature given by $\kappa \nabla \cdot (T \nabla \Phi)$ in order to detect different ways of tumor development.

On the other hand, necrosis and vasculature have not diffusion movement. Furthermore, the areas of poor vasculature commented at the beginning of this Chapter (see Figure 1.1) are modelled by the destruction of the vasculature by the tumor, which is a term that appears in all the models that we will study.

The reaction functions of (1.1) are given by:

$$\left\{ \begin{array}{l} f_1(T, N, \Phi) = \underbrace{\rho P(\Phi, T) T \left(1 - \frac{T + N + \Phi}{K}\right)}_{\text{Tumor growth}} - \underbrace{\alpha S(\Phi, T) T}_{\text{Hypoxia}} - \underbrace{\beta_1 N T}_{\text{Tumor destruction by necrosis}}, \\ f_2(T, N, \Phi) = \alpha S(\Phi, T) T + \beta_1 N T + \delta Q(\Phi, T) \Phi + \beta_2 N \Phi, \\ f_3(T, N, \Phi) = \underbrace{\gamma R(\Phi, T) \Phi \left(1 - \frac{T + N + \Phi}{K}\right)}_{\text{Vasculature growth}} - \underbrace{\delta Q(\Phi, T) \Phi}_{\text{Vasculature destruction by the tumor}} - \underbrace{\beta_2 N \Phi}_{\text{Vasculature destruction by necrosis}}, \end{array} \right. \quad (1.4)$$

where $\rho, \alpha, \beta_1, \beta_2, \delta, \gamma \geq 0$ are reaction parameters and $K > 0$ is the carrying capacity. All the parameters are given by the following description corresponding to the relevant studies [30, 36, 37]:

Variable	Description	Value
κ	Speed chemotaxis	$\frac{\text{cm}^2}{\text{sec} \cdot \text{density}}$
κ_1	Anisotropic diffusion	cm^2/day
κ_0	Isotropic diffusion	cm^2/day
ρ	Tumor proliferation rate	day^{-1}
α	Hypoxic death rate by persistent anoxia	cell/day
β_1	Tumor destruction by the necrosis	day^{-1}
β_2	Vasculature destruction by the necrosis	day^{-1}
γ	Vasculature proliferation rate	day^{-1}
δ	Vasculature destruction by tumor action	day^{-1}
K	Carrying capacity	cell/cm^3

Table 1.1: Parameters.

Now, we are going to describe the biological meaning of the reaction terms:

- Since tumour cells and vasculature must have enough space to proliferate, two logistic growth terms have been included respectively, for tumor and vasculature:

$$T \left(1 - \frac{T + N + \Phi}{K}\right) \text{ in } f_1(T, N, \Phi) \quad \text{and} \quad \Phi \left(1 - \frac{T + N + \Phi}{K}\right) \text{ in } f_3(T, N, \Phi)$$

- Since vasculature supplies nutrients and oxygenation to tumor cells, speed tumor growth depends on the amount of vasculature. This effect is given by the term $\rho P(\Phi, T)$, where $P(\Phi, T)$ will be a volume fraction of vasculature.

1. Introduction

- We consider the hypoxia term, $\alpha S(\Phi, T) T$, that is, a decreasing tumor term due to lack of vasculature which is transformed into necrosis. Low vasculature produces more tumor destruction and high vasculature less destruction. In fact, the non-dimensional factor $S(\Phi, T)$ must be increasing if Φ decreases.
- The vasculature growth term is given by $\gamma R(\Phi, T)$. It depends on the amount of tumor. In fact, vasculature can growth when there is a high demand for nutrients by the tumor cells. In particular, where there is not tumor, there is not growth of vasculature.
- Interaction between tumor (resp. vasculature) with necrosis produces a lost of tumor (resp. vasculature) which is transformed in necrosis. These effects are given by the terms: $\pm\beta_1 T N$ and $\pm\beta_2 \Phi N$.
- The destruction of vasculature by tumor is transformed into necrosis by the terms: $\pm\delta Q(\Phi, T) \Phi$, and the factor $Q(\Phi, T)$ increases depending on the amount of tumor. If there is not tumor, there will not be vascular destruction.

Once presented the general model (1.1), we will consider some particular cases in the different Chapters of this thesis.

I) Linear Diffusion Model without chemotaxis, that is, $\kappa = \kappa_1 = 0$ in (1.1).

II) Nonlinear Diffusion Model without chemotaxis, that is, $\kappa = 0$ in (1.1).

III) Chemotaxis model with linear diffusion, that is, $\kappa_1 = 0$ in (1.1).

1.2 Linear Diffusion Model without chemotaxis

In Chapter 2, we analyse (1.1) for the case of linear diffusion without chemotaxis ($\kappa = \kappa_1 = 0$) and taking $\kappa_0 = 1$ for simplicity. Specifically, we consider the following PDE-ODE system

$$\left\{ \begin{array}{l} \frac{\partial T}{\partial t} - \underbrace{\Delta T}_{\text{Linear diffusion}} = f_1(T, N, \Phi) \\ \frac{\partial N}{\partial t} = f_2(T, N, \Phi) \\ \frac{\partial \Phi}{\partial t} = f_3(T, N, \Phi) \end{array} \right. \quad (1.5)$$

endowed with non tumor flux boundary condition

$$-\nabla T \cdot n = 0 \quad (1.6)$$

and initial conditions (1.3).

The nonlinear reaction functions $f_i : \mathbb{R}^3 \rightarrow \mathbb{R}$ for $i = 1, 2, 3$ given in (1.5) have the following form

$$\left\{ \begin{array}{l} f_1(T, N, \Phi) := \rho P(\Phi, T) T \left(1 - \frac{T + N + \Phi}{K}\right) - \alpha \underbrace{\sqrt{1 - P(\Phi, T)^2}}_{S(\Phi, T)} T - \beta_1 N T \\ f_2(T, N, \Phi) := \alpha \underbrace{\sqrt{1 - P(\Phi, T)^2}}_{S(\Phi, T)} T + \beta_1 N T + \delta \underbrace{T}_{Q(\Phi, T)} \Phi + \beta_2 N \Phi \\ f_3(T, N, \Phi) := \gamma \underbrace{\frac{T}{K} \sqrt{1 - P(\Phi, T)^2}}_{R(\Phi, T)} \Phi \left(1 - \frac{T + N + \Phi}{K}\right) - \delta \underbrace{T}_{Q(\Phi, T)} \Phi - \beta_2 N \Phi \end{array} \right. \quad (1.7)$$

where

$$P(\Phi, T) = \frac{\Phi_+}{\Phi_+ + T_+} \quad \text{if } (\Phi, T) \neq (0, 0) \quad (1.8)$$

with $T_+ = \max\{0, T\}$ and similar to Φ_+ . Notice that $P(\Phi, T)$ is the vasculature volume fraction and it has the pointwise estimates

$$0 \leq P(\Phi, T) \leq 1, \quad \forall (T, \Phi) \in \mathbb{R}^2 \setminus \{(0, 0)\}.$$

It is easy to check that the rest of factors

$$S(\Phi, T) = \sqrt{1 - P(\Phi, T)^2}, \quad R(\Phi, T) = \frac{T}{K} \sqrt{1 - P(\Phi, T)^2} \quad \text{and} \quad Q(\Phi, T) = T$$

defined in (1.7) satisfy the biological conditions commented previously.

There is an extensive literature devoted to the study of PDE-ODE systems, see for instance the recent papers [9, 15, 16, 44] and the references therein. As far as we know, a great quantity of works related to solve this kind of problems for classical solutions are based in generic results of Amann [4, 5], see for instance [31, 58].

1. Introduction

The aim of Chapter 2 is to analyse (1.5)-(1.7) in a theoretical way. Firstly, we show the existence and uniqueness of global in time classical solution using a fixed point argument. In fact, the fixed point operator is built by computing first the ODE system, and then the PDE. One important difficulty here is to obtain classical regularity of solutions with respect to the spatial variable (which is a parameter for the ODE system). Secondly, we study the asymptotic behaviour of solutions of (1.5)-(1.7), showing three main results:

1. Vasculature goes to zero pointwisely in space as time goes to infinity for any choice of parameters
2. If the destruction of vasculature by tumor is large regarding to the vasculature growth, specifically if $\delta \geq \gamma/K$, then tumor and vasculature go to zero in an exponential way (uniformly in space) and necrosis is uniformly bounded.
3. If the destruction of tumor by necrosis dominates to tumor growth, specifically if $\beta_1 \gg \rho$ (see hypothesis (2.40) below), then tumor and vasculature go to zero in an exponential way (uniformly in space) and necrosis is uniformly bounded.

1.3 Nonlinear Diffusion Model without chemotaxis

Chapter 3 is dedicated to the study of (1.1) for the case of nonlinear diffusion without chemotaxis ($\kappa = 0$). Thus, we study the PDE-ODE system given by:

$$\left\{ \begin{array}{l} \frac{\partial T}{\partial t} - \underbrace{\nabla \cdot ((\kappa_1 P(\Phi, T) + \kappa_0) \nabla T)}_{\text{Nonlinear Diffusion}} = f_1(T, N, \Phi) \\ \frac{\partial N}{\partial t} = f_2(T, N, \Phi) \\ \frac{\partial \Phi}{\partial t} = f_3(T, N, \Phi) \end{array} \right. \quad (1.9)$$

endowed with non-flux boundary condition (1.6) and initial conditions (1.3). We also consider the nonlinear reactions terms (1.7) with the description of the parameters given in Table 1.1

However, now the vasculature volume fraction $P(\Phi, T)$ is regularized by:

$$P(\Phi, T) = \frac{\Phi_+}{\left(\frac{\Phi_+ + K}{2}\right) + T_+}. \quad (1.10)$$

Notice that $P(\Phi, T)$ is continuous in \mathbb{R}^2 , satisfies the pointwise estimates

$$0 \leq P(\Phi, T) \leq 1 \quad \forall (T, \Phi) \in [0, K] \times [0, K] \quad (1.11)$$

and $P(\Phi, T) = 0$ for $\Phi = 0$ (without vasculature) and $P(\Phi, T) = 1$ for $(\Phi, T) = (K, 0)$ (maximum of vasculature). This regularization is motivated for the introduction of the nonlinear diffusion term $\kappa_1 P(\Phi, T)$ in model (1.9) since the factor $P(\Phi, T)$ defined in (1.8), degenerates in $(0, 0)$.

As we use the same nonlinear reactions functions $f_i : \mathbb{R}^3 \rightarrow \mathbb{R}$ for $i = 1, 2, 3$, defined in (1.7), the relation between biological effects and reaction terms is the same that in Chapter 2. The diffusion term in (1.9) includes the nonlinear term, $\kappa_1 P(\Phi, T)$, and the linear self-diffusion term with parameter $\kappa_0 > 0$, what makes the diffusion non-degenerate (although from a biological point of view κ_0 must be small). Therefore, as we commented at the beginning of the Introduction, tumor cells show a random movement when there is not nutrient limitation (included in the linear self-diffusion term) whereas they have an anisotropic diffusion speed increasing with the vasculature. Thus, we express this anisotropic diffusion speed through factor $P(\Phi, T)$, defined in (1.10) which measures the quotient between the amount of vasculature and the amount of vasculature and tumor together.

In [34], the study of a PDE-ODE system is based on approximating regularized problems with pointwise estimates. Moreover, the results obtained in [34] are used in a recent work of the same authors for other PDE-ODE system, see [62].

There are many previous results according to the analysis of Finite Element (FE) schemes which preserves energy estimates and pointwise estimates related to parabolic PDEs with maximum principle, see for instance [19]. Specifically, in order to obtain pointwise estimates for FE numerical scheme of nonlinear PDE-ODE systems with maximum principle, we highlight works such as [21, 59, 60] or [12] where an acute triangulation is considered to have the pointwise estimates and [29] for energy estimates. Another relevant paper in the study of FE method for nonlinear PDE is [42] where the authors use a mass-lumping technique with quadrature formula.

In Chapter 2, we have studied the PDE-ODE system (1.5) with linear diffusion ($\kappa = \kappa_1 = 0$) where we get existence and uniqueness of classical solution using a fixed point argument. Nevertheless, in Chapter 3, due to the complexity of the nonlinear diffusion term, we will prove existence of a so-called

1. Introduction

weak-strong solution of problem (1.9) (see Definition 3.1 below). Roughly speaking, it will be a variational solution for the tumor-PDE and pointwise for the ODE system with necrosis and vasculature variables.

The inclusion of the nonlinear diffusion term gives rise to the model more realistic than model studied in Chapter 2, but it entails technical complications that we try to overcome in Chapter 3. Specifically, the main contributions of Chapter 3 are the following:

1. The existence of global in time weak solutions of (1.6)-(1.9). For that, we regularize (1.6)-(1.9) including an artificial diffusion in the ODE-system. This regularized problem maintains the same pointwise estimates as (1.6)-(1.9) and it is solved by a fixed point argument. Finally, we get some estimates for the regularized problem which let us to pass to the limit arriving at one weak solution of (1.6)-(1.9).
2. We investigate the asymptotic behaviour of (1.6)-(1.9). Mainly, we prove that the vasculature tends to zero “pointwisely” as time goes to infinity and, under some constraints on the parameters, tumor also goes to the extinction and necrosis grows to an upper limit. Looking at the asymptotic behaviour of the linear diffusion problem (1.5)-(1.7), we conclude that the nonlinear diffusion model has a similar behaviour.
3. We design an uncoupled and linear numerical scheme of (1.6)-(1.9) by means of an Implicit-Explicit finite difference scheme in time and a finite element with “mass-lumping” approximation in space which preserves the pointwise and energy estimates of the continuous model whenever an acute triangulation be considered.

Once presented the two main characteristics of the GBM at the beginning of the introduction (tumor vs necrosis quotient and regular vs irregular tumor surface), our goal in Chapter 4 is to use the differential model studied in Chapter 3 to capture the two phenomena showed in Figs 1.2 and 1.3 through numerical simulations in $2D$ domains and to detect which parameters are more important in each kind of GBM behaviour. Thus, we will study two different growths: the first one consists of computing the so-called tumor-ring via ratio proliferative tumor/necrosis, and the second one is about to detect regular vs irregular growth of the tumor surface depending on vasculature. For that, we have introduced two coefficients depending on the density and area of tumor and necrosis, respectively, with the following definition:

1. The “ring quotient” (RQ) coefficient:

$$0 \leq \mathbf{RQ} = \frac{\int_{\Omega} T \, dx}{\int_{\Omega} (T + N) \, dx} \leq 1. \quad (1.12)$$

If RQ is near to zero, tumor ring will be slim whereas it will be thick if RQ is close to one.

2. The “surface quotient” (SQ) coefficient:

$$0 \leq \mathbf{SQ} = \frac{\int_{\Omega} (T + N)_{\min} \, dx}{\pi \cdot (\mathbf{R}_{\max})^2} \leq 1 \quad (1.13)$$

where $(T + N)_{\min}$ and \mathbf{R}_{\max} are defined as:

$$(T + N)_{\min} = \begin{cases} 1 & \text{if } T + N \geq 0.001, \\ 0 & \text{otherwise,} \end{cases} \quad (1.14)$$

$$\mathbf{R}_{\max} = \max \{ \text{radio of the subdomain where } (T + N)_{\min} = 1 \}. \quad (1.15)$$

If SQ is near to zero, tumor will have a very irregular surface whereas if SQ is close to one, tumor will be rather similar to a circle.

Therefore, using the coefficients RQ of (1.12) and SQ of (1.13), changing the value of the parameters of (1.9), we obtain the relevancy of the parameters in the different tumor growths.

Let us point out that, recently in [46], the authors have proposed a GBM mathematical model, simpler than (1.9), in order to quantify the tumor ring and obtain a relation with the survival that we can see in Figure 1.2. Then, we have completed the model of [46] in order to not only capture the ring width but also the regularity surface of the GBM.

The main advantage of (1.9) over the model of [46] is the presence of the vasculature as an additional variable which is essential in the study of the regularity surface, as we will see in the Sections 4.4 and 6.3.2, since the amount and spatial distribution of vasculature can orientate the growth of the tumor. Moreover, the introduction of vasculature would allow the application of chemical therapies in the model because this type of therapy arrives to the tumor by the vasculature.

1.4 Chemotaxis model with linear diffusion

In Chapter 5, we present the third model obtained from (1.1) which corresponds to the chemotaxis model ($\kappa_1 = 0$). In particular, the chemotaxis model is giving by the following PDE-ODE system:

$$\left\{ \begin{array}{l} \frac{\partial T}{\partial t} - \underbrace{\kappa_0 \Delta T}_{\text{Linear diffusion}} + \underbrace{\kappa \nabla \cdot (T \nabla \Phi)}_{\text{Chemotaxis}} = f_1(T, N, \Phi) \\ \frac{\partial N}{\partial t} = f_2(T, \Phi) \\ \frac{\partial \Phi}{\partial t} = f_3(T, N, \Phi) \end{array} \right. \quad (1.16)$$

endowed with non-flux boundary condition

$$(-\kappa_0 \nabla T + \kappa T \nabla \Phi) \cdot n = 0 \quad (1.17)$$

and initial conditions (1.3).

The nonlinear reactions functions $f_i : \mathbb{R}^3 \rightarrow \mathbb{R}$ for $i = 1, 2, 3$ given in (1.16), are defined by:

$$\left\{ \begin{array}{l} f_1(T, N, \Phi) := \rho \underbrace{\frac{\Phi}{\Phi + T}}_{P(\Phi, T)} T \left(1 - \frac{T + N + \Phi}{K} \right) - \alpha \underbrace{\frac{K - \Phi}{T + \Phi + K}}_{S(\Phi, T)} T \\ f_2(T, N, \Phi) := \alpha \underbrace{\frac{K - \Phi}{T + \Phi + K}}_{S(\Phi, T)} T + \delta \underbrace{\frac{T}{\Phi + T}}_{Q(\Phi, T)} \Phi \\ f_3(T, N, \Phi) := \gamma \underbrace{\frac{T}{\frac{T^2}{K} + \Phi + K}}_{R(\Phi, T)} \Phi \left(1 - \frac{T + N + \Phi}{K} \right) - \delta \underbrace{\frac{T}{\Phi + T}}_{Q(\Phi, T)} \Phi \end{array} \right. \quad (1.18)$$

Here, we have modified the nonlinear reactions terms $f_i : \mathbb{R}^3 \rightarrow \mathbb{R}$ for $i = 1, 2, 3$ given in Chapters 2 and 3 in order to reduce some aspects such as the interactions between tumor (resp. vasculature) with necrosis.

Although in (1.18), we have considered particular factors $P(\Phi, T)$, $S(\Phi, T)$, $R(\Phi, T)$ and $Q(\Phi, T)$, the results of Chapter 5 are proved for general factors that satisfy the modelling hypotheses:

$$0 \leq P(\Phi, T), S(\Phi, T), Q(\Phi, T), R(\Phi, T) \leq 1 \quad \forall (T, \Phi) \in \mathbb{R}^2, \quad (1.19)$$

and,

$$P(\Phi, T) = 0 \text{ for } \Phi = 0 \text{ and } P(\Phi, T) \text{ increases if } \Phi \text{ increases.} \quad (1.20)$$

$$S(\Phi, T) \text{ increases if } \Phi \text{ decreases.} \quad (1.21)$$

$$R(\Phi, T) = 0 \text{ for } T = 0 \text{ and } R(\Phi, T) \text{ increases if } T \text{ increases (at least for } T \leq K). \quad (1.22)$$

$$Q(\Phi, T) = 0 \text{ for } T = 0 \text{ and } Q(\Phi, T) \text{ increases if } T \text{ increases.} \quad (1.23)$$

and mathematical conditions:

$$C_1 P(\Phi, T) \geq R(\Phi, T) \Phi, \quad (1.24)$$

$$\left| \frac{\partial (R(\Phi, T) \Phi)}{\partial \Phi} \right|, \left| \frac{\partial (R(\Phi, T) \Phi)}{\partial T} \right| \leq C_2, \quad (1.25)$$

$$\left| \frac{\partial (Q(\Phi, T) \Phi)}{\partial \Phi} \right|, \left| \frac{\partial (Q(\Phi, T) \Phi)}{\partial T} \right| \leq C_3 \quad (1.26)$$

and

$$\left| \frac{\partial (S(\Phi, T) T)}{\partial \Phi} \right|, \left| \frac{\partial (S(\Phi, T) T)}{\partial T} \right| \leq C_4 \quad (1.27)$$

for some constants $C_i > 0$ for $i = 2, 3, 4$ and for all $0 \leq \Phi \leq K$, and $T \geq 0$.

Some chemotactic PDE-ODE models have been studied in the literature, see for instance [6, 11, 52, 53, 54] where the authors model the movement cells with a parabolic-ODE system. Specifically, in [54] a system of PDEs is considered using a probabilistic framework of reinforced random walks. The authors analyse in [54] various combinations of taxis and local dynamics giving examples of aggregation, blow-up and collapse. Later, in [52], some analytical and numerical results supporting the numerical observations of [54] are presented using a similar model than in [54]. Moreover, in [6, 11] a model of tumor inducing angiogenesis is proposed consisting of an equation with chemotaxis and haptotaxis terms, and two nonlinear ODEs. Finally, in [53] a stochastic system related to bacteria and particles of chemical substances is discussed where the position of each particle is described by an equation of a chemotaxis system.

Several works such as [55, 56, 57] have shown results of existence for systems of three differential equations modelling cancer invasion. In [55] is proved the global existence and boundedness for a

1. Introduction

parabolic-parabolic-ODE system with nonlinear density-dependent chemotaxis and haptotaxis and logistic source. Furthermore, in [56], the authors have proved global existence of solutions for a parabolic-elliptic-ODE system with chemotaxis, haptotaxis and logistic growth. The existence of solutions for a chemotaxis and haptotaxis model with nonlinear diffusion is presented in [57].

Recently, a PDE-ODE model with chemotaxis is studied in [32] obtaining asymptotic stability results using a proper transformation and energy estimates. Another PDE-ODE with chemotaxis problem is considered in [41] modelling the evolution of biological species and they obtain analytical results concerning the bifurcation of constant steady states and global existence of solutions for a range of initial data.

The chemotaxis term introduced in Chapter 5 provides another different perspective do not considered until now in the previous Chapters but it involves some technical complications. In particular, the main contributions of Chapter 5 are the following:

1. The obtaining of a priori estimates for the possible solutions of (1.16)-(1.18). For that, we need to impose that the chemotaxis and vasculature growth rate do not dominate with respect to the tumor growth rate and linear diffusion, in fact, we impose $\rho \kappa_0 \geq \kappa \gamma C_1$ with $C_1 > 0$ the constant appearing in (5.6). To get it, we will use the change variable $T = e^{\frac{\kappa}{\kappa_0} \Phi} u$, similar to the used in [14, 16, 35], in order to obtain a PDE without chemotaxis for the new variable u . Moreover, we use an Alikakos' argument, see [3], to obtain the L^∞ estimate of this new variable u (which drives to the L^∞ estimate for T).
2. The design of an uncoupled and linear numerical scheme using the same change variable than in continuous case by means of an Implicit-Explicit finite difference scheme in time and a finite element with "mass-lumping" approximation in space. Assuming an acute triangulation we deduce some pointwisely estimates. for the discrete solution.

Finally, in Chapter 6, we use the PDE-ODE model with chemotaxis presented in Chapter 5 in order to identify which parameters are more important for the same two phenomena of GBMs studied in Chapter 4 with the nonlinear diffusion model (tumor-ring ratio proliferative tumor/necrosis and regular vs irregular growth of the tumor depending on vasculature). Thus, we will study through numerical simulations these two different growths using the coefficients RQ and SQ defined in (1.12) and (1.13) for the tumor ring and the regularity surface of tumor, respectively, by changing the value of the parameters of the chemotaxis model (1.16) as we did in Chapter 4 for the nonlinear diffusion model.

1.5 Comparison between two models

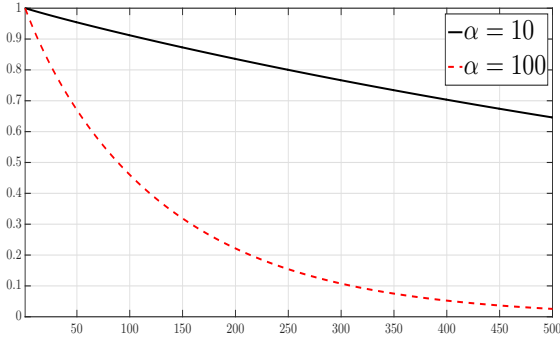
Furthermore, we present the comparison of the results between the nonlinear diffusion model (1.9) and chemotaxis model (1.16) that supplies a better idea according to which kind of movement (nonlinear diffusion or chemotaxis) is more realistic when we want to model the development of a GBM.

Summarizing the results obtained with respect to the ring width and the regularity surface for the nonlinear diffusion model and chemotactic one studied in Chapters 4 and 6 related to GBM growth model, we deduce that both models can capture these two properties varying some parameters. Moreover, we have proved that the more relevant parameters according to the tumor growth are κ_1 (anisotropic diffusion parameter) and α (hypoxic death rate by persistent anoxia parameter) for the nonlinear diffusion model (1.9) and κ (speed chemotaxis parameter) and α (hypoxic death rate) for the chemotaxis with linear diffusion model (1.16).

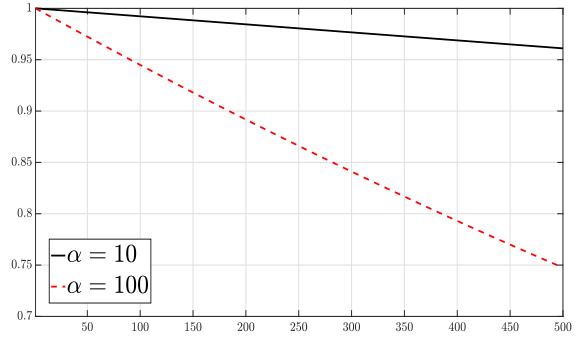
Hence, we can compare the results obtained in the Chapter 4 with the results of Chapter 6. Mainly, we show the similarities and differences between the hypoxia parameter, α in both models and between the chemotaxis parameter κ of system (1.16) and the nonlinear diffusion parameter κ_1 of system (1.9) for each kind of tumor growth.

For the tumor ring, where the vasculature is uniformly distributed, the numerical simulations of the nonlinear diffusion model show that the hypoxia parameter α is the most relevant parameter, see Figure 1.4a. This effect is also observed for the chemotaxis model in Figure 1.4b for the same hypoxia parameter α . Consequently, in both chemotaxis and nonlinear diffusion models, the hypoxia parameter α has the highest influence for the behaviour of the tumor ring.

1. Introduction



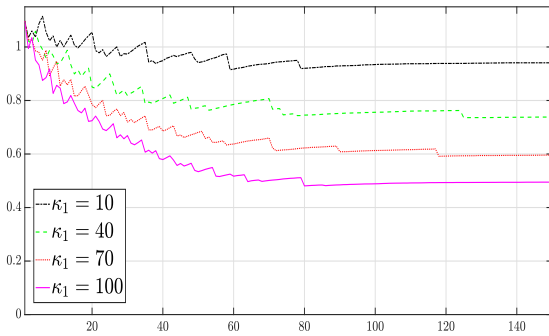
(a) Nonlinear diffusion model.



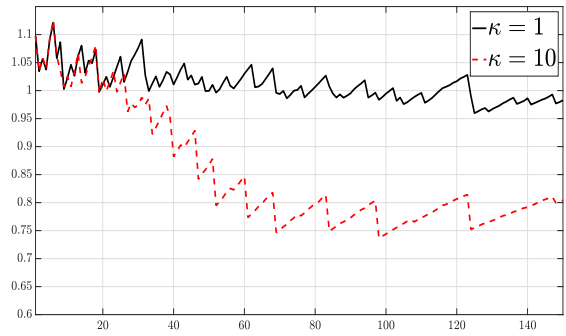
(b) Chemotaxis model.

Figure 1.4: RQ versus time for α in the nonlinear diffusion model and the chemotaxis model.

In the case of regularity surface, where the vasculature is non-uniformly distributed, the parameter which produces more irregularity in the tumor surface for the nonlinear diffusion model is the anisotropic diffusion parameter κ_1 , see Figure [1.5a](#). For the chemotaxis model, we obtained that the speed chemotaxis parameter κ is the most significant in the irregular growth, see Figure [1.5b](#). Thus, both κ_1 and κ are the main parameters in order to capture the regularity surface in its respective model.



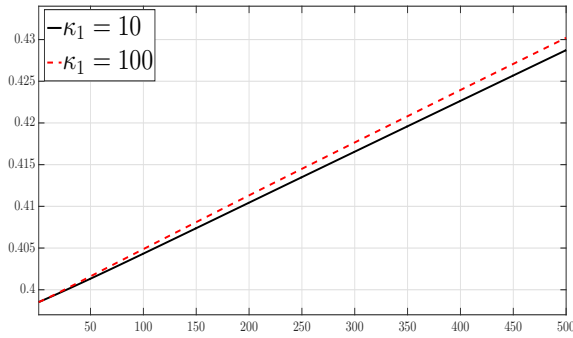
(a) Nonlinear diffusion model.



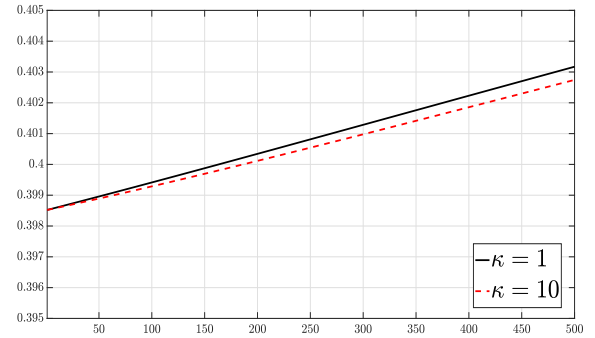
(b) Chemotaxis model.

Figure 1.5: SQ versus time for κ_1 in the nonlinear diffusion model and for κ in the chemotaxis model.

However, the first difference between the nonlinear diffusion and the chemotactic model appears for the total density in the ring width study, where the initial vasculature is uniformly distributed. Thus, in Figure [1.6a](#), we observe that the anisotropic diffusion parameter κ_1 satisfies that the highest density is achieved for the maximum value of κ_1 , whereas in Figure [1.6b](#), the speed chemotaxis parameter κ achieves the highest total density for small κ .



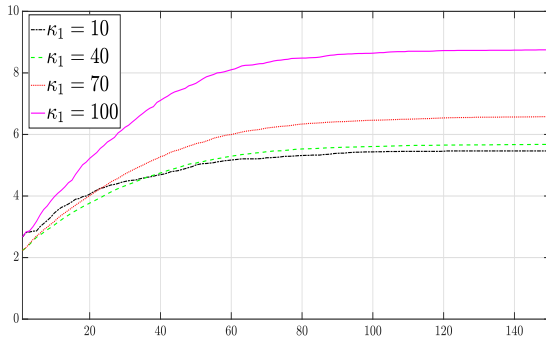
(a) Nonlinear diffusion model.



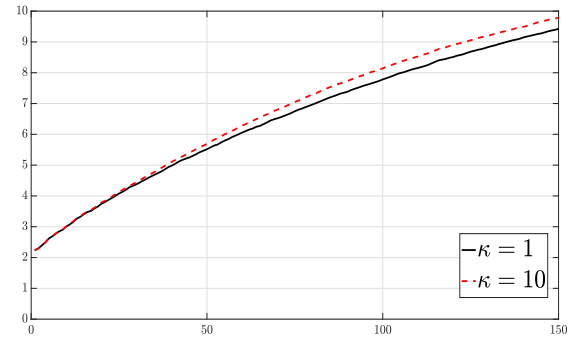
(b) Chemotaxis model.

Figure 1.6: $\int_{\Omega} (T + N) dx$ versus time for κ_1 in the nonlinear diffusion model and for κ in the chemotaxis model.

Another difference occurs for the total area in the regularity surface study. In fact, in Figure 1.7a, a high difference between the total areas for two different values of the anisotropic diffusion parameter κ_1 can be seen, whereas the total area for the speed chemotaxis parameter κ is similar for different values of κ , see Figure 1.7b. Despite this fact, we obtain more total area with the chemotaxis parameter κ than for the anisotropic diffusion parameter κ_1 .



(a) Nonlinear diffusion model.



(b) Chemotaxis model.

Figure 1.7: Area of total tumor versus time for κ_1 in the nonlinear diffusion model and for κ in the chemotaxis model.

Now, we show the spatial movement of the tumor in the nonlinear diffusion model, Figure 1.8, and in the chemotaxis model, Figure 1.9. We observe that the surface of the tumor occupies more space in Figure 1.8 than in Figure 1.9. Nevertheless, the tumor density values in Figure 1.8 are smaller than in

1. Introduction

Figure 1.9 (see Figs 1.8e and 1.9e).

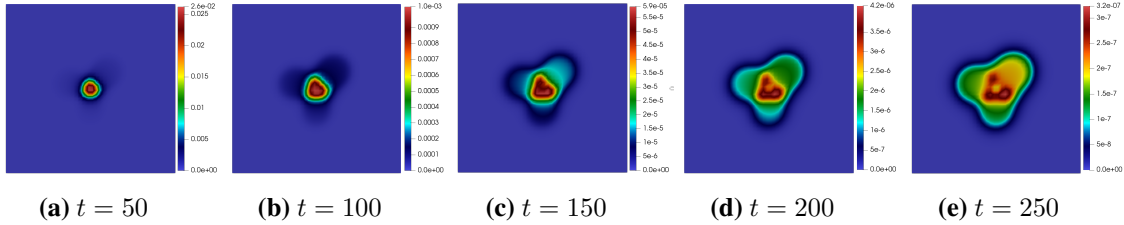


Figure 1.8: Tumor growth for $\kappa_1 = 100$ in the nonlinear diffusion model.

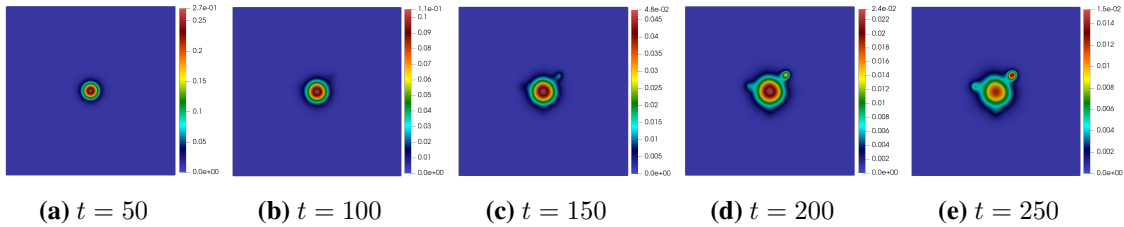


Figure 1.9: Tumor growth for $\kappa = 10$ in the chemotaxis model.

Finally, after the reduction in the nonlinear diffusion model (1.9) from 9 initial parameters to 2 (κ_1 and α) and in the chemotaxis with linear diffusion model (1.16) from 7 initial parameters to 2 (κ and α) which capture the different behaviour of tumor growth, we conclude that:

- For the nonlinear diffusion model (1.9), we obtain that α is the most relevant parameter for the tumor ring, for the density and area of tumor independently the distribution of the vasculature and the anisotropic diffusion parameter κ_1 is the principal parameter with respect to the regularity surface.
- In the chemotaxis with linear diffusion model (1.16), the hypoxia parameter α is the main parameter for the tumor ring and area of tumor and κ is the most influential parameter for the regularity surface.

1.6 Current and future research lines

There are many interesting facts which could be investigated concerning the model with nonlinear diffusion and chemotaxis because of the large variety of applications of this model. This is the reason which encourages us to continue working on this model and, due to that, we will summarize in the following paragraphs some possibilities that we consider really interesting.

- I) The existence of solution for the chemotaxis with linear diffusion model (1.16)-(1.3). We have obtained some estimates about the possible solutions of this model giving in particular a constraint on the parameters that avoids blow-up. But, the next step in this study must be to prove existence of global in time weak solutions.
- II) The asymptotic behaviour study for the solution of the chemotaxis with linear diffusion model (1.16)-(1.3). As we did with linear and nonlinear diffusion model without chemotaxis, the analysis of the long time behaviour for the solution of (1.16)-(1.3) could contribute to understand in a better way this model and observe if the presence of chemotaxis adds news results of asymptotic behaviour in comparison with the results obtained for the linear and nonlinear diffusion model in Chapters 2 and 3.
- III) The research of the model with nonlinear diffusion and chemotaxis (1.1)-(1.3). Once we have studied the sub-models obtained from (1.1)-(1.3), the analysis of existence and uniqueness of solution of (1.1)-(1.3), the long time behaviour and the design of a numerical scheme, which satisfies the estimates of the solution, could add a new point of view for the process of modelling the tumor development with the presence of vasculature. Moreover, we would compare the results, theoretical and numerically, with the obtained for the different sub-models studied in this thesis. Eventually, the numerical simulations of this complete model are also interesting in order to observe the relation between the nonlinear diffusion and chemotaxis in the tumor growth.
- IV) The introduction of chemical therapies in any model obtained from (1.1)-(1.3) since thanks to the presence of vasculature in (1.1)-(1.3), this type of therapy can be applied through the vasculature variable and could be considered more effective in the zones with more vasculature concentration. Furthermore, the study of different therapies could add functions such as $-\beta(t, \Phi)T$ in the tumor equation or could change the tumor growth term to $(1 - \beta(t, \Phi))P(\Phi, T)$.

Theoretical analysis for a PDE-ODE system with linear diffusion related to a Glioblastoma tumor with vasculature

In this Chapter we study the linear diffusion model introduced in the Introduction (1.1) for $\kappa = \kappa_1 = 0$ and $\kappa_0 = 1$. Specifically:

$$\left\{ \begin{array}{l} \frac{\partial T}{\partial t} - \Delta T = f_1(T, N, \Phi) \\ \frac{\partial N}{\partial t} = f_2(T, N, \Phi) \\ \frac{\partial \Phi}{\partial t} = f_3(T, N, \Phi) \end{array} \right. \quad (2.1)$$

endowed with non tumor flux boundary condition

$$-\nabla T \cdot n = 0 \quad (2.2)$$

where n is the outward unit normal vector to $\partial\Omega$ and initial conditions

$$T(0, x) = T_0(x), \quad N(0, x) = N_0(x), \quad \Phi(0, x) = \Phi_0(x) \quad x \in \Omega. \quad (2.3)$$

and where $\Omega \subset \mathbb{R}^3$ is a smooth bounded domain and $T_f > 0$ the final time.

2. Theoretical analysis for a PDE-ODE system with linear diffusion related to a Glioblastoma tumor with vasculature

The nonlinear reaction functions $f_i : \mathbb{R}^3 \rightarrow \mathbb{R}$ for $i = 1, 2, 3$ of (2.1), are defined by:

$$\begin{cases} f_1(T, N, \Phi) = \rho P(\Phi, T) T \left(1 - \frac{T + N + \Phi}{K}\right) - \alpha T \sqrt{1 - P(\Phi, T)^2} - \beta_1 N T, \\ f_2(T, N, \Phi) = \alpha T \sqrt{1 - P(\Phi, T)^2} + \beta_1 N T + \delta T \Phi + \beta_2 N \Phi, \\ f_3(T, N, \Phi) = \gamma \frac{T}{K} \sqrt{1 - P(\Phi, T)^2} \Phi \left(1 - \frac{T + N + \Phi}{K}\right) - \delta T \Phi - \beta_2 N \Phi, \end{cases} \quad (2.4)$$

where the $\rho, \alpha, \beta_1, \beta_2, \delta, \gamma, K > 0$ are defined in Table 1.1 and $P(\Phi, T)$ is defined in (1.8).

The Chapter is organized as follows: In Section 2.1, we present preliminary results which we will use along this thesis. In Section 2.2 we prove the existence (and uniqueness) of classical solution of (2.1)-(2.3). Section 2.3 is dedicated to the long time behaviour of the classical solutions and we show some numerical simulations according to the results proved previously. Finally, in Section 2.4, we discuss our findings and summarize our main results of this Chapter.

The results of this Chapter have been published in [24].

2.1 Preliminaries

Although $P(\Phi, T)$ defined in (1.8) is not evaluated in $(0, 0)$, we can deduce the following

Lemma 2.1. *The functions $B : \mathbb{R}^2 \rightarrow \mathbb{R}$ and $D : \mathbb{R}^2 \rightarrow \mathbb{R}$ given by*

$$B(\Phi, T) = T_+ \sqrt{1 - P(\Phi, T)^2}$$

and

$$D(\Phi, T) = T_+ P(\Phi, T)$$

are well defined, continuous and globally lipschitz in \mathbb{R}^2 .

Proof. We only show the proof for $B(\Phi, T)$ because for $D(\Phi, T)$ is similar, even easier. Since $0 \leq P(\Phi, T) \leq 1$, it is clear that $B(\Phi, T)$ is well defined and continuous in \mathbb{R}^2 (in particular, $B(0, 0) = 0$). To prove the global lipschitz condition for B , it suffices to show that the two partial derivatives of $B(\Phi, T)$ are continuous and bounded in the subdomain $A = \{(\Phi, T) \in \mathbb{R}^2 : \Phi, T > 0\}$ (in the rest, is equal to zero). By means of direct calculations, it follows that for any $(\Phi, T) \in A$,

$$\left| \frac{\partial B}{\partial \Phi} \right| \leq \left| \frac{1}{2} \frac{\sqrt{T}}{\sqrt{T + 2\Phi}} \right| \leq \frac{1}{2}, \quad (2.5)$$

2. Theoretical analysis for a PDE-ODE system with linear diffusion related to a Glioblastoma tumor with vasculature

and

$$\left| \frac{\partial B}{\partial T} \right| \leq \left| 1 + \frac{T}{\sqrt{T}\sqrt{T+2\Phi}} \right| \leq 2. \quad (2.6)$$

Hence, we deduce that $B(\Phi, T)$ is globally lipschitz in \mathbb{R}^2 . □

As consequence, we get the following result

Lemma 2.2. *The functions $f_i : \mathbb{R}^3 \rightarrow \mathbb{R}$ for $i = 1, 2, 3$ defined in (2.4) are continuous and locally lipschitz in \mathbb{R}^3 .*

Proof. Rewriting the definition of $f_i(T, N, \Phi)$ for every $i = 1, 2, 3$ according to the functions $B(\Phi, T)$ and $D(\Phi, T)$, it is easy to deduce that functions $f_i(T, N, \Phi)$ are continuous and their partial derivatives are bounded in compact sets of \mathbb{R}^3 for every $i = 1, 2, 3$, because they are products and sums of the globally lipschitz functions $B(\Phi, T)$ and $D(\Phi, T)$ and polynomials in (T, N, Φ) . □

In order to obtain some regularity result, we need to define the following spaces for $p > 3$:

$$W_n^{2-2/p,p}(\Omega) = \left\{ u \in W^{2-2/p,p}(\Omega) : \frac{\partial u}{\partial n} = 0 \text{ on } \partial\Omega \right\},$$

$$V_p = \left\{ \begin{array}{l} u \in L^p(0, T_f; W^{2,p}(\Omega)) \cap C^0([0, T_f]; W_n^{2-2/p,p}(\Omega)) \\ \text{and } u_t \in L^p(0, T_f; L^p(\Omega)) \end{array} \right\}$$

with the norm,

$$\|u\|_{V_p} := \|u\|_{C^0([0, T_f]; W_n^{2-2/p,p}(\Omega))} + \|\partial_t u\|_{L^p(0, T_f; L^p(\Omega))} + \|u\|_{L^p(0, T_f; W^{2,p}(\Omega))}.$$

The following result follows by [22, p. 344]

Lemma 2.3. *Assume $\Omega \in C^2$, let $p > 3$, $u_0 \in W_n^{2-2/p,p}(\Omega)$ and $g \in L^p(0, T_f; L^p(\Omega))$. Then, the problem*

$$\left\{ \begin{array}{l} \partial_t u - \Delta u = g \quad \text{in } (0, T_f) \times \Omega, \\ u(0, \cdot) = u_0 \quad \text{in } \Omega, \\ \frac{\partial u}{\partial n} = 0 \quad \text{on } (0, T_f) \times \partial\Omega, \end{array} \right.$$

admits an unique solution $u \in V_p$. Moreover, there exists a positive constant $C := C(p, \Omega, T_f)$ such that

$$\|u\|_{V_p} \leq C \left(\|g\|_{L^p(0, T_f; L^p(\Omega))}, \|u_0\|_{W_n^{2-2/p,p}(\Omega)} \right).$$

2. Theoretical analysis for a PDE-ODE system with linear diffusion related to a Glioblastoma tumor with vasculature

Remark 2.1. Along the thesis, the constant C will denote different constants which appear in the Chapters.

It will be necessary to obtain existence and uniqueness of global in time classical solution for an ordinary differential system depending on parameters. The first result is a classical extension result while the second one provides us the continuous dependence of the solutions of an ODE system with respect to parameters and initial conditions, see [13] for instance.

Lemma 2.4 (Continuous extension). *Let $g \in C^0(\overline{\Omega})$ with $\Omega \subseteq \mathbb{R}^d$ an open bounded set of class C^0 and $d \in \mathbb{N}$. Then, there exists an extension $Ext(g) \in C^0(\mathbb{R}^d)$ such that $Ext(g)|_{\overline{\Omega}} = g$.*

Theorem 2.1 (Continuous dependence of ODEs with respect to parameters and initial data). *Let $U \subseteq \mathbb{R} \times \mathbb{R}^N \times \mathbb{R}^M$ an open set and $F : U \rightarrow \mathbb{R}^N$ a continuous map such that, for any parameter $\lambda \in \mathbb{R}^M$ and for any initial data $y_0(\lambda) \in \mathbb{R}^N$ such that $(0, y_0(\lambda), \lambda) \in U$, the Cauchy's problem*

$$\begin{cases} y'(t) = F(t, y, \lambda) \\ y(0) = y_0(\lambda) \end{cases}$$

has an unique maximal solution $\phi(\cdot; y_0(\lambda), \lambda) : I_{(y_0(\lambda), \lambda)} \rightarrow \mathbb{R}^N$ being $I_{(y_0(\lambda), \lambda)}$ an open interval. Then,

$$\Theta = \{(t; y_0(\lambda), \lambda) \in \mathbb{R} \times \mathbb{R}^N \times \mathbb{R}^M : (t, y_0(\lambda), \lambda) \in U \text{ and } t \in I_{(y_0(\lambda), \lambda)}\}$$

is an open set and the map $\phi(\cdot; \cdot, \cdot)$ is continuous from Θ to \mathbb{R}^N .

Finally, we will use this classical fixed point theorem.

Theorem 2.2 (Leray-Schauder's theorem). *Let V a Banach space, $\lambda \in [0, 1]$ and $\mathcal{R} : V \rightarrow V$ a continuous and compact map such that for every $v \in V$ with $v = \lambda \mathcal{R}(v)$, it holds $\|v\|_V \leq C$ with $C > 0$ independent of $\lambda \in [0, 1]$. Then, there exists a fixed point v of \mathcal{R} .*

2.2 Existence and uniqueness of Classical Solution of Problem (2.1)-(2.3)

First of all, by biological considerations, we assume along the thesis the following assumption on the initial data

$$0 \leq T_0(x), N_0(x), \Phi_0(x) \leq K \text{ in } \Omega. \quad (2.7)$$

Now, we define the concept of classical solution of (2.1)-(2.3).

Definition 2.1. (Classical solution of (2.1)-(2.3)) *Given $T_0 \in W^{2-2/p, p}(\Omega)$ for some $p > 3$ and $N_0, \Phi_0 \in C^0(\overline{\Omega})$, then (T, N, Φ) is called a classical solution of (2.1)-(2.3) if:*

$$i) T \in V_p, N, \Phi \in C^1([0, T_f]; C^0(\overline{\Omega})),$$

2. Theoretical analysis for a PDE-ODE system with linear diffusion related to a Glioblastoma tumor with vasculature

ii) • $T_t - \Delta T = f_1(T, N, \Phi)$ a.e. in $(0, T_f) \times \Omega$,

$$\bullet \begin{pmatrix} \frac{\partial N}{\partial t} \\ \frac{\partial \Phi}{\partial t} \end{pmatrix} = \begin{pmatrix} f_2(T, N, \Phi) \\ f_3(T, N, \Phi) \end{pmatrix} \quad \forall (t, x) \in [0, T_f] \times \bar{\Omega}.$$

iii) (T, N, Φ) satisfies the boundary and the initial conditions given in (2.2) and (2.3), respectively.

Theorem 2.3. *If there exists a classical solution of (2.1)-(2.3), then, it is unique.*

Proof. Let (T_1, N_1, Φ_1) and (T_2, N_2, Φ_2) two possible classical solutions of (2.1)-(2.3). Since both solutions are classical solutions, fixed a final time $0 < T_f < +\infty$, we have that (T_1, N_1, Φ_1) and (T_2, N_2, Φ_2) are bounded pointwise. Then, the graphs $(T_i(t, x), N_i(t, x), \Phi_i(t, x))$ for any $(t, x) \in [0, T_f] \times \bar{\Omega}$ are bounded for $i = 1, 2$ and therefore the union of both graphs is contained in a compact \mathcal{K} of \mathbb{R}^3 . We consider the problem which satisfies the differences $T = T_1 - T_2$, $N = N_1 - N_2$, $\Phi = \Phi_1 - \Phi_2$,

$$\begin{cases} \frac{\partial T}{\partial t} - \Delta T = f_1(T_1, N_1, \Phi_1) - f_1(T_2, N_2, \Phi_2) \\ \frac{\partial N}{\partial t} = f_2(T_1, N_1, \Phi_1) - f_2(T_2, N_2, \Phi_2) \\ \frac{\partial \Phi}{\partial t} = f_3(T_1, N_1, \Phi_1) - f_3(T_2, N_2, \Phi_2) \end{cases} \quad (2.8)$$

with non-flux boundary condition and zero initial data

$$\frac{\partial T}{\partial n} \Big|_{\partial \Omega} = 0, \quad T \Big|_{t=0} = N \Big|_{t=0} = \Phi \Big|_{t=0} = 0.$$

It is sufficient to prove that $(T, N, \Phi) \equiv (0, 0, 0)$. Multiplying the first equation of (2.8) by T and integrating in Ω , we obtain

$$\begin{aligned} \frac{1}{2} \frac{d}{dt} \int_{\Omega} T^2 dx + \int_{\Omega} |\nabla T|^2 dx &\leq \int_{\Omega} |(f_1(T_1, N_1, \Phi_1) - f_1(T_2, N_2, \Phi_2)) T| dx \\ &\leq C_1 \left(\int_{\Omega} (T^2 + |N| |T| + |\Phi| |T|) dx \right) \leq C_1 \left(\int_{\Omega} (T^2 + N^2 + \Phi^2) dx \right) \end{aligned} \quad (2.9)$$

because $f_1(T, N, \Phi)$ is locally lipschitz in \mathbb{R}^3 and $(T_i, N_i, \Phi_i)(t, x)$ is bounded in \mathbb{R}^3 for $i = 1, 2$. We repeat the same argument for the second and third equations, multiplying by N and Φ , respectively.

2. Theoretical analysis for a PDE-ODE system with linear diffusion related to a Glioblastoma tumor with vasculature

We conclude that,

$$\frac{1}{2} \frac{d}{dt} \int_{\Omega} (T^2 + N^2 + \Phi^2) dx + \int_{\Omega} |\nabla T|^2 dx \leq C \int_{\Omega} (T^2 + N^2 + \Phi^2). \quad (2.10)$$

Consequently, $T, N, \Phi \equiv 0$. □

In order to obtain existence of solution for the system (2.1)-(2.3), we define the following truncated system of (2.1):

$$\begin{cases} \frac{\partial T}{\partial t} - \Delta T = f_1(T_+, N_+, \Phi_+), \\ \frac{\partial N}{\partial t} = f_2(T_+^K, N_+, \Phi_+), \\ \frac{\partial \Phi}{\partial t} = f_3(T_+^K, N_+, \Phi_+), \end{cases} \quad (2.11)$$

endowed with the boundary and initial conditions given in (2.2) and (2.3), where

$$T_+^K = \min \{K, \max \{T, 0\}\} \quad (2.12)$$

and $N_+ = \max \{N, 0\}$ and similar to Φ_+ .

Once we prove the existence of classical solution of the problem (2.11) and its positivity, we will deduce in fact that this solution is also a classical solution of (2.1)-(2.3).

Before studying the existence of classical solution of (2.11), we prove a priori estimates for any possible classical solution.

Lemma 2.5 (Pointwise a priori estimates). *Under assumptions of Definition 2.1 any classical solution (T, N, Φ) of the truncated system (2.11) with initial data verifying (2.7) satisfies the following pointwise bounds*

$$\begin{cases} 0 \leq T \leq K, & a.e. (t, x) \in (0, T_f) \times \Omega, \\ 0 \leq N \leq C(T_f), & \forall (t, x) \in [0, T_f] \times \bar{\Omega}, \\ 0 \leq \Phi \leq K, & \forall (t, x) \in [0, T_f] \times \bar{\Omega}, \end{cases} \quad (2.13)$$

where $C(T_f)$ is a positive constant depending exponentially on the final time T_f , which we will define below in (2.14).

2. Theoretical analysis for a PDE-ODE system with linear diffusion related to a Glioblastoma tumor with vasculature

Proof. Let (T, N, Φ) be a classical solution of (2.11). Multiplying the first equation of (2.11) by $T_- = \min\{T, 0\}$ and integrating in Ω , if we rewrite $f_1(T_+, N_+, \Phi_+) = T_+ \tilde{f}_1(T_+, N_+, \Phi_+)$, we get

$$\frac{1}{2} \frac{d}{dt} \int_{\Omega} (T_-)^2 dx + \int_{\Omega} |\nabla T_-|^2 dx = \int_{\Omega} T_- T_+ \tilde{f}_1(T_+, N_+, \Phi_+) dx = 0, \quad \text{a.e. } t \in (0, T_f).$$

Hence, since $T_-(0, x) = 0$, we get $T_-(t, x) = 0$ a.e. $(t, x) \in (0, T_f) \times \Omega$. We can repeat the same argument for the other two equations of (2.11), using now that

$$\Phi_- f_3(T_+^K, N_+, \Phi_+) = 0 \quad \text{and} \quad N_- f_2(T_+^K, N_+, \Phi_+) \leq 0.$$

To obtain the upper bounds of (2.13), we multiply the first equation of (2.11) by $(T - K)_+ = \max\{0, T - K\}$ and integrate in Ω ,

$$\begin{aligned} & \frac{1}{2} \frac{d}{dt} \int_{\Omega} ((T - K)_+)^2 dx + \int_{\Omega} |\nabla (T - K)_+|^2 dx \\ &= \int_{\Omega} f_1(T_+, N_+, \Phi_+) (T - K)_+ dx \leq 0, \quad \text{a.e. } t \in (0, T_f) \end{aligned}$$

where in the last inequality we have used $f_1(T_+, N_+, \Phi_+) \leq \rho T_+ \left(1 - \frac{T_+}{K}\right)$.

Hence, since $(T(0, x) - K)_+ = 0$, then $(T(t, x) - K)_+ = 0$ a.e. $(t, x) \in (0, T_f) \times \Omega$. We repeat the same argument for the third equation of (2.11) using now that $(\Phi - K)_+ f_3(T_+^K, N_+, \Phi_+) \leq 0$.

Finally, given a fixed final time $T_f > 0$, for any $t \leq T_f$ and $x \in \bar{\Omega}$, we have

$$\frac{\partial N}{\partial t} = \alpha B(\Phi_+, T_+^K) + \delta T_+^K \Phi_+ + N(\beta_1 T_+^K + \beta_2 \Phi_+) \leq C_1 + C_2 N$$

where C_1 and C_2 depend on $\alpha, \beta_1, \beta_2, \delta$ and K . Hence,

$$N(t, x) \leq \frac{C_1}{C_2} (e^{C_2 t} - 1) + e^{C_2 t} N_0(x) \leq C(T_f) = e^{C_2 T_f} \left(\frac{C_1}{C_2} + K \right) = C(T_f). \quad (2.14)$$

In particular, $C(T_f) > 0$ is an upper bound with an exponential growth depending on the final time T_f . \square

By Lemma 2.5, we deduce that if (T, N, Φ) is a classical solution of (2.11) then $T_+^K = T$, $N_+ = N$ and $\Phi_+ = \Phi$ and $f_i(T_+^K, N_+, \Phi_+) = f_i(T, N, \Phi)$ for $i = 1, 2, 3$. Hence, we obtain the following crucial corollary

Corollary 2.1. *Under hypotheses of Lemma 2.5 if (T, N, Φ) is a classical solution of the truncated problem (2.11), then (T, N, Φ) is also a classical solution of the non truncated problem (2.1)-(2.3) and (T, N, Φ) satisfies the pointwise bounds (2.13).*

2. Theoretical analysis for a PDE-ODE system with linear diffusion related to a Glioblastoma tumor with vasculature

Theorem 2.4 (Existence of classical solution of (2.11)). *Let $\Omega \subseteq \mathbb{R}^3$ be a bounded domain of class C^2 and $(0, T_f)$ a time interval, with $0 < T_f < +\infty$ and let $T_0 \in W_n^{2-2/p, p}(\Omega)$ for some $p > 3$ and $N_0, \Phi_0 \in C^0(\bar{\Omega})$ satisfying (2.7). Then, there exists an unique classical solution (T, N, Φ) of system (2.11) in the sense of Definition 2.1. Moreover, (T, N, Φ) satisfies estimates (2.13).*

Remark 2.2. *In the revision process of [24], one of the referees pointed out that the proof of the existence and uniqueness of the global classical solution could be deduced from the Rothe's book [50]. In fact, the part II of [50] is devoted to degenerate parabolic systems with linear diffusion, where some variables have zero diffusion coefficient, remaining a mixed PDE-ODE system as (2.1). The argument developed in [50] is completely different to ours made in this Chapter. In fact, in [50] the existence and uniqueness of a mild solution (satisfying an integral system) is proved in three steps, first local existence via a contractive map, second the length of the local time existence interval is a bounded from below and third proving an extensibility result. By the contrary, here we will prove the existence of global in time solution directly by applying the Leray-Schauder fixed-point Theorem.*

Proof. The proof splits in several steps:

2.2.1 Step 1. Define the fixed-point map

We define the map

$$\mathbf{R} : C^0([0, T_f]; C^0(\bar{\Omega})) \xrightarrow{R_1} (C^1([0, T_f]; C^0(\bar{\Omega})))^2 \xrightarrow{R_2} C^0([0, T_f]; C^0(\bar{\Omega}))$$

$$\tilde{T} \qquad \qquad \qquad (N, \Phi) \qquad \qquad \qquad T$$

where $R_1(\tilde{T}) := (N, \Phi)$ is the solution of the ordinary differential problem

$$\left\{ \begin{array}{l} \left(\begin{array}{l} \frac{\partial N}{\partial t} \\ \frac{\partial \Phi}{\partial t} \end{array} \right) = \left(\begin{array}{l} f_2(\tilde{T}_+, N_+, \Phi_+) \\ f_3(\tilde{T}_+, N_+, \Phi_+) \end{array} \right) \\ \left(\begin{array}{l} N(0, x) \\ \Phi(0, x) \end{array} \right) = \left(\begin{array}{l} N_0(x) \\ \Phi_0(x) \end{array} \right) \end{array} \right. \quad (2.15)$$

and $R_2(N, \Phi) := T$ is the solution of the nonlinear parabolic problem,

2. Theoretical analysis for a PDE-ODE system with linear diffusion related to a Glioblastoma tumor with vasculature

$$\begin{cases} T_t - \Delta T = f_1(T_+, N_+, \Phi_+), \\ \frac{\partial T}{\partial n} \Big|_{\partial\Omega} = 0, \\ T(0, \cdot) = T_0(x). \end{cases} \quad (2.16)$$

2.2.2 Step 2. The map is well-defined and continuous

Lemma 2.6. *The map $R_1 : C^0([0, T_f]; C^0(\bar{\Omega})) \rightarrow (C^1([0, T_f]; C^0(\bar{\Omega})))^2$ is well defined and it is continuous.*

Proof. Step 1: R_1 is well defined. Observe that to obtain the solution (N, Φ) of (2.15), we have to solve an ordinary differential system which depends on the parameter $x \in \bar{\Omega}$, appearing in the ODE system via the function $\tilde{T}_+^K(t, x)$ and on the initial data $(N_0(x), \Phi_0(x))$.

We are going to define time and space extensions, respectively. First, we define the constant time extension as follows

$$\begin{aligned} Ext_t : C^0([0, T_f]) &\rightarrow C^0(\mathbb{R}) \\ f &\mapsto Ext_t(f) = \begin{cases} f(0) & t \leq 0, \\ f(t) & 0 \leq t \leq T_f, \\ f(T_f) & t \geq T_f. \end{cases} \end{aligned}$$

For the space extension, we use Lemma 2.4

$$\begin{aligned} Ext_x : C^0(\bar{\Omega}) &\rightarrow C^0(\mathbb{R}^3) \\ f &\mapsto Ext_x(f). \end{aligned}$$

Finally, we consider the global extension

$$\begin{aligned} Ext : C^0([0, T_f]; C^0(\bar{\Omega})) &\rightarrow C^0(\mathbb{R}; C^0(\mathbb{R}^3)) \\ f &\mapsto Ext(f) := (Ext_t \circ Ext_x)(f). \end{aligned}$$

Hence, we can rewrite (2.15) defined in open sets as

$$\begin{cases} y'(t) = F(t, y, x) \in \mathbb{R}^2 & \text{for } (t, y, x) \in \mathbb{R} \times \mathbb{R}^2 \times \mathbb{R}^3 \\ y(0) = y_0(x) \in \mathbb{R}^2 \end{cases} \quad (2.17)$$

2. Theoretical analysis for a PDE-ODE system with linear diffusion related to a Glioblastoma tumor with vasculature

where we denote $y = (N, \Phi)$ and

$$F(t, y, x) = \begin{pmatrix} f_2 \left(\left(Ext \left(\tilde{T}(t, x) \right) \right)_+^K, N_+, \Phi_+ \right) \\ f_3 \left(\left(Ext \left(\tilde{T}(t, x) \right) \right)_+^K, N_+, \Phi_+ \right) \end{pmatrix}, \quad (2.18)$$

$$y_0(x) = \begin{pmatrix} Ext_x(N_0(x)) \\ Ext_x(\Phi_0(x)) \end{pmatrix}. \quad (2.19)$$

Since

$$0 \leq \left(Ext \left(\tilde{T}(t, x) \right) \right)_+^K \leq K \quad \forall (t, x) \in [0, T_f] \times \bar{\Omega}$$

and

$$0 \leq Ext_x(N_0(x)), Ext_x(\Phi_0(x)) \leq K \quad \forall x \in \bar{\Omega},$$

we can argue similarly to Lemma 2.5 to conclude that the solution of (2.17) satisfies that $0 \leq \Phi(t, x) \leq K$ and $0 \leq N(t, x) \leq C(T_f)$ for all $(t, x) \in [0, T_f] \times \bar{\Omega}$.

Then, by Lemmas 2.1 and 2.2 and definition of F , we have that $F(t, y, x)$ is continuous in $\mathbb{R} \times \mathbb{R}^2 \times \mathbb{R}^3$ and locally lipschitz with respect to $y \in \mathbb{R}^2$. Hence for each $x \in \bar{\Omega}$ we can apply the Picard's theorem to obtain a local in time unique solution $y(\cdot, x)$ of (2.17). Moreover, since we know that the solution of (2.17) is bounded for all $t \in [0, T_f]$, the solution can be extended to $[0, T_f]$ for each $x \in \bar{\Omega}$.

Now, we can apply Theorem 2.1, with $U = \mathbb{R} \times \mathbb{R}^2 \times \mathbb{R}^3$, $\lambda = x \in \mathbb{R}^3$ and $y_0(x)$ defined in (2.19) to the Cauchy's problem (2.17). Thus, we have that for each $y_0 = y_0(x) \in \mathbb{R}^2$ defined in (2.19) such that $0 \leq Ext_x(N_0(x)), Ext_x(\Phi_0(x)) \leq K$ in \mathbb{R}^3 , the interval $[0, T_f] \subseteq I_{(Ext_x(N_0(x)), Ext_x(\Phi_0(x)))}$ and hence, the set

$$\tilde{\Theta} = \left\{ (t, (Ext_x(N_0(x)), Ext_x(\Phi_0(x))), x) \in \mathbb{R} \times \mathbb{R}^2 \times \mathbb{R}^3 : t \in I_{(0, (Ext_x(N_0(x)), Ext_x(\Phi_0(x)))} \right\}$$

is an open set of \mathbb{R}^6 and the map $y = y(t; (Ext_x(N_0(x)), Ext_x(\Phi_0(x))), x)$ is continuous from $\tilde{\Theta}$ to \mathbb{R}^2 .

In conclusion, given $N_0, \Phi_0 \in C^0(\bar{\Omega})$ such that $0 \leq N_0, \Phi_0 \leq K$ in $\bar{\Omega}$, there exists a solution $y = y(t; (Ext_x(N_0(x)), Ext_x(\Phi_0(x))), x)$ of (2.17) whose restriction to $[0, T_f] \times \bar{\Omega}$

$$(N, \Phi)(t, x) = y(t; (Ext_x(N_0(x)), Ext_x(\Phi_0(x))), x) \quad \forall (t, x) \in [0, T_f] \times \bar{\Omega}$$

2. Theoretical analysis for a PDE-ODE system with linear diffusion related to a Glioblastoma tumor with vasculature

satisfies that

$$(N, \Phi) \in (C^1([0, T_f]; C^0(\bar{\Omega})))^2$$

and it is the unique solution of (2.15).

Step 2: R_1 is continuous. Take $\tilde{T}_n \rightarrow \tilde{T}$ in $C^0([0, T_f]; C^0(\bar{\Omega}))$. We use the same vectorial notation as before and we consider the following integral formulation of (2.15),

$$y(t; y_0(x)) = y_0(x) + \int_0^t \tilde{F}(s, y(s, x), x) ds$$

where in this case $y = (N, \Phi)$ and

$$\tilde{F}(t, y, x) = \begin{pmatrix} f_2(\tilde{T}_+^K(t, x), N, \Phi) \\ f_3(\tilde{T}_+^K(t, x), N, \Phi) \end{pmatrix}. \quad (2.20)$$

Now, we take $R_1(\tilde{T}_n) = y_n$ and $R_1(\tilde{T}) = y$ the solutions of (2.15) associated to \tilde{T}_n and \tilde{T} , respectively. Thus, denoting $y(t, \cdot) = y(t; y_0(\cdot), \cdot)$, we get

$$\|y_n(t) - y(t)\|_{(C^0(\bar{\Omega}))^2} = \left\| \int_0^t \tilde{F}(s, y_n(s), x) - \tilde{F}(s, y(s), x) ds \right\|_{(C^0(\bar{\Omega}))^2}.$$

By Lemma 2.2 and the form of (2.20), we deduce that $\tilde{F}(t, y, x)$ is locally lipschitz in $\mathbb{R} \times \mathbb{R}^2 \times \mathbb{R}^3$ with respect to (t, y, x) . Moreover, y_n and y are bounded in $C^0([0, T_f]; C^0(\bar{\Omega}))$, then, we have that

$$\|y_n(t) - y(t)\|_{C^0(\bar{\Omega})^2} \leq C \int_0^t \left(\| (y_n - y)(s) \|_{(C^0(\bar{\Omega}))^2} + \left\| \left((\tilde{T}_n)_+^K - \tilde{T}_+^K \right)(s) \right\|_{C^0(\bar{\Omega})} \right) ds.$$

Applying Gronwall's lemma, we deduce

$$\| (y_n - y)(t) \|_{C^0(\bar{\Omega})^2} \leq C e^{Ct} \left(\int_0^{T_f} \left\| \left((\tilde{T}_n)_+^K - \tilde{T}_+^K \right)(s) \right\|_{C^0(\bar{\Omega})} ds \right). \quad (2.21)$$

Now, in (2.21) we take maximum in $t \in [0, T_f]$ in the left side and we bound in the right side. Thus,

$$\| (y_n - y) \|_{C^0([0, T_f]; C^0(\bar{\Omega}))^2} \leq C e^{CT_f} \left\| \left((\tilde{T}_n)_+^K - \tilde{T}_+^K \right) \right\|_{C^0([0, T_f]; C^0(\bar{\Omega}))} \xrightarrow{n \rightarrow \infty} 0.$$

Hence, we obtain that $y_n \rightarrow y$ in $(C^0([0, T_f]; C^0(\bar{\Omega})))^2$.

2. Theoretical analysis for a PDE-ODE system with linear diffusion related to a Glioblastoma tumor with vasculature

Moreover, it follows

$$\tilde{F}(y_n(t, x), t, x) \xrightarrow[n \rightarrow \infty]{} \tilde{F}(y(t, x), t, x) \quad \text{in } (C^0([0, T_f]; C^0(\bar{\Omega})))^2$$

whence we deduce that

$$\partial_t y_n(t, x) = \tilde{F}(y_n(t, x), t, x) \xrightarrow[n \rightarrow \infty]{} \tilde{F}(y(t, x), t, x) = \partial_t y(t, x) \quad \text{in } (C^0([0, T_f]; C^0(\bar{\Omega})))^2.$$

Hence, we get that R_1 is continuous from $C^0([0, T_f]; C^0(\bar{\Omega}))$ to $(C^1([0, T_f]; C^0(\bar{\Omega})))^2$. \square

Lemma 2.7. *The map $R_2 : (C^1([0, T_f]; C^0(\bar{\Omega})))^2 \rightarrow C^0([0, T_f]; C^0(\bar{\Omega}))$ is well defined.*

Proof. Observe that the pair of constant functions $(\underline{T}, \bar{T}) = (0, K)$ is a sub-super solution of (2.16) and the reaction term in (2.16) is bounded a.e. $(t, x) \in (0, T_f) \times \Omega$ and for $T \in [\underline{T}, \bar{T}]$. Then, applying Theorem of [17, p. 94], there exists at least a weak solution T of (2.16) such that $0 \leq T \leq K$ a.e. in $(0, T_f) \times \Omega$.

Since $T \in [0, K]$, we get that the application $(t, x, T_+) \rightarrow f_1(T_+(t, x), N_+(t, x), \Phi_+(t, x))$ is bounded in $L^\infty(0, T_f; L^\infty(\Omega))$. Hence, applying Lemma 2.3 since $T_0 \in W_n^{2-2/p, p}(\Omega)$, we deduce that $T \in V_p$.

In particular, since $W_n^{2-2/p, p}(\Omega) \hookrightarrow C^0(\bar{\Omega})$, we get

$$T \in C^0([0, T_f]; C^0(\bar{\Omega})).$$

The uniqueness of $T = R_2(N, \Phi)$ can be deduced by a comparison argument using the regularity of (T, N, Φ) . \square

Before proving that R_2 is continuous, we show the following result:

Lemma 2.8. *For any bounded set A of $(C^1([0, T_f]; C^0(\bar{\Omega})))^2$, then $R_2(A)$ is bounded in V_p for some $p > 3$, where V_p is the Banach space defined in Lemma 2.3*

Notice that, by Aubion-Lions lemma (see [33, Théorème 5.1, p. 58]) and [51, Corollary 4], one has the compact embedding

$$V_p \hookrightarrow C^0([0, T_f]; C^0(\bar{\Omega})).$$

Proof. Given $(N, \Phi) \in A$ a bounded set of $(C^1([0, T_f]; C^0(\bar{\Omega})))^2$, then

$$\|N\|_{C^1([0, T_f]; C^0(\bar{\Omega}))}, \|\Phi\|_{C^1([0, T_f]; C^0(\bar{\Omega}))} \leq \tilde{C} \quad (2.22)$$

and there exists an unique $T = R_2(N, \Phi)$ solution of (2.16). Moreover, we have that the application $(t, x) \rightarrow f_1(T_+(t, x), N(t, x), \Phi(t, x))$ is bounded in $L^\infty((0, T_f); L^\infty(\Omega))$. Thus by Lemma 2.3 and (2.22),

2. Theoretical analysis for a PDE-ODE system with linear diffusion related to a Glioblastoma tumor with vasculature

$$\|T\|_{V_p} \leq C \left(\|f_1(T_+, N_+, \Phi_+)\|_{L^p((0, T_f); L^p(\Omega))}, \|T_0\|_{W^{2-2/p, p}(\Omega)} \right) \leq \widehat{C}.$$

□

Lemma 2.9. *The map $R_2 : (C^1([0, T_f]; C^0(\overline{\Omega})))^2 \rightarrow C^0([0, T_f]; C^0(\overline{\Omega}))$ is continuous.*

Proof. Given

$$(N_n, \Phi_n) \rightarrow (N, \Phi) \quad \text{in } (C^1([0, T_f]; C^0(\overline{\Omega})))^2 \quad (2.23)$$

we are going to check that $T_n = R_2(N_n, \Phi_n) \rightarrow T = R_2(N, \Phi)$ in $C^0([0, T_f]; C^0(\overline{\Omega}))$.

Applying Lemma 2.8, it holds that $T_n = R_2(N_n, \Phi_n)$ is bounded in V_p , hence there exists a subsequence $T_{n_k} \in V_p$ and a limit $T^* \in V_p$ such that

$$T_{n_k} \rightharpoonup T^* \text{ weakly in } V_p \text{ and strongly in } C^0([0, T_f]; C^0(\overline{\Omega}))$$

and

$$\frac{\partial T_{n_k}}{\partial t} \rightharpoonup \frac{\partial T^*}{\partial t} \text{ weakly in } L^p(0, T_f; L^p(\Omega)).$$

In particular,

$$\Delta T_{n_k} \rightharpoonup \Delta T^* \text{ weakly in } L^p(0, T_f; L^p(\Omega)).$$

Using these convergences and (2.23), the continuity of $f_1(T_+, N_+, \Phi_+)$ and the locally lipschitz property of the application $(T, N, \Phi) \rightarrow f_1(T_+, N_+, \Phi_+)$ respect to all the variables, we deduce

$$f_1((T_{n_k})_+, (N_{n_k})_+, (\Phi_{n_k})_+) \rightarrow f_1((T^*)_+, N_+, \Phi_+) \text{ strongly in } C^0([0, T_f]; C^0(\overline{\Omega})).$$

Taking $n_k \rightarrow \infty$ we have that $T^* = R_2(N, \Phi)$ and since the solution of (2.16) is unique, then $T^* = T$ and

$$T_n \rightarrow T \text{ in } C^0([0, T_f]; C^0(\overline{\Omega})).$$

□

From Lemmas 2.6, 2.7 and 2.9, we obtain that:

Corollary 2.2. *The map*

$$\mathbf{R} : C^0([0, T_f]; C^0(\overline{\Omega})) \rightarrow C^0([0, T_f]; C^0(\overline{\Omega}))$$

is well defined and continuous.

2. Theoretical analysis for a PDE-ODE system with linear diffusion related to a Glioblastoma tumor with vasculature

2.2.3 Step 3. The map is compact

Lemma 2.10. *The operator $\mathbf{R} : C^0([0, T_f]; C^0(\bar{\Omega})) \rightarrow C^0([0, T_f]; C^0(\bar{\Omega}))$ is compact.*

Proof. Let $\tilde{T} \in C^0([0, T_f]; C^0(\bar{\Omega}))$ then by Lemmas 2.6 and 2.7 there exists an unique $T = \mathbf{R}(\tilde{T})$ such that $0 \leq T \leq K$ a.e. $(t, x) \in (0, T_f) \times \Omega$ and being T the solution of (2.16).

Moreover, there exists an unique $(N, \Phi) \in (C^0([0, T_f]; C^0(\bar{\Omega})))^2$ such that $0 \leq N, \Phi \leq K$ for all $(t, x) \in [0, T_f] \times \bar{\Omega}$. Hence, $f_1(T_+, N_+, \Phi_+)$ is bounded in $L^\infty(0, T_f; L^\infty(\Omega))$, in particular, in $L^p(0, T_f; L^p(\Omega))$ for all $p < \infty$. Following a similar argument of Lemma 2.8, we obtain that T is bounded in V_p for some $p > 3$.

Finally, applying the compact embedding of V_p in $C^0([0, T_f]; C^0(\bar{\Omega}))$, we obtain that \mathbf{R} is compact from $C^0([0, T_f], C^0(\bar{\Omega}))$ to itself. □

2.2.4 Step 4. A priori estimates of possible fixed-points and conclusion

Lemma 2.11. *For any $T = \lambda \mathbf{R}(T)$, for some $\lambda \in [0, 1]$, then $\|T\|_{C^0([0, T_f], C^0(\Omega))} \leq C$ with $C > 0$ independent of $\lambda \in [0, 1]$.*

Proof. For $\lambda = 0$ the result is trivial, hence we suppose $\lambda \in (0, 1]$.

On the one hand, if we rewrite $f_1(T_+, N_+, \Phi_+) = T_+ \tilde{f}_1(T_+, N_+, \Phi_+)$, we have that,

$$T_t - \Delta T = \lambda f_1(T_+/\lambda, N_+, \Phi_+) = \lambda \frac{T_+}{\lambda} \tilde{f}_1(T_+/\lambda, N_+, \Phi_+) \leq \rho T_+ \left(1 - \frac{T_+}{\lambda K}\right).$$

Since $0 \leq T(0, x) \leq K$ in $\bar{\Omega}$, we can argue similarly to Lemma 2.5 and conclude that $0 \leq T \leq K$ in $[0, T_f] \times \bar{\Omega}$. Thus, T is bounded $C^0([0, T_f], C^0(\bar{\Omega}))$ independently of $\lambda \in [0, 1]$. □

Finally, from Corollary 2.2 and Lemmas 2.10 and 2.11, the operator \mathbf{R} satisfies the hypotheses of Theorem 2.2. Thus, we conclude that the map \mathbf{R} has a fixed point $T = \mathbf{R}(T)$ which is a classical solution of (2.11) and consequently it is also a classical solution of (2.1)-(2.3). □

2.3 Asymptotic behaviour

2.3.1 Stability of the (non-diffusion) ODE system

Once we have proved the existence and uniqueness of solution for (2.1) for any finite time, let us study the long time behaviour of this solution. For that, first of all, we will study the non-diffusion problem

2. Theoretical analysis for a PDE-ODE system with linear diffusion related to a Glioblastoma tumor with vasculature

$$\begin{cases} \frac{dT}{dt} = f_1(T, N, \Phi) \\ \frac{dN}{dt} = f_2(T, N, \Phi) \\ \frac{d\Phi}{dt} = f_3(T, N, \Phi) \end{cases} \quad (2.24)$$

with initial data

$$(T, N, \Phi)(0) = (T_0, N_0, \Phi_0) \in \mathbb{R}^3 \quad (2.25)$$

such that $0 \leq T_0, N_0, \Phi_0 \leq K$ and the functions $f_i = f_i(T, N, \Phi) \in \mathbb{R}$ for $i = 1, 2, 3$ are defined in (2.4). Since problem (2.24) is decoupled for each $x \in \Omega$, it suffices to study the ODE system (2.24) with a fixed $(T_0, N_0, \Phi_0) \in \mathbb{R}_+^3$. First of all, we can deduce the same bounds for the solution (T, N, Φ) as in problem (2.1)-(2.3) and hence $(T(t), N(t), \Phi(t)) \in \mathbb{R}_+^3 \forall t \geq 0$.

In order to obtain the equilibrium points, we solve the nonlinear algebraic system $f_i(T, N, \Phi) = 0$ for $i = 1, 2, 3$. From $f_2(T, N, \Phi) = 0$ we obtain that

$$\begin{cases} T \sqrt{1 - (P(\Phi, T))^2} = 0, \\ T \Phi = 0, \\ N(T + \Phi) = 0. \end{cases}$$

From $T \sqrt{1 - (P(\Phi, T))^2} = 0$ and $T \Phi = 0$, we have $T = 0$. From the third condition, we obtain that $N = 0$ or $\Phi = 0$.

Thus, the equilibria of (2.24) are

- $P_1 = \{(0, 0, 0)\}$.
 - $P_2 = \{(0, N, 0), \quad N > 0\}$.
 - $P_3 = \{(0, 0, \Phi), \quad \Phi > 0\}$.
- (2.26)

Remark 2.3. Observe that $P_1 \cup P_2 \cup P_3$ is a continuum of equilibrium points.

Remark 2.4. The linearisation technique around the equilibria P_1, P_2 and P_3 doesn't give any relevant information because one of the eigenvalue of this linearisation is zero.

2. Theoretical analysis for a PDE-ODE system with linear diffusion related to a Glioblastoma tumor with vasculature

Now, we consider the differential equation for the sum $S = T + N + \Phi$, which satisfies

$$\begin{cases} \frac{dS}{dt} = \underbrace{\left(\rho T P(\Phi, T) + \frac{\gamma \Phi}{K} T \sqrt{1 - (P(\Phi, T))^2} \right)}_{=0 \text{ if } T=0 \text{ or } \Phi=0} \left(1 - \frac{S}{K} \right), \\ S(0) = S_0 := T_0 + N_0 + \Phi_0. \end{cases} \quad (2.27)$$

Hence, we see that $S(t)$ is increasing if $S_0 < K$, and, $S(t) \nearrow S_* \leq K$ as $t \rightarrow +\infty$. On the other hand, if $S_0 = K$, then $S(t) = K \quad \forall t \in [0, +\infty)$. Finally, if $S_0 > K$ then $S(t)$ is decreasing and $S(t) \searrow S_* \leq K$ as $t \rightarrow +\infty$. For brevity, we only study the case $S_0 \leq K$.

We show two particular cases:

- If $T_0 = 0$, then $T(t) = 0 \quad \forall t \geq 0$. This implies from (2.27) that $\frac{dS}{dt} = 0 \quad \forall t > 0$. Hence $S(t) = N_0 + \Phi_0 \quad \forall t > 0$. In terms of the subsystem (N, Φ) , we obtain that

$$\begin{cases} \frac{dN}{dt} = \beta_2 N \Phi, \\ \frac{d\Phi}{dt} = -\beta_2 N \Phi, \end{cases}$$

with $N(0) = N_0 \geq 0$ and $\Phi(0) = \Phi_0 \geq 0$. Hence $N(t) \nearrow N_*$ and, $\Phi(t) \searrow 0$ with $N_* = N_0 + \Phi_0$.

- If $\Phi_0 = 0$, then $\Phi(t) = 0 \quad \forall t > 0$. Hence, from (2.27), $S(t) = T_0 + N_0$ for all $t > 0$. Since $N(t) \nearrow N_*$ then, $T(t) \searrow 0$ with $N_* = N_0 + T_0$.

In order to study the stability of (2.24), we use the properties of ω -limit sets. Given $y_0 = (T_0, N_0, \Phi_0) \in \mathbb{R}_+^3$ such that $T_0 + N_0 + \Phi_0 \leq K$, then there exists an unique solution $y(t) = (T, N, \Phi)(t) \in \mathbb{R}_+^3 \quad \forall t \in [0, +\infty)$ of (2.24)-(2.25) such that $T(t) + N(t) + \Phi(t) \leq K$. Therefore the corresponding ω -limit set is defined by

$$\omega(y_0) = \{y_* \in \mathbb{R}_+^3, \exists t_n \rightarrow \infty : y(t_n) \rightarrow y_* \text{ in } \mathbb{R}^3\}$$

and is a nonempty compact and invariant set of \mathbb{R}_+^3 . Since $0 < S_0 \leq K$ then $S(t) \nearrow S_* \leq K$ and $N(t) \nearrow N_* \leq S_*$ for $t \rightarrow \infty$, where $S_* = S_*(S_0)$ and $N_* = N_*(T_0, N_0, \Phi_0)$, because both functions are increasing and bounded from above. Therefore,

$$\omega(T_0, N_0, \Phi_0) \subseteq \left\{ (\tilde{T}, N_*, S_* - N_* - \tilde{T}), \tilde{T} \in [0, S_* - N_*] \right\}. \quad (2.28)$$

2. Theoretical analysis for a PDE-ODE system with linear diffusion related to a Glioblastoma tumor with vasculature

Theorem 2.5. Given $y_0 = (T_0, N_0, \Phi_0) \in \mathbb{R}_+^3$ and $S_0 = T_0 + N_0 + \Phi_0 \leq K$. If $y_0 \neq (0, 0, \Phi_0)$ with $\Phi_0 \geq 0$, then the ω -limit set is an unitary set

$$\omega(T_0, N_0, \Phi_0) = \left\{ (0, N_*, 0) \right\}.$$

Remark 2.5. If $y_0 \notin P_1 \cup P_3$, then $\omega(y_0)$ is unitary and belongs to P_2 .

Proof. Let (T_p, N_p, Φ_p) be the solution starting from a point

$$p = \left(\tilde{T}, N_*, S_* - N_* - \tilde{T} \right) \in \omega(T_0, N_0, \Phi_0).$$

Since $\omega(T_0, N_0, \Phi_0)$ is an invariant set, it holds that $N_p(t) = N_* \forall t$. Hence $\frac{d}{dt}N_p = 0$. Now, from the N_p equation,

$$0 = \frac{d}{dt}N_p = T_p \left(\alpha \sqrt{1 - \left(\frac{\Phi_p}{\Phi_p + T_p} \right)^2} + \beta_1 N_p \right) + \Phi_p (\delta T_p + \beta_2 N_p) \geq \beta_1 T_p N_p. \quad (2.29)$$

Hence $T_p(t) = 0$ for all $t \geq 0$ and $\tilde{T} = 0$. Then, $p = (0, N_*, S_* - N_*)$.

Since in particular p is an equilibrium point and $N_* > 0$, then p must be a point of type P_2 , hence $p = (0, N_*, 0)$. In particular, $N_* = S_*$. \square

As consequence of this result, we deduce:

Corollary 2.3. P_3 is a continuum of unstable equilibria. Indeed, for any (T_0, N_0, Φ_0) with $T_0 > 0$ or $N_0 > 0$, then its solution satisfies

$$(T(t), N(t), \Phi(t)) \rightarrow (0, N_*, 0) \text{ as } t \rightarrow \infty$$

with $N_* \geq T_0 + N_0 + \Phi_0$.

2.3.2 Stability of the Diffusion Model (2.1)-(2.3)

In this Section, we study the stability of the constant equilibria of (2.1)-(2.3) to spatio-temporal perturbations for $t \rightarrow +\infty$. The constant solutions of (2.1)-(2.3) are the same of (2.24)-(2.25) given in (2.26). In this case, the main difference is that we do not have a differential problem for $S(t)$ as in (2.27). Before showing the results we will discuss the following remark.

Remark 2.6. The condition $N_0(x) > 0$ for $x \in \bar{\Omega}$ used in the followings results can be relaxed by $N(t_*, x) > 0$ for some $t_* > 0$ since $N(\cdot, x)$ is increasing in time. On the other hand, applying the strong maximum principle to the parabolic problem that satisfies the tumor variable T (since the reaction can

2. Theoretical analysis for a PDE-ODE system with linear diffusion related to a Glioblastoma tumor with vasculature

be rewrite as $f_1(T, N, \Phi) = T \tilde{f}_1(T, N, \Phi)$ with \tilde{f}_1 bounded), it holds that $T(t_1, x) > 0$ for any $t_1 > 0$ and for all $x \in \bar{\Omega}$. Due to the hypoxia term, in particular one has $\frac{\partial N}{\partial t} \geq \alpha T \sqrt{1 - P^2(\Phi, T)} > 0$ hence $N(t_*, x) > 0$ for any $t_* > t_1$ and for all $x \in \bar{\Omega}$.

We introduce some results of pointwise and uniform convergence as time goes to infinity. First of all, we will see that vasculature always goes to zero.

Lemma 2.12. *Given a solution (T, N, Φ) of (2.1)-(2.3), then for each $x \in \bar{\Omega}$ such that $N_0(x) > 0$ one has $\Phi(t, x) \rightarrow 0$ when $t \rightarrow +\infty$.*

Proof. Let $x \in \bar{\Omega}$ such that $N_0(x) > 0$. Since $N(\cdot, x)$ is increasing, then, $0 < N_0(x) \leq N(t, x)$ for all $t > 0$. Now, we separate this proof in two cases depending on the value of $N(t, x)$:

a) If there exists $t_* > 0$ such that $N(t, x) \geq K$ for all $t \geq t_*$, then we get

$f_3(T(t, x), N(t, x), \Phi(t, x)) \leq -\beta_2 K \Phi(t, x)$ for all $t \geq t_*$. Hence we have the following

$$\begin{cases} \frac{\partial \Phi}{\partial t}(t, x) \leq -\beta_2 K \Phi(t, x) & \text{in } [t_*, +\infty), \\ \Phi(t_*, x) \geq 0. \end{cases} \quad (2.30)$$

Therefore for all $t \geq t_*$,

$$\Phi(t, x) \leq \Phi(t_*, x) e^{-\beta_2 K (t-t_*)} \rightarrow 0 \quad \text{as } t \rightarrow +\infty.$$

b) If $N(t, x) < K$ for all $t \geq 0$ we reason by contradiction. Assume that there exists a sequence $\{t_n\}_{n \in \mathbb{N}}$ such that $t_n \rightarrow +\infty$ and $t_{n+1} - t_n \geq 1$ for all $n \in \mathbb{N}$ and there exists $\eta(x)$ such that $\Phi(t_n, x) \geq \eta(x) > 0$ for all $n \in \mathbb{N}$. Since

$$\begin{cases} \frac{\partial N}{\partial t}(t, x) \geq \beta_2 N(t, x) \Phi(t, x) & \text{in } (0, +\infty), \\ N(0, x) \geq 0, \end{cases} \quad (2.31)$$

we have the following estimates for $N(t, x)$.

$$K > N(t, x) \geq N_0(x) e^{\beta_2 \int_0^t \Phi(s, x) ds}. \quad (2.32)$$

Since $0 \leq T, \Phi \leq K$ and $N(t, x) < K$ for all $t > 0$, we get the following lower bound

$$\begin{aligned} \frac{\partial \Phi}{\partial t} = f_3(T, N, \Phi) &\geq -\frac{\gamma}{K} T \sqrt{1 - P(\Phi, T)^2} \Phi \left(\frac{T + \Phi}{K} \right) - \delta T \Phi - \beta_2 N \Phi \geq \\ &\geq -2\gamma \Phi - \delta K \Phi - \beta_2 K \Phi = -C_0 \Phi. \end{aligned}$$

2. Theoretical analysis for a PDE-ODE system with linear diffusion related to a Glioblastoma tumor with vasculature

Hence,

$$\Phi(t, x) \geq e^{-C_0(t-t_n)} \Phi(t_n, x) \geq e^{-C_0(t-t_n)} \eta(x) \quad \forall t \in (t_n, t_{n+1}).$$

Integrating in $[t_n, t_{n+1}]$ and using that $t_{n+1} - t_n \geq 1$

$$\int_{t_n}^{t_{n+1}} \Phi(t, x) dt \geq \frac{\eta(x)}{C_0} \left(1 - e^{-C_0(t_{n+1}-t_n)}\right) \geq \frac{\eta(x)}{C_0} (1 - e^{-C_0}) > 0.$$

Finally, adding all t_n

$$\sum_{n=1}^{+\infty} \int_{t_n}^{t_{n+1}} \Phi(t, x) dt = +\infty.$$

Hence, $\int_0^{+\infty} \Phi(t, x) dt = +\infty$ and we arrive at contradiction with (2.32) and the proof is completed. □

As consequence of Lemma 2.12, we deduce:

Corollary 2.4. *The equilibria P_3 are unstable.*

Remark 2.7. *As consequence of $t \mapsto N(t, x)$ is increasing for all $x \in \bar{\Omega}$, we deduce that P_1 is not asymptotically stable.*

In the following result, adding a constraint on some parameters of the problem, we can deduce the behaviour of the solution of the system (2.1)-(2.3) as $t \rightarrow +\infty$.

Lemma 2.13. *Given a classical solution (T, N, Φ) of (2.1)-(2.3) such that $N_0(x) > 0$ for all $x \in \bar{\Omega}$ and assume that*

$$\delta \geq \frac{\gamma}{K}. \tag{2.33}$$

Then, for all $t \geq 0$:

$$\|\Phi(t, \cdot)\|_{C^0(\bar{\Omega})} \leq \|\Phi_0\|_{C^0(\bar{\Omega})} e^{-\beta_2 N_0^{\min} t},$$

where $N_0^{\min} = \min_{x \in \bar{\Omega}} N_0(x)$. In addition, there exists $\mu \in (0, \min\{\beta_1, \beta_2\} N_0^{\min})$ such that

$$\|T(t, \cdot)\|_{C^0(\bar{\Omega})} \leq M e^{-\mu t}, \quad \forall t \geq 0$$

with $M = \max \left\{ \|T_0\|_{C^0(\bar{\Omega})}, \frac{\rho \|\Phi_0\|_{C^0(\bar{\Omega})}}{\beta_1 N_0^{\min} - \mu} \right\} > 0$. Moreover, there exists $N_{\max} > 0$ such that

$$N(t, x) \leq N_{\max} \quad \forall (t, x) \in [0, +\infty) \times \bar{\Omega}.$$

2. Theoretical analysis for a PDE-ODE system with linear diffusion related to a Glioblastoma tumor with vasculature

Proof. Using hypothesis (2.33) and the bounds $T, \Phi \geq 0$ and $N \geq N_0$, we can estimate

$$f_3(T, N, \Phi) \leq \frac{\gamma}{K} \Phi T - \delta \Phi T - \beta_2 \Phi N \leq -\beta_2 \Phi N_0.$$

Hence, Φ satisfies the differential inequality problem

$$\begin{cases} \frac{\partial \Phi}{\partial t} \leq -\beta_2 \Phi N_0(x) & \text{in } [0, +\infty) \times \overline{\Omega}, \\ \Phi(0, x) = \Phi_0(x) \leq \|\Phi_0\|_{C^0(\overline{\Omega})} & \text{in } \overline{\Omega}, \end{cases} \quad (2.34)$$

Using that $N_0^{\min} > 0$, we conclude that

$$\Phi(t, x) \leq \Phi_0(x) e^{-\beta_2 N_0(x) t} \leq \|\Phi_0\|_{C^0(\overline{\Omega})} e^{-\beta_2 N_0^{\min} t}. \quad (2.35)$$

In particular, $\Phi(t, x) \rightarrow 0$ as $t \rightarrow +\infty$ uniformly in $x \in \overline{\Omega}$.

Using (2.35) and the bounds $T, \Phi \geq 0, N \geq N_0$ and $P(\Phi, T) T \leq \Phi$, we can estimate $f_1(T, N, \Phi)$ as follows:

$$\begin{aligned} f_1(T, N, \Phi) &\leq \rho P(\Phi, T) T - \alpha T \sqrt{1 - P^2(\Phi, T)} - \beta_1 N T \\ &\leq \rho \Phi - \beta_1 N T \leq \rho \|\Phi_0\|_{L^\infty(\Omega)} e^{-\beta_2 N_0^{\min} t} - \beta_1 N_0^{\min} T. \end{aligned}$$

Therefore, $T \leq S$, where S is the unique solution of the following parabolic problem

$$\begin{cases} \frac{\partial S}{\partial t} - \Delta S = \rho \|\Phi_0\|_{C^0(\overline{\Omega})} e^{-\beta_2 N_0^{\min} t} - \beta_1 N_0^{\min} S & \text{in } (0, +\infty) \times \overline{\Omega}, \\ S(0, x) = \|T_0\|_{C^0(\overline{\Omega})} & \text{in } \Omega, \\ \frac{\partial S}{\partial n} \Big|_{\partial \Omega} = 0. \end{cases} \quad (2.36)$$

Now, we can find a super solution of (2.36) with the form

$$\overline{T}(t) = M e^{-\mu t}$$

such that $\min\{\beta_1, \beta_2\} N_0^{\min} > \mu > 0$ and $M = \max\left\{\|T_0\|_{C^0(\overline{\Omega})}, \frac{\rho \|\Phi_0\|_{C^0(\overline{\Omega})}}{\beta_1 N_0^{\min} - \mu}\right\} > 0$ for all $t \geq 0$.

Consequently, \overline{T} is a super solution of (2.36) and we have

$$T(t, x) \leq S(t, x) \leq \overline{T}(t) = M e^{-\mu t}. \quad (2.37)$$

In particular, $T(t, x) \rightarrow 0$ as $t \rightarrow +\infty$ uniformly for $x \in \overline{\Omega}$.

2. Theoretical analysis for a PDE-ODE system with linear diffusion related to a Glioblastoma tumor with vasculature

Then, we can obtain an uniform upper bound in time and space for $N(t, x)$ since,

$$\frac{\partial N}{\partial t} = a(t, x) N + b(t, x) \quad (2.38)$$

where

$$a(t, x) = \beta_2 \Phi(t, x) + \beta_1 T(t, x)$$

and

$$b(t, x) = \alpha B(\Phi(t, x), T(t, x)) + \delta \Phi(t, x) T(t, x).$$

Hence, one has the variation of constants formula

$$N(t, x) = \left(N_0(x) + \int_0^t b(s, x) e^{-A(s, x)} ds \right) e^{A(t, x)} \quad (2.39)$$

with $A(t, x) = \int_0^t a(s, x) ds$.

Using now the exponential upper bounds of $\Phi(t, x)$ and $T(t, x)$ given in (2.35) and (2.37) respectively,

$$a(t, x) \leq \widehat{a}(t) = \beta_2 \|\Phi_0\|_{C^0(\overline{\Omega})} e^{-\beta_2 N_0^{\min} t} + \beta_1 M e^{-\mu t},$$

$$b(t, x) \leq \widehat{b}(t) = \alpha M e^{-\mu t} + \delta \|\Phi_0\|_{C^0(\overline{\Omega})} e^{-\beta_2 N_0^{\min} t} M e^{-\mu t},$$

and then,

$$A(t, x) = \int_0^t a(s, x) ds \leq \int_0^t \widehat{a}(s) ds \leq C_1 \quad \text{and} \quad \int_0^t b(s, x) e^{-A(s, x)} ds \leq C_2.$$

Hence, we conclude that there exists a constant $N_{\max} > 0$ such that $N(t, x) \leq N_{\max} \forall (t, x) \in [0, +\infty) \times \overline{\Omega}$. Since $N(t, x)$ is increasing, it holds that there exists $N_*(x) \leq N_{\max}$ such that $N(t, x) \rightarrow N_*(x) \leq N_{\max}$ pointwise in space when $t \rightarrow +\infty$.

□

Our third result shows that when β_1 is large with respect to ρ (that is, destruction of tumor by necrosis dominates to tumor growth), then the tumor tends to the extinction. For that, we need to introduce some notation. Given $b \in L^\infty(\Omega)$ we denote by $\lambda_1(-\Delta + b)$ the first eigenvalue of the problem

$$\begin{cases} -\Delta u + b(x)u = \lambda u & \text{in } \Omega, \\ \frac{\partial u}{\partial n} = 0 & \text{on } \partial\Omega. \end{cases}$$

2. Theoretical analysis for a PDE-ODE system with linear diffusion related to a Glioblastoma tumor with vasculature

Lemma 2.14. *Given a classical solution (T, N, Φ) of (2.1)-(2.3) such that $N_0(x) > 0$ for all $x \in \bar{\Omega}$ and assume that*

$$\rho < \lambda_1(-\Delta + \beta_1 N_0(x)). \quad (2.40)$$

Then, for all $t \geq 0$:

$$\|T(t, \cdot)\|_{C^0(\bar{\Omega})} \leq \|T_0\|_{C^0(\bar{\Omega})} e^{-(\lambda_1(-\Delta + \beta_1 N_0(x)) - \rho)t} \quad \forall t > 0$$

and there exists $0 < \mu_ < \beta_2 N_0^{\min}$ and $t_* > 0$ large enough, such that*

$$\|\Phi(t, \cdot)\|_{C^0(\bar{\Omega})} \leq \|\Phi(t_*, \cdot)\|_{C^0(\bar{\Omega})} e^{-\mu_*(t-t_*)} \quad \forall t > t_*.$$

Moreover, there exists $N_{\max} > 0$ such that

$$N(t, x) \leq N_{\max} \quad \forall (t, x) \in [0, +\infty) \times \bar{\Omega}.$$

Proof. Since $N(t, x) \geq N_0(x)$ for all $x \in \bar{\Omega}$ and $t \geq 0$, and using the positivity of Φ and that $0 \leq P(\Phi, T) \leq 1$, we get

$$T_t - \Delta T \leq \rho T \left(1 - \frac{T}{K}\right) - \beta_1 N_0(x) T.$$

Hence,

$$T(x, t) \leq S(x, t) \quad \forall t \geq 0, \forall x \in \Omega, \quad (2.41)$$

where S is the unique positive solution of the classical logistic equation

$$\begin{cases} S_t - \Delta S + \beta_1 N_0(x) S = \rho S \left(1 - \frac{S}{K}\right) & t > 0, x \in \Omega, \\ S(x, 0) = T_0(x) & x \in \Omega, \\ \frac{\partial S}{\partial n} = 0 & t > 0, x \in \partial\Omega. \end{cases} \quad (2.42)$$

Now, it is known (see for instance [10]) that if ρ satisfies (2.40) then the problem (2.42) has a super solution with the form

$$\bar{S}(t, x) = \|T_0\|_{C^0(\bar{\Omega})} e^{-(\lambda_1(-\Delta + \beta_1 N_0(x)) - \rho)t} \varphi(x)$$

where $\varphi(x)$ is the positive eigenfunction associated with $\lambda_1(-\Delta + \beta_1 N_0(x))$ with $\|\varphi\|_\infty = 1$. Consequently, we have that

$$T(t, x) \leq S(t, x) \leq \bar{S}(t, x) \leq \|T_0\|_{C^0(\bar{\Omega})} e^{-(\lambda_1(-\Delta + \beta_1 N_0(x)) - \rho)t} \rightarrow 0 \quad (2.43)$$

as $t \rightarrow +\infty$ uniformly for $x \in \bar{\Omega}$.

2. Theoretical analysis for a PDE-ODE system with linear diffusion related to a Glioblastoma tumor with vasculature

Now, since $T, N, \Phi \geq 0$, we can bound $f_3(T, N, \Phi)$ as follows:

$$f_3(T, N, \Phi) \leq \frac{\gamma}{K} T \Phi \left(1 - \frac{T + N + \Phi}{K}\right) - \beta_2 N \Phi \leq \Phi \left(\frac{\gamma}{K} T - \beta_2 N\right) \leq \Phi \left(\frac{\gamma}{K} T - \beta_2 N_0(x)\right).$$

Since $N_0(x) > 0$ for all $x \in \bar{\Omega}$ and using (2.43), there exists $t_* > 0$ large enough such that for all $t \geq t_*$, $f_3(T, N, \Phi) \leq -\mu_* \Phi$ with $0 < \mu_* < \beta_2 N_0^{\min}$. Hence, Φ satisfies the differential inequality problem

$$\begin{cases} \frac{\partial \Phi}{\partial t} \leq -\mu_* \Phi & \text{in } [t_*, +\infty) \times \bar{\Omega}, \\ \Phi(t_*, x) = \|\Phi(t_*, \cdot)\|_{C^0(\bar{\Omega})} & \text{in } \bar{\Omega}. \end{cases} \quad (2.44)$$

Solving (2.44), we conclude that

$$\Phi(t, x) \leq \|\Phi(t_*, \cdot)\|_{C^0(\bar{\Omega})} e^{-\mu_*(t-t_*)}. \quad (2.45)$$

In particular, $\Phi(t, x) \rightarrow 0$ as $t \rightarrow +\infty$ uniformly in $x \in \bar{\Omega}$.

Using now the exponential upper bounds of $\Phi(t, x)$ and $T(t, x)$ given in (2.45) and (2.43) respectively, we can obtain an uniform upper bound in time and space for $N(t, x)$ using the same argument that in (2.38) with the following estimates

$$\begin{aligned} a(t, x) &\leq \hat{a}(t) = \beta_2 \|\Phi(t_*, \cdot)\|_{C^0(\bar{\Omega})} e^{-\mu_*(t-t_*)} + \beta_1 \|T_0\|_{C^0(\bar{\Omega})} e^{-(\lambda_1(-\Delta + \beta_1 N_0(x)) - \rho)t}, \\ b(t, x) &\leq \hat{b}(t) = \alpha \|T_0\|_{C^0(\bar{\Omega})} e^{-(\lambda_1(-\Delta + \beta_1 N_0(x)) - \rho)t} \\ &\quad + \delta \|\Phi(t_*, \cdot)\|_{C^0(\bar{\Omega})} e^{-\mu_*(t-t_*)} \|T_0\|_{C^0(\bar{\Omega})} e^{-(\lambda_1(-\Delta + \beta_1 N_0(x)) - \rho)t} \end{aligned}$$

and then,

$$A(t, x) = \int_{t_*}^t a(s, x) ds \leq \int_{t_*}^t \hat{a}(s) ds \leq C_1 \quad \text{and} \quad \int_{t_*}^t b(s, x) e^{-A(s, x)} ds \leq C_2.$$

With a similar reasoning to the used in Lemma 2.13 we conclude the existence of $N_* \in L^\infty(\Omega)$ and $N_{\max} > 0$ such that $N(t, x) \rightarrow N_*(x) \leq N_{\max}$ pointwise in space when $t \rightarrow +\infty$. \square

Remark 2.8. It is well-known that the map $\beta_1 \mapsto \lambda_1(-\Delta + \beta_1 N_0(x))$ is continuous and increasing. Moreover, if $N_0(x) > 0$ for $x \in \bar{\Omega}$ we have that $\lambda_1(-\Delta + \beta_1 N_0(x)) \rightarrow \infty$ as $\beta_1 \rightarrow \infty$. Hence, given $\rho > 0$ there exists $\beta_0(\rho) > 0$ large enough such that for $\beta_1 \geq \beta_0(\rho)$, condition (2.40) holds, and then the tumor tends to zero.

Corollary 2.5. Assume hypotheses of Lemma 2.13 or Lemma 2.14 and given $N_*(x) \in C^0(\bar{\Omega})$ such that $N_*(x) \geq N_*^{\min} > 0 \forall x \in \bar{\Omega}$, then the semi-trivial steady solution $(0, N_*, 0)$ is locally stable in $C^0(\bar{\Omega})$.

2. Theoretical analysis for a PDE-ODE system with linear diffusion related to a Glioblastoma tumor with vasculature

Proof. Let $\epsilon > 0$ and $\|T_0\|_{C^0(\bar{\Omega})}$, $\|\Phi_0\|_{C^0(\bar{\Omega})}$, $\|N_0 - N_*\|_{C^0(\bar{\Omega})} \leq \bar{\delta}$ for $\bar{\delta} > 0$ to choice in function of ϵ . Following the same argument that in Lemma 2.13 or Lemma 2.14, it is possible to prove that $\|T(t, \cdot)\|_{C^0(\bar{\Omega})}$, $\|\Phi(t, \cdot)\|_{C^0(\bar{\Omega})}$, $\|N(t, \cdot) - N_*\|_{C^0(\bar{\Omega})} \leq \epsilon$ for all $t \geq 0$. \square

In the following result, we are able to know the long time behaviour of the system (2.1)-(2.3) when $N_0(x)$ is close to the capacity K .

Lemma 2.15. *Let $\epsilon > 0$ small enough such that $N_0(x) \geq K - \epsilon$ for all $x \in \bar{\Omega}$. Then, the classical solution (T, N, Φ) of (3.1)-(3.3) satisfies*

$$T(t, x) \leq \|T_0\|_{C^0(\bar{\Omega})} e^{-\left(\beta_1(K-\epsilon) - \rho \frac{\epsilon}{K}\right) t},$$

$$\Phi(t, x) \leq \|\Phi_0\|_{C^0(\bar{\Omega})} e^{-\left(\beta_2(K-\epsilon) - \gamma \frac{\epsilon}{K}\right) t},$$

for all $(t, x) \in [0, +\infty) \times \bar{\Omega}$. In particular, if $\rho \frac{\epsilon}{K} - \beta_1(K - \epsilon) < 0$ and $\gamma \frac{\epsilon}{K} - \beta_2(K - \epsilon) < 0$ we get that $T(t, x), \Phi(t, x) \rightarrow 0$ uniformly in x as $t \rightarrow +\infty$. Finally, there exists N_{\max} such that $N(t, x) \leq N_{\max}$ for all $(t, x) \in [0, +\infty) \times \bar{\Omega}$.

Proof. Since N is increasing, we get

$$N(t, x) \geq N_0(x) > K - \epsilon \quad \forall t \geq 0, \quad \forall x \in \bar{\Omega}.$$

Using now that $T, \Phi \geq 0$,

$$1 - \frac{T + N + \Phi}{K} \leq 1 - \frac{N}{K} < 1 - \frac{K - \epsilon}{K} = \frac{\epsilon}{K}.$$

Therefore, T satisfies

$$\frac{\partial T}{\partial t} - \Delta T = f_1(T, N, \Phi) \leq \rho T \frac{\epsilon}{K} - \beta_1(K - \epsilon) T = \left(\rho \frac{\epsilon}{K} - \beta_1(K - \epsilon)\right) T.$$

In particular, $T \leq S$, where S is the unique solution of the following problem

$$\begin{cases} \frac{\partial S}{\partial t} - \Delta S = -\left(\beta_1(K - \epsilon) - \rho \frac{\epsilon}{K}\right) S & \text{in } [0, +\infty) \times \bar{\Omega}, \\ S(0, x) = \|T_0\|_{C^0(\bar{\Omega})} & \text{in } \Omega, \\ \frac{\partial S}{\partial n} \Big|_{\partial\Omega} = 0. \end{cases} \quad (2.46)$$

Solving (2.46) we conclude that

2. Theoretical analysis for a PDE-ODE system with linear diffusion related to a Glioblastoma tumor with vasculature

$$T(t, x) \leq S(t, x) = \|T_0\|_{C^0(\bar{\Omega})} e^{-\left(\beta_1(K-\epsilon) - \rho \frac{\epsilon}{K}\right)t}.$$

Therefore, if $\left(\rho \frac{\epsilon}{K} - \beta_1(K - \epsilon)\right) < 0$, then, $S(t, x)$ satisfies that

$$T(t, x) \leq S(t, x) = \|T_0\|_{C^0(\bar{\Omega})} e^{-\left(\beta_1(K-\epsilon) - \rho \frac{\epsilon}{K}\right)t} \rightarrow 0 \quad (2.47)$$

uniformly for $x \in \bar{\Omega}$ as $t \rightarrow +\infty$.

On the other hand, since $T \leq K$ and $N \geq K - \epsilon$, we get

$$f_3(T, N, \Phi) \leq \frac{\gamma}{K} T \Phi \frac{\epsilon}{K} - \beta_2(K - \epsilon) \Phi \leq \left(\gamma \frac{\epsilon}{K} - \beta_2(K - \epsilon)\right) \Phi.$$

Hence, we deduce that Φ satisfies

$$\begin{cases} \frac{\partial \Phi}{\partial t} \leq -\left(\beta_2(K - \epsilon) - \gamma \frac{\epsilon}{K}\right) \Phi \text{ in } [0, +\infty) \times \bar{\Omega}, \\ \Phi(0, x) \leq \|\Phi_0\|_{C^0(\bar{\Omega})} \text{ in } \bar{\Omega}. \end{cases} \quad (2.48)$$

As consequence, if $\left(\gamma \frac{\epsilon}{K} - \beta_2(K - \epsilon)\right) < 0$,

$$\Phi(t, x) \leq \|\Phi_0\|_{C^0(\bar{\Omega})} e^{-\left(\beta_2(K-\epsilon) - \gamma \frac{\epsilon}{K}\right)t} \rightarrow 0 \quad (2.49)$$

as $t \rightarrow +\infty$ uniformly for $x \in \bar{\Omega}$.

Finally, we can obtain an uniform upper bound in time and space for $N(t, x)$ using the same argument that in (2.38). Now, using the upper bound for $T(t, x)$ and $\Phi(t, x)$ given in (2.47) and (2.49) one has,

$$a(t, x) \leq \hat{a}(t) = \beta_2 \|\Phi_0\|_{C^0(\bar{\Omega})} e^{-\left(\beta_2(K-\epsilon) - \gamma \frac{\epsilon}{K}\right)t} + \beta_1 \|T_0\|_{C^0(\bar{\Omega})} e^{-\left(\beta_1(K-\epsilon) - \rho \frac{\epsilon}{K}\right)t},$$

hence,

$$\int_0^t a(s, x) ds \leq \hat{A}(t) = \int_0^t \hat{a}(s) ds \leq C_1,$$

and

$$\begin{aligned} b(t, x) \leq \hat{b}(t) &= \alpha \|T_0\|_{C^0(\bar{\Omega})} e^{-\left(\beta_1(K-\epsilon) - \rho \frac{\epsilon}{K}\right)t} \\ &+ \delta \|\Phi_0\|_{C^0(\bar{\Omega})} e^{-\left(\beta_2(K-\epsilon) - \gamma \frac{\epsilon}{K}\right)t} \|T_0\|_{C^0(\bar{\Omega})} e^{-\left(\beta_1(K-\epsilon) - \rho \frac{\epsilon}{K}\right)t}, \end{aligned}$$

2. Theoretical analysis for a PDE-ODE system with linear diffusion related to a Glioblastoma tumor with vasculature

hence,

$$\int_0^t b(s, x) e^{-A(s, x)} \leq C_2.$$

With a similar reasoning to the used in Lemmas 2.13 and 2.14 we conclude the existence of $N_* \in L^\infty(\Omega)$ and $N_{\max} > 0$ such that $N(t, x) \rightarrow N_*(x) \leq N_{\max}$ pointwisely in space when $t \rightarrow +\infty$. \square

Corollary 2.6. Assume hypotheses of Lemma 2.15 and given $N_* \in C^0(\bar{\Omega})$ such that $N_*(x) \geq N_*^{\min} \geq K - \epsilon$ with $\epsilon > 0$ small enough, then the semi-trivial steady solution $(0, N_*(x), 0)$ is locally stable in $C^0(\bar{\Omega})$

Proof. Using the argument of Lemma 2.15, it is similar to the proof of Corollary 2.5. \square

2.3.3 Numerical Simulations

In order to see the asymptotic behaviour of problem (2.1) with the boundary condition (2.2) graphically, we will show three numerical simulations for different initial conditions in the domain $\Omega = (-2, 2)^2$. In all of them, we have considered the constant initial vasculature $\Phi_0(x) = 0.5$ and initial necrosis zero, $N_0(x) = 0$ for all $x \in \bar{\Omega}$. The parameters are taken as:

Parameter	ρ	α	β_1	β_2	γ	δ	K
Value	1	0.03	0.03	0.03	0.003	0.3	1

Table 2.1: Parameter values.

Note that hypothesis (2.33) is satisfied, hence tumor and vasculature will vanish at infinity time. Indeed, starting with the different initial conditions for the tumor given in Figure 2.1:

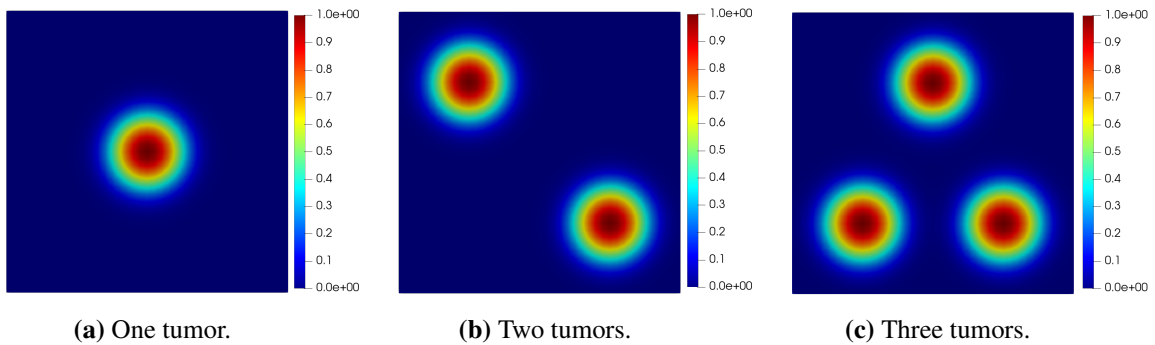


Figure 2.1: Initial tumor.

we obtain the different equilibrium solutions for the necrosis given in Figure 2.2:

2. Theoretical analysis for a PDE-ODE system with linear diffusion related to a Glioblastoma tumor with vasculature

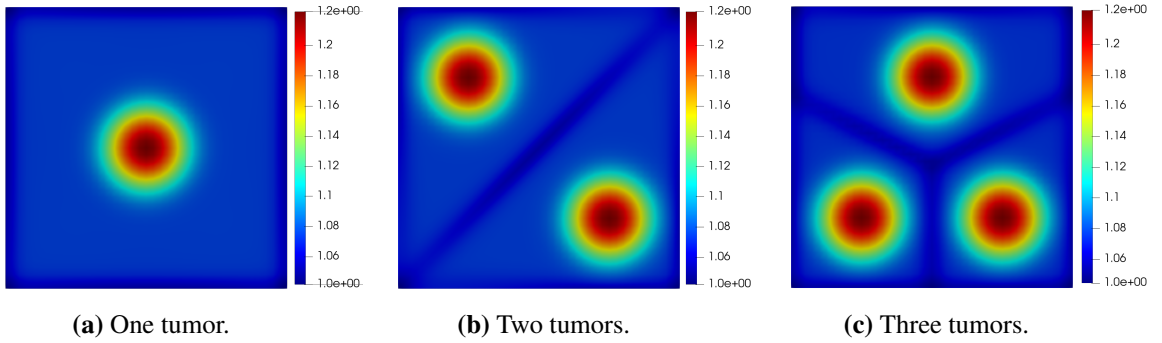


Figure 2.2: Final necrosis.

We observe as necrosis occupies all the domain but mainly where the tumor was initially, and tumor and vasculature disappear in all the cases. Moreover, the maximum value of necrosis is the same in each simulation.

In order to see the importance of hypothesis (2.33), now we consider the value of the parameters as follows:

Parameter	ρ	α	β_1	β_2	γ	δ	K
Value	1	0.03	0.03	0.03	0.3	0.03	1

Table 2.2: Parameter values.

where (2.33) is not satisfied. Then, starting with the same initial conditions for the tumor given in Figure 2.1, we obtain the different equilibrium solutions for the necrosis given in Figure 2.3:

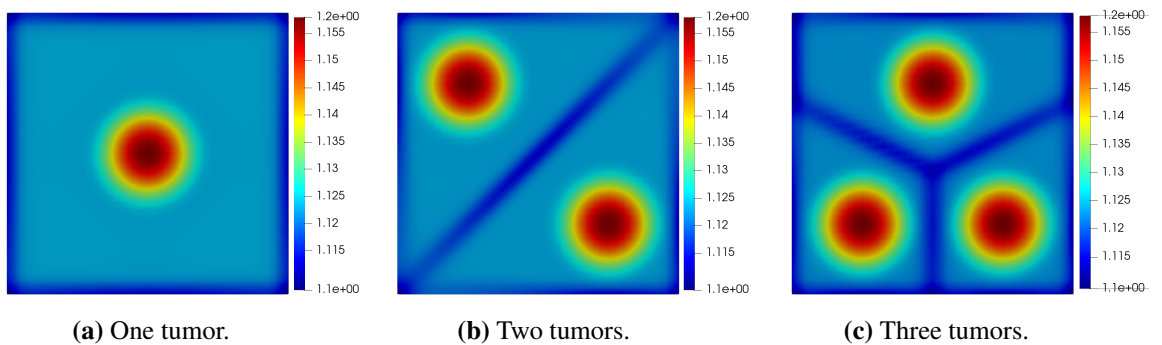


Figure 2.3: Final necrosis.

We observe a similar behaviour that in Figure 2.2.

2.4 Conclusions

In this Chapter we have completed the model studied in [46] introducing a new variable, the vasculature, giving rise a more realistic model. Thus, after the theoretical and numerical study made of (2.1)-(2.3), we can conclude:

1. The model (2.1) is well-posed: we have proved that there exists an unique global in time classical solution of the model.
2. The long time behaviour of (2.1)-(2.3) asserts that vasculature always disappears and, under conditions on the parameters of the problem, tumor proliferative also disappears. Moreover, we show numerical simulations that highlight our results.

Theoretical and numerical analysis for a hybrid tumor model with nonlinear diffusion depending on vasculature

In this Chapter we investigate the nonlinear parabolic PDE-ODE system considered in the introduction (1.1) for $\kappa = 0$. In particular,

$$\left\{ \begin{array}{l} \frac{\partial T}{\partial t} - \nabla \cdot ((\kappa_1 P(\Phi, T) + \kappa_0) \nabla T) = f_1(T, N, \Phi) \quad \text{in } (0, T_f) \times \Omega \\ \frac{\partial N}{\partial t} = f_2(T, N, \Phi) \quad \text{in } (0, T_f) \times \Omega \\ \frac{\partial \Phi}{\partial t} = f_3(T, N, \Phi) \quad \text{in } (0, T_f) \times \Omega \end{array} \right. \quad (3.1)$$

endowed with non-flux boundary condition

$$-(\kappa_1 P(\Phi, T) + \kappa_0) \nabla T \cdot n = 0 \quad (3.2)$$

where n is the outward unit normal vector to $\partial\Omega$ and initial conditions

$$T(0, \cdot) = T_0, \quad N(0, \cdot) = N_0, \quad \Phi(0, \cdot) = \Phi_0 \quad \text{in } \Omega \quad (3.3)$$

and where $\Omega \subset \mathbb{R}^3$ is a smooth bounded domain and $T_f > 0$ the final time. The nonlinear reaction terms $f_i : \mathbb{R}^3 \rightarrow \mathbb{R}$ for $i = 1, 2, 3$ of (3.1) have the same definition that in (2.4) with the factor $P(\Phi, T)$

3. Theoretical and numerical analysis for a hybrid tumor model with nonlinear diffusion depending on vasculature

defined by:

$$P(\Phi, T) = \frac{\Phi_+}{\left(\frac{\Phi_+ + K}{2}\right) + T_+}. \quad (3.4)$$

The outline of the Chapter is as follows. In Section 3.1, we present preliminary results which we will use along the study of system (3.1)-(3.3). In Section 3.2 we prove the existence of weak-strong solutions of (3.1)-(3.3). Section 3.3 is dedicated to the long time behaviour of the solution. Finally, in Section 3.4 we present a numerical scheme of our model (3.1)-(3.3) which preserves the same estimates as the continuous model.

The results of this Chapter have been published in [25].

3.1 Preliminaries

In this Section we include some necessary results to study the existence of solutions of the system (3.1)-(3.3).

The continuity and locally lipschitz condition of functions $P(\Phi, T)$ and $f_i(T, N, \Phi)$ for $i = 1, 2, 3$ are proved in Lemma 2.2 of Chapter 2.

In order to define the concepts of weak and strong solution for a parabolic problem, we introduce the following “weak” space

$$\mathcal{W}_2 = \left\{ u \in L^\infty(0, T_f; L^2(\Omega)) \cap L^2(0, T_f; H^1(\Omega)) : u_t \in L^2\left(0, T_f; (H^1(\Omega))'\right) \right\}, \quad (3.5)$$

and the “strong” space

$$\mathcal{S}_2 = \left\{ u \in L^\infty(0, T_f; H^1(\Omega)) \cap L^2(0, T_f; H^2(\Omega)), u_t \in L^2(0, T_f; L^2(\Omega)) \right\}. \quad (3.6)$$

\mathcal{W}_2 and \mathcal{S}_2 are Banach spaces with the respective norms:

$$\|u\|_{\mathcal{W}_2} = \|u\|_{L^\infty(0, T_f; L^2(\Omega))} + \|u\|_{L^2(0, T_f; H^1(\Omega))} + \|u_t\|_{L^2(0, T_f; (H^1(\Omega))')},$$

$$\|u\|_{\mathcal{S}_2} = \|u\|_{L^\infty(0, T_f; H^1(\Omega))} + \|u\|_{L^2(0, T_f; H^2(\Omega))} + \|u_t\|_{L^2(0, T_f; L^2(\Omega))}.$$

Thus, we can use the following result about existence and uniqueness of weak and strong solution for a linear parabolic problem, see for instance [20].

3. Theoretical and numerical analysis for a hybrid tumor model with nonlinear diffusion depending on vasculature

Theorem 3.1. Given $\Omega \subseteq \mathbb{R}^3$ a bounded open set and $(0, T_f)$ a time interval for a fixed time $T_f > 0$, we consider the following linear parabolic problem

$$\begin{cases} u_t + L u = f & \text{in } (0, T_f) \times \Omega, \\ u(0, \cdot) = u_0 & \text{in } \Omega, \\ \left. \frac{\partial u}{\partial n} \right|_{\partial\Omega} = 0 & \text{on } (0, T_f) \times \partial\Omega \end{cases} \quad (3.7)$$

where $f \in L^2(0, T_f; L^2(\Omega))$,

$$L u = - \sum_{i,j=1}^3 (a_{ij}(t, x) u_{x_j})_{x_i} + \sum_{i=1}^3 b_i(t, x) u_{x_i} + c(t, x) u$$

denotes a second-order partial elliptic differential operator with $a_{ij}, b_i, c \in L^\infty(0, T_f; L^\infty(\Omega))$, $a_{ij} = a_{ji}$ and there exists $C > 0$ such that

$$\sum_{i,j=1}^3 a_{ij}(t, x) p_i p_j \geq C \|p\|^2, \quad \text{a.e. } (t, x) \in (0, T_f) \times \Omega, \quad \forall p \in \mathbb{R}^3.$$

Then:

a) For every $u_0 \in L^2(\Omega)$, (3.7) has an unique weak solution $u \in \mathcal{W}_2$ and

$$\|u\|_{\mathcal{W}_2} \leq C \left(\|u_0\|_{L^2(\Omega)}, \|f\|_{L^2(0, T_f; L^2(\Omega))} \right).$$

b) Assume $a_{ij} = \delta_{ij}$ (Kronecker delta) for $i, j = 1, 2, 3$ hence

$$L u = -\Delta u + \sum_{i=1}^3 b_i(t, x) u_{x_i} + c(t, x) u.$$

Then, for every $u_0 \in H^1(\Omega)$, (3.7) has an unique strong solution $u \in \mathcal{S}_2$ and

$$\|u\|_{\mathcal{S}_2} \leq C \left(\|u_0\|_{H^1(\Omega)}, \|f\|_{L^2(0, T_f; L^2(\Omega))} \right).$$

3.2 Existence of Solution of Problem (3.1)-(3.3)

First of all, we define the concept of solution used in this Chapter.

3. Theoretical and numerical analysis for a hybrid tumor model with nonlinear diffusion depending on vasculature

Definition 3.1 (Weak-Strong solution of (3.1)-(3.3)). Given $T_0 \in L^\infty(\Omega)$ and $N_0, \Phi_0 \in H^1(\Omega) \cap L^\infty(\Omega)$ satisfying (2.7), then (T, N, Φ) is called a weak-strong solution of problem (3.1)-(3.3) if $T \in \mathcal{W}_2$, $N, \Phi \in L^\infty(0, T_f; H^1(\Omega))$, $N_t, \Phi_t \in L^2(0, T_f; L^2(\Omega))$ and they satisfy

$$\int_0^{T_f} \langle T_t, v \rangle_{(H^1(\Omega))'} dt + \int_0^{T_f} \int_\Omega (\kappa_1 P(\Phi, T) + \kappa_0) \nabla T \cdot \nabla v \, dx \, dt = \int_0^{T_f} \int_\Omega f_1(T, N, \Phi) v \, dx \, dt,$$

$\forall v \in L^2(0, T_f; H^1(\Omega))$ and

$$\begin{cases} N_t = f_2(T, N, \Phi) \\ \Phi_t = f_3(T, N, \Phi) \end{cases} \quad \text{a.e. in } (0, T_f) \times \Omega$$

and the boundary and initial conditions (3.2) and (3.3) are satisfied by T and (T, N, Φ) , respectively.

3.2.1 Truncated problem

In order to obtain a solution of (3.1)-(3.3), we define the following truncated system of (3.1):

$$\begin{cases} \frac{\partial T}{\partial t} - \nabla \cdot ((\kappa_1 P(\Phi_+^K, T_+^K) + \kappa_0) \nabla T) = f_1(T_+^K, N_+^{C(T_f)}, \Phi_+^K) \\ \frac{\partial N}{\partial t} = f_2(T_+^K, N_+^{C(T_f)}, \Phi_+^K) \\ \frac{\partial \Phi}{\partial t} = f_3(T_+^K, N_+^{C(T_f)}, \Phi_+^K) \end{cases} \quad (3.8)$$

subject to (3.2) and (3.3). We have denoted T_+^K as in (2.12) and similar to Φ_+^K and $N_+^{C(T_f)}$ with $C(T_f)$ an exponential positive constant which depends on the final time $T_f > 0$ and the carrying capacity K (see Lemma 2.5 of Chapter 2).

Once we obtain the existence of solution of the truncated problem (3.8), we will prove that this solution is also a positive solution of (3.1)-(3.3), due to the following estimates for any possible weak-strong solution of (3.8).

Lemma 3.1. Any weak-strong solution (T, N, Φ) of (3.8) with initial data satisfying (2.7) satisfies the following bounds:

a) Pointwise estimates:

$$0 \leq T, \Phi \leq K \quad \text{and} \quad 0 \leq N \leq C(T_f), \quad \text{a.e. in } (0, T_f) \times \Omega. \quad (3.9)$$

3. Theoretical and numerical analysis for a hybrid tumor model with nonlinear diffusion depending on vasculature

b) *Energy estimates:*

$$\|T\|_{L^\infty(0,T_f;L^2(\Omega))} + \|T\|_{L^2(0,T_f;H^1(\Omega))} \leq C (\|T_0\|_{L^2(\Omega)}, K, |\Omega|, T_f).$$

Proof. a) Let (T, N, Φ) a weak-strong solution of (3.8). Since one can rewrite

$$f_1(T, N, \Phi) = T \tilde{f}_1(T, N, \Phi),$$

multiplying the first equation of (3.8) by T_- and integrating in Ω , we get

$$\begin{aligned} & \frac{1}{2} \frac{d}{dt} \int_{\Omega} (T_-)^2 dx + \int_{\Omega} (\kappa_1 P(\Phi_+^K, T_+^K) + \kappa_0) |\nabla T_-|^2 dx \\ &= \int_{\Omega} T_- T_+^K \tilde{f}_1(T_+^K, N_+^{C(T_f)}, \Phi_+^K) dx = 0, \quad \text{a.e. in } (0, T_f). \end{aligned}$$

Hence, since $T_-(0, x) = 0$, then $T_-(t, x) = 0$ a.e. $(t, x) \in (0, T_f) \times \Omega$. To obtain the upper bound $T \leq K$, we multiply the first equation of (3.8) by $(T - K)_+$ and integrate in Ω

$$\begin{aligned} & \frac{1}{2} \frac{d}{dt} \int_{\Omega} ((T - K)_+)^2 dx + \int_{\Omega} (\kappa_1 P(\Phi_+^K, T_+^K) + \kappa_0) |\nabla (T - K)_+|^2 dx \\ &= \int_{\Omega} f_1(T_+^K, N_+^{C(T_f)}, \Phi_+^K) (T - K)_+ dx, \quad \text{a.e. in } (0, T_f). \end{aligned}$$

Since $f_1(T_+^K, N_+^{C(T_f)}, \Phi_+^K) \leq \rho T_+^K (1 - \frac{T_+^K}{K})$, then

$$f_1(T_+^K, N_+^{C(T_f)}, \Phi_+^K) (T - K)_+ \leq \rho T_+^K \left(1 - \frac{T_+^K}{K}\right) (T - K)_+ = 0.$$

Since $(T(0, x) - K)_+ = 0$, then $(T(t, x) - K)_+ = 0$ a.e. $(t, x) \in (0, T_f) \times \Omega$.

For the corresponding bounds of N and Φ given in (3.9), we can use the same argument as in Lemma 2.2 of Chapter 2.

b) Using the pointwise bounds for (T, N, Φ) given in a), multiplying the first equation of (3.8) by T and integrating in Ω , we get

$$\begin{aligned} & \frac{1}{2} \frac{d}{dt} \int_{\Omega} T^2 dx + \int_{\Omega} (\kappa_1 P(\Phi_+^K, T_+^K) + \kappa_0) |\nabla T|^2 dt dx = \int_{\Omega} T^2 \tilde{f}_1(T, N, \Phi) \\ & \leq \int_{\Omega} \rho T^2 dx \leq \rho K^2 |\Omega|. \end{aligned}$$

Integrating in time, the proof is finished. □

3. Theoretical and numerical analysis for a hybrid tumor model with nonlinear diffusion depending on vasculature

By Lemma 3.1 a), for any (T, N, Φ) a weak-strong solution of (3.8), we deduce that $T_+^K = T$, $N_+^{C(T_f)} = N$ and $\Phi_+^K = \Phi$ and then, $f_i \left(T_+^K, N_+^{C(T_f)}, \Phi_+^K \right) = f_i(T, N, \Phi)$ for $i = 1, 2, 3$. Hence, we obtain the following crucial corollary

Corollary 3.1. *If (T, N, Φ) is a weak-strong solution of the truncated problem (3.8), then (T, N, Φ) is also a weak-strong solution of (3.1)-(3.3) and (T, N, Φ) satisfies the pointwise bounds (3.9).*

3.2.2 Existence of Weak-Strong Solution of Problem (3.8)

Theorem 3.2. *There exists a weak-strong solution (T, N, Φ) of (3.8) in the sense of Definition 3.1*

Remark 3.1. *We can not guarantee the uniqueness of the weak-strong solution of (3.1)-(3.3) due to T is not sufficiently regular by the influence of the nonlinear diffusion. Notice that, unlike in Chapter 2 and due to nonlinear diffusion, we are not able to prove that T is a pointwise solution of (3.1).*

Proof. The proof of this theorem follows the next steps:

1. Regularize the problem via an artificial diffusion with parameter $\epsilon > 0$ for (N, Φ) .
2. Solve the regularized problem for any fixed value of ϵ .
3. Taking limits $\epsilon \rightarrow 0$ to get solution of the non-regularized problem (3.8).

Step 1. Regularizing the problem (3.8)

We will study the following family of regularized problems related to system (3.8). For any $\epsilon > 0$. We define $(T_\epsilon, N_\epsilon, \Phi_\epsilon)$ as the solution of

$$\left\{ \begin{array}{l} \frac{\partial T}{\partial t} - \nabla \cdot ((\kappa_1 P(\Phi_+^K, T_+^K) + \kappa_0) \nabla T) = f_1 \left(T_+^K, N_+^{C(T_f)}, \Phi_+^K \right) \\ \frac{\partial N}{\partial t} - \epsilon \Delta N = f_2 \left(T_+^K, N_+^{C(T_f)}, \Phi_+^K \right) \\ \frac{\partial \Phi}{\partial t} - \epsilon \Delta \Phi = f_3 \left(T_+^K, N_+^{C(T_f)}, \Phi_+^K \right) \end{array} \right. \quad (3.10)$$

with the boundary conditions

$$\frac{\partial T}{\partial n} \Big|_{\partial \Omega} = \epsilon \frac{\partial N}{\partial n} \Big|_{\partial \Omega} = \epsilon \frac{\partial \Phi}{\partial n} \Big|_{\partial \Omega} = 0 \quad (3.11)$$

and the initial conditions

$$T|_{t=0} = T_0, \quad N|_{t=0} = N_0, \quad \Phi|_{t=0} = \Phi_0 \quad \text{in } \Omega. \quad (3.12)$$

Now, we can define the kind of solution which we will obtain

3. Theoretical and numerical analysis for a hybrid tumor model with nonlinear diffusion depending on vasculature

Definition 3.2 (Weak-Strong solution of (3.10)-(3.12)). *Given $T_0 \in L^\infty(\Omega)$ and $N_0, \Phi_0 \in L^\infty(\Omega) \cap H^1(\Omega)$, then (T, N, Φ) is called a weak-strong solution of problem (3.10)-(3.12) if $T \in \mathcal{W}_2$ and $N, \Phi \in \mathcal{S}_2$ and they satisfy*

$$\begin{aligned} & \int_0^{T_f} \langle T_t, v \rangle_{(H^1(\Omega))'} dt + \int_0^{T_f} \int_\Omega (\kappa_1 P(\Phi_+^K, T_+^K) + \kappa_0) \nabla T \cdot \nabla v \, dx \, dt \\ & = \int_0^{T_f} \int_\Omega f_1(T_+^K, N_+^{C(T_f)}, \Phi_+^K) v \, dx \, dt, \end{aligned}$$

$\forall v \in L^2(0, T_f; H^1(\Omega))$, the PDE system

$$\begin{cases} N_t - \epsilon \Delta N = f_2(T_+^K, N_+^{C(T_f)}, \Phi_+^K) \\ \Phi_t - \epsilon \Delta \Phi = f_3(T_+^K, N_+^{C(T_f)}, \Phi_+^K) \end{cases} \quad \text{a.e. in } (0, T_f) \times \Omega$$

and the boundary and initial conditions (3.11) and (3.12).

Remark 3.2. *It is easy to prove for T and Φ the estimates (3.9) following the same argument as in Lemma 3.1. For N , the following differential inequality is satisfied*

$$\frac{\partial N}{\partial t} - \epsilon \Delta N \leq C_1 + C_2 N. \quad (3.13)$$

Hence, $N \leq \tilde{N}$ where \tilde{N} is the solution of the ODE equation

$$\frac{\partial \tilde{N}}{\partial t} = C_1 + C_2 \tilde{N}.$$

Thus, any solution of (3.10)-(3.12) satisfies that

$$0 \leq T, \Phi \leq K, \quad 0 \leq N \leq C(T_f), \quad \text{a.e. in } (0, T_f) \times \Omega. \quad (3.14)$$

Theorem 3.3 (Existence of weak-strong solution of (3.10)-(3.12)). *There exists a weak-strong solution (T, N, Φ) of system (3.10)-(3.12) in the sense of Definition 3.2.*

3.2.2.1 Proof of Theorem 3.3

We define the following operator

$$\begin{aligned} \mathbf{R} : (L^2(0, T_f; L^2(\Omega)))^3 & \longrightarrow (L^2(0, T_f; L^2(\Omega)))^3 \\ (\tilde{T}, \tilde{N}, \tilde{\Phi}) & \longrightarrow (T, N, \Phi) = \mathbf{R}(\tilde{T}, \tilde{N}, \tilde{\Phi}) \end{aligned}$$

where (T, N, Φ) is the weak-strong solution of the linear and decoupled problem

3. Theoretical and numerical analysis for a hybrid tumor model with nonlinear diffusion depending on vasculature

$$\left\{ \begin{array}{l} \frac{\partial T}{\partial t} - \nabla \cdot \left((\kappa_1 P(\tilde{\Phi}_+^K, \tilde{T}_+^K) + \kappa_0) \nabla T \right) = f_1 \left(\tilde{T}_+^K, \tilde{N}_+^{C(T_f)}, \tilde{\Phi}_+^K \right) \\ \frac{\partial N}{\partial t} - \epsilon \Delta N = f_2 \left(\tilde{T}_+^K, \tilde{N}_+^{C(T_f)}, \tilde{\Phi}_+^K \right) \\ \frac{\partial \Phi}{\partial t} - \epsilon \Delta \Phi = f_3 \left(\tilde{T}_+^K, \tilde{N}_+^{C(T_f)}, \tilde{\Phi}_+^K \right) \end{array} \right. \quad (3.15)$$

subject to (3.11) and (3.12). Observe that thanks to (3.14), a weak-strong solution of (3.10)-(3.12) is a fixed point of \mathbf{R} . Therefore, we look for a fixed point of \mathbf{R} using Leray-Schauder's theorem 2.2.

Lemma 3.2. *The operator \mathbf{R} is well defined from $(L^2(0, T_f; L^2(\Omega)))^3$ to itself.*

Proof. Using (1.11),

$$0 \leq P \left(\left(\tilde{\Phi}(t, x) \right)_+^K, \left(\tilde{T}(t, x) \right)_+^K \right) \leq 1, \quad \text{a.e. } (t, x) \in (0, T_f) \times \Omega. \quad (3.16)$$

On the other hand, one has

$$\left\| f_i \left(\tilde{T}_+^K, \tilde{N}_+^{C(T_f)}, \tilde{\Phi}_+^K \right) \right\|_{L^\infty(0, T_f; L^\infty(\Omega))} \leq C_i \quad \forall i = 1, 2, 3, \quad (3.17)$$

with C_i independent of \tilde{T} , \tilde{N} and $\tilde{\Phi}$. Hence, we can apply Theorem 3.1 to conclude that there exists a unique weak solution of (3.15) with the following regularity

$$(T, N, \Phi) \in \mathcal{W}_2 \times \mathcal{S}_2 \times \mathcal{S}_2.$$

In particular,

$$(T, N, \Phi) \in (L^2(0, T_f; L^2(\Omega)))^3.$$

□

Lemma 3.3. *The operator \mathbf{R} is compact from $(L^2(0, T_f; L^2(\Omega)))^3$ to itself.*

Proof. Let $(\tilde{T}, \tilde{N}, \tilde{\Phi}) \in (L^2(0, T_f; L^2(\Omega)))^3$. Then, applying the same argument of Lemma 3.2 and estimates (3.16) and (3.17), we prove that there exists a unique $(T, N, \Phi) = \mathbf{R}(\tilde{T}, \tilde{N}, \tilde{\Phi})$ such that (T, N, Φ) is solution of (3.15) with the following estimates:

$$\begin{aligned} \|T\|_{\mathcal{W}_2} &\leq C \left(\|T_0\|_{L^2(\Omega)}, K, C(T_f) \right), \\ \|N\|_{\mathcal{S}_2} &\leq C \left(\|N_0\|_{L^2(\Omega)}, K, C(T_f) \right), \\ \|\Phi\|_{\mathcal{S}_2} &\leq C \left(\|\Phi_0\|_{L^2(\Omega)}, K, C(T_f) \right). \end{aligned} \quad (3.18)$$

3. Theoretical and numerical analysis for a hybrid tumor model with nonlinear diffusion depending on vasculature

Hence, (T, N, Φ) is bounded in $\mathcal{W}_2 \times \mathcal{S}_2 \times \mathcal{S}_2$. Applying Aubin-Lions Theorem, we conclude that the embedding

$$\mathcal{W}_2 \times \mathcal{S}_2 \times \mathcal{S}_2 \hookrightarrow (L^2(0, T_f; L^2(\Omega)))^3$$

is compact. Thus, \mathbf{R} is compact from $(L^2(0, T_f; L^2(\Omega)))^3$ to itself. □

Lemma 3.4. *The operator $\mathbf{R} : (L^2(0, T_f; L^2(\Omega)))^3 \rightarrow (L^2(0, T_f; L^2(\Omega)))^3$ is continuous.*

Proof. Given

$$(\tilde{T}_n, \tilde{N}_n, \tilde{\Phi}_n) \rightarrow (\tilde{T}, \tilde{N}, \tilde{\Phi}) \in (L^2((0, T_f); L^2(\Omega)))^3, \quad (3.19)$$

we are going to check that

$$(T_n, N_n, \Phi_n) := \mathbf{R}(\tilde{T}_n, \tilde{N}_n, \tilde{\Phi}_n) \rightarrow \mathbf{R}(\tilde{T}, \tilde{N}, \tilde{\Phi}) := (T, N, \Phi) \text{ in } (L^2((0, T_f); L^2(\Omega)))^3.$$

Since $(T_n, N_n, \Phi_n) = \mathbf{R}(\tilde{T}_n, \tilde{N}_n, \tilde{\Phi}_n)$ is solution of (3.15), from (3.18) we obtain that (T_n, N_n, Φ_n) is bounded in $\mathcal{W}_2 \times \mathcal{S}_2 \times \mathcal{S}_2$.

By Aubin-Lions Theorem the embeddings $\mathcal{W}_2 \hookrightarrow L^2(0, T_f; L^2(\Omega))$ and $\mathcal{S}_2 \hookrightarrow L^2(0, T_f; H^1(\Omega))$ are compact, hence there exists a subsequence $(T_{n_k}, N_{n_k}, \Phi_{n_k}) \in \mathcal{W}_2 \times \mathcal{S}_2 \times \mathcal{S}_2$ and a limit $(T^*, N^*, \Phi^*) \in \mathcal{W}_2 \times \mathcal{S}_2 \times \mathcal{S}_2$ such that

$$\mathbf{R}(\tilde{T}_{n_k}, \tilde{N}_{n_k}, \tilde{\Phi}_{n_k}) = (T_{n_k}, N_{n_k}, \Phi_{n_k}) \rightharpoonup_{k \rightarrow \infty} (T^*, N^*, \Phi^*) \text{ weakly in } \mathcal{W}_2 \times \mathcal{S}_2 \times \mathcal{S}_2,$$

$$\mathbf{R}(\tilde{T}_{n_k}, \tilde{N}_{n_k}, \tilde{\Phi}_{n_k}) = (T_{n_k}, N_{n_k}, \Phi_{n_k}) \rightarrow_{k \rightarrow \infty} (T^*, N^*, \Phi^*) \text{ strongly in } (L^2(0, T_f, L^2(\Omega)))^3$$

and

$$(N_{n_k}, \Phi_{n_k}) \rightarrow_{k \rightarrow \infty} (N^*, \Phi^*) \text{ strongly in } (L^2(0, T_f, H^1(\Omega)))^2.$$

In particular,

$$((T_{n_k})_t, (N_{n_k})_t, (\Phi_{n_k})_t) \rightharpoonup_{k \rightarrow \infty} ((T^*)_t, (N^*)_t, (\Phi^*)_t) \text{ weakly in } \left(L^2(0, T_f; (H^1(\Omega))') \right)^3,$$

$$((N_{n_k})_t, (\Phi_{n_k})_t) \rightharpoonup_{k \rightarrow \infty} ((N^*)_t, (\Phi^*)_t) \text{ weakly in } (L^2(0, T_f; L^2(\Omega)))^2,$$

and

$$(\nabla T_{n_k}, \nabla N_{n_k}, \nabla \Phi_{n_k}) \rightharpoonup_{k \rightarrow \infty} (\nabla T^*, \nabla N^*, \nabla \Phi^*) \text{ weakly in } (L^2(0, T_f; L^2(\Omega)))^3.$$

Using the pointwise convergence

$$(\tilde{T}_n(t, x), \tilde{N}_n(t, x), \tilde{\Phi}_n(t, x)) \rightarrow (\tilde{T}(t, x), \tilde{N}(t, x), \tilde{\Phi}(t, x)), \quad \text{a.e. } (t, x) \in (0, T_f) \times \Omega$$

3. Theoretical and numerical analysis for a hybrid tumor model with nonlinear diffusion depending on vasculature

one also has

$$\left(\left(\tilde{T}_n(t, x) \right)_+^K, \left(\tilde{N}_n(t, x) \right)_+^{C(T_f)}, \left(\tilde{\Phi}_n(t, x) \right)_+^K \right) \rightarrow \left(\left(\tilde{T}(t, x) \right)_+^K, \left(\tilde{N}(t, x) \right)_+^{C(T_f)}, \left(\tilde{\Phi}(t, x) \right)_+^K \right)$$

a.e. $(t, x) \in (0, T_f) \times \Omega$.

Since $\left\| P \left(\tilde{\Phi}_+^K, \tilde{T}_+^K \right) \right\|_{L^\infty(0, T_f; L^\infty(\Omega))} \leq 1$ and $P \left(\tilde{\Phi}, \tilde{T} \right)$ is continuous in \mathbb{R}^2 , applying dominated convergence Theorem, we can deduce that

$$P \left(\left(\tilde{\Phi}_{n_k} \right)_+^K, \left(\tilde{T}_{n_k} \right)_+^K \right) \xrightarrow{k \rightarrow \infty} P \left(\tilde{\Phi}_+^K, \tilde{T}_+^K \right) \text{ in } L^p(0, T_f; L^p(\Omega)), \quad \forall p < \infty. \quad (3.20)$$

Since $\left\| f_1 \left(\tilde{T}_+^K, \tilde{N}_+^{C(T_f)}, \tilde{\Phi}_+^K \right) \right\|_{L^\infty(0, T_f; L^\infty(\Omega))} \leq C$ and (3.19), applying dominated convergence Theorem, we deduce that

$$f_i \left(\left(\tilde{T}_{n_k} \right)_+^K, \left(\tilde{N}_{n_k} \right)_+^{C(T_f)}, \left(\tilde{\Phi}_{n_k} \right)_+^K \right) \xrightarrow{k \rightarrow \infty} f_i \left(\tilde{T}_+^K, \tilde{N}_+^{C(T_f)}, \tilde{\Phi}_+^K \right)$$

in $L^p(0, T_f; L^p(\Omega))$ for all $p < \infty$ and for $i = 1, 2, 3$.

On the other hand, $\nabla T_{n_k} \rightharpoonup \nabla T^*$ weakly in $L^2(0, T_f; L^2(\Omega))$. Thus, we obtain

$P \left(\left(\tilde{\Phi}_{n_k} \right)_+^K, \left(\tilde{T}_{n_k} \right)_+^K \right) \nabla T_{n_k}$ is bounded in $L^2(0, T_f; L^2(\Omega))$. Consequently,

$$P \left(\left(\tilde{\Phi}_{n_k} \right)_+^K, \left(\tilde{T}_{n_k} \right)_+^K \right) \nabla T_{n_k} \rightharpoonup P \left(\tilde{\Phi}_+^K, \tilde{T}_+^K \right) \nabla T^* \text{ weakly in } (L^2(0, T_f; L^2(\Omega)))^3.$$

Thus, passing to the limit in the problem satisfied by $(T_{n_k}, N_{n_k}, \Phi_{n_k})$, we have that $(T^*, N^*, \Phi^*) = \mathbf{R} \left(\tilde{T}, \tilde{N}, \tilde{\Phi} \right)$ and since the solution $\mathbf{R} \left(\tilde{T}, \tilde{N}, \tilde{\Phi} \right)$ of (3.15) is unique, we conclude the convergence of the whole sequence, that is,

$$\mathbf{R} \left(\tilde{T}_n, \tilde{N}_n, \tilde{\Phi}_n \right) = (T_n, N_n, \Phi_n) \rightarrow \mathbf{R} \left(\tilde{T}, \tilde{N}, \tilde{\Phi} \right) = (T, N, \Phi) \text{ in } (L^2(0, T_f; L^2(\Omega)))^3.$$

□

Now we introduce a notation for vectorial norms. Given a space X and $f, g, h \in X$,

$$\|f, g, h\|_X^2 = \|f\|_X^2 + \|g\|_X^2 + \|h\|_X^2.$$

3. Theoretical and numerical analysis for a hybrid tumor model with nonlinear diffusion depending on vasculature

Lemma 3.5. *If $(T, N, \Phi) = \lambda \mathbf{R}(T, N, \Phi)$ for some $\lambda \in [0, 1]$, then*

$$\|T, N, \Phi\|_{L^2(0, T_f; L^2(\Omega))} \leq C$$

with $C > 0$ independent of $\lambda \in [0, 1]$.

Proof. For $\lambda = 0$ is trivial, hence we suppose $\lambda \in (0, 1]$. Let $(T, N, \Phi) \in L^2(0, T_f; L^2(\Omega))$ such that $(T, N, \Phi) = \lambda \mathbf{R}(T, N, \Phi)$. Then (T, N, Φ) is solution of a system similar to (3.10)-(3.12) with λ multiplying in the right hand side. Therefore, we can follow the same argument that in Lemma 3.1 to obtain that $0 \leq T, \Phi \leq K$ and $0 \leq N \leq C(T_f)$ a.e. $(0, T_f) \times \Omega$.

Thus, (T, N, Φ) is bounded in $(L^\infty(0, T_f; L^\infty(\Omega)))^3$ and also in $(L^2(0, T_f; L^2(\Omega)))^3$ independently of $\lambda \in [0, 1]$. □

Finally, from Lemmas 3.3, 3.4 and 3.5 the operator \mathbf{R} satisfies the hypotheses of Theorem 2.2. Thus, we conclude that the map \mathbf{R} has a fixed point $(T_\epsilon, N_\epsilon, \Phi_\epsilon)$ which is a weak-strong solution of problem (3.10)-(3.12).

Step 2. ϵ -independent estimates

Once we have proved the existence of weak-strong solution for the regularized problem (3.10)-(3.12), we are going to take $\epsilon \rightarrow 0$ in order to obtain a weak-strong solution of problem (3.8).

We can deduce the following ϵ independent estimates for the solution $(T_\epsilon, N_\epsilon, \Phi_\epsilon)$:

- Following the proof of Lemma 3.1, we can obtain that

$$0 \leq T_\epsilon, \Phi_\epsilon \leq K \text{ and } 0 \leq N_\epsilon \leq C(T_f), \quad \text{a.e. in } (0, T_f) \times \Omega. \quad (3.21)$$

- Following the proof of Lemma 3.1 b) for the problems satisfied by N_ϵ and Φ_ϵ , we have the bounds

$$\|N_\epsilon, \Phi_\epsilon\|_{L^\infty(0, T_f; L^2(\Omega))}^2 + \|\nabla(\sqrt{\epsilon} N_\epsilon), \nabla(\sqrt{\epsilon} \Phi_\epsilon)\|_{L^2(0, T_f; L^2(\Omega))}^2 \leq C(\|N_0, \Phi_0\|_{L^2(\Omega)}, |\Omega|, K, T_f).$$

Hence,

$$(\sqrt{\epsilon} \nabla N_\epsilon, \sqrt{\epsilon} \nabla \Phi_\epsilon) \text{ is bounded in } L^2(0, T_f; L^2(\Omega)). \quad (3.22)$$

- From Lemma 3.1 b), we obtain that

$$T_\epsilon \text{ is bounded in } L^\infty(0, T_f; L^2(\Omega)) \cap L^2(0, T_f; H^1(\Omega)).$$

3. Theoretical and numerical analysis for a hybrid tumor model with nonlinear diffusion depending on vasculature

- From (3.22), we obtain the bounds

$$(\sqrt{\epsilon} \Delta \Phi_\epsilon, \sqrt{\epsilon} \Delta N_\epsilon) \text{ in } L^2 \left(0, T_f; (H^1(\Omega))' \right). \quad (3.23)$$

- Moreover, from (3.10) we obtain that

$$\begin{cases} (T_\epsilon)_t \text{ is bounded in } L^2 \left(0, T_f; (H^1(\Omega))' \right), \\ (N_\epsilon)_t, (\Phi_\epsilon)_t \text{ are bounded in } L^\infty \left(0, T_f; L^\infty(\Omega) \right) \end{cases} \quad (3.24)$$

because $f_i \left((\tilde{T}_\epsilon)_+^K, (\tilde{N}_\epsilon)_+^{C(T_f)}, (\tilde{\Phi}_\epsilon)_+^K \right)$ is bounded in $L^\infty \left(0, T_f; L^\infty(\Omega) \right)$ for $i = 1, 2, 3$.

We will see the following additional estimate.

Lemma 3.6. *Assume $N_0, \Phi_0 \in H^1(\Omega)$, then $N_\epsilon, \Phi_\epsilon$ are bounded in $L^\infty \left(0, T_f; H^1(\Omega) \right)$.*

Proof. We only make the proof for N_ϵ because for Φ_ϵ is similar. Multiplying the N_ϵ equation by $-\Delta N_\epsilon \in L^2 \left(0, T_f; L^2(\Omega) \right)$ and integrating in Ω , we obtain

$$\frac{1}{2} \frac{d}{dt} \|\nabla N_\epsilon\|_{L^2(\Omega)}^2 + \epsilon \|\Delta N_\epsilon\|_{L^2(\Omega)}^2 dx = \int_\Omega f_2 \left((T_\epsilon)_+^K, (N_\epsilon)_+^{C(T_f)}, (\Phi_\epsilon)_+^K \right) (-\Delta N_\epsilon) dx \quad (3.25)$$

where the right hand side of (3.25) after integrating by parts can be bounded as follows

$$\begin{aligned} \int_\Omega f_2 \left((T_\epsilon)_+^K, (N_\epsilon)_+^{C(T_f)}, (\Phi_\epsilon)_+^K \right) (-\Delta N_\epsilon) dx &\leq C \left(\|\nabla T_\epsilon \cdot \nabla N_\epsilon\|_{L^2(\Omega)} + \|\nabla N_\epsilon\|_{L^2(\Omega)}^2 \right. \\ &\quad \left. + \|\nabla \Phi_\epsilon \cdot \nabla N_\epsilon\|_{L^2(\Omega)} \right) \leq C \left(1 + \|\nabla T_\epsilon\|_{L^2(\Omega)}^2 \right) \|\nabla N_\epsilon, \nabla \Phi_\epsilon\|_{L^2(\Omega)}^2. \end{aligned} \quad (3.26)$$

Here, we have used that every partial derivative $\frac{\partial f_2}{\partial T}$, $\frac{\partial f_2}{\partial N}$ and $\frac{\partial f_2}{\partial \Phi}$ evaluated at $((T_\epsilon)_+^K, (N_\epsilon)_+^{C(T_f)}, (\Phi_\epsilon)_+^K)$ is bounded in $L^\infty \left(0, T_f; L^\infty(\Omega) \right)$ and the fact that $|\nabla (T_\epsilon)_+^K| \leq |\nabla T_\epsilon|$ and the same for $\nabla (N_\epsilon)_+^{C(T_f)}$ and $\nabla (\Phi_\epsilon)_+^K$. Taking into account this estimate in (3.25), we obtain that

$$\frac{1}{2} \frac{d}{dt} \|\nabla N_\epsilon, \nabla \Phi_\epsilon\|_{L^2(\Omega)}^2 + \epsilon \|\Delta N_\epsilon, \Delta \Phi_\epsilon\|_{L^2(\Omega)}^2 \leq C \left(1 + \|\nabla T_\epsilon\|_{L^2(\Omega)}^2 \right) \|\nabla N_\epsilon, \nabla \Phi_\epsilon\|_{L^2(\Omega)}^2. \quad (3.27)$$

Since ∇T_ϵ is bounded in $L^2 \left(0, T_f; L^2(\Omega) \right)$, applying Gronwall Lemma, we deduce that

$$(\nabla N_\epsilon, \nabla \Phi_\epsilon) \text{ is bounded in } L^\infty \left(0, T_f; L^2(\Omega) \right).$$

3. Theoretical and numerical analysis for a hybrid tumor model with nonlinear diffusion depending on vasculature

Hence,

$$(N_\epsilon, \Phi_\epsilon) \text{ is bounded in } L^\infty(0, T_f; H^1(\Omega)).$$

Finally, integrating in time the inequality (3.27), we obtain the following bounds

$$\| \Delta(\sqrt{\epsilon} N_\epsilon), \Delta(\sqrt{\epsilon} \Phi_\epsilon) \|_{L^2(0, T_f; L^2(\Omega))}^2 \leq C.$$

Hence one has the bound of $(\sqrt{\epsilon} N_\epsilon, \sqrt{\epsilon} \Phi_\epsilon)$ in $L^2(0, T_f; H^2(\Omega))$.

□

Step 3. Taking limits as $\epsilon \rightarrow 0$

Using (3.21), (3.22), (3.23), (3.24) and Lemma 3.1 b), we can conclude that there exists a subsequence $(T_\epsilon, N_\epsilon, \Phi_\epsilon) \in \mathcal{W}_2$, with $N_\epsilon, \Phi_\epsilon \in L^\infty(0, T_f; H^1(\Omega))$ and a limit (T, N, Φ) such that as $\epsilon \rightarrow 0$,

$$\left\{ \begin{array}{ll} T_\epsilon \rightharpoonup T & \text{weakly in } \mathcal{W}_2, \\ (N_\epsilon, \Phi_\epsilon) \overset{*}{\rightharpoonup} (N, \Phi) & \text{weakly } * \text{ in } (L^\infty(0, T_f; H^1(\Omega)))^2, \\ (T_\epsilon)_t \rightharpoonup T_t & \text{weakly in } L^2(0, T_f; (H^1(\Omega))'), \\ ((N_\epsilon)_t, (\Phi_\epsilon)_t) \overset{*}{\rightharpoonup} (N_t, \Phi_t) & \text{weakly } * \text{ in } (L^\infty(0, T_f; L^\infty(\Omega)))^2, \\ \nabla T_\epsilon \rightharpoonup \nabla T & \text{weakly in } L^2(0, T_f; L^2(\Omega)), \\ (\sqrt{\epsilon} \Delta N_\epsilon, \sqrt{\epsilon} \Delta \Phi_\epsilon) \rightharpoonup (\theta_1, \theta_2) & \text{weakly in } L^2(0, T_f; L^2(\Omega)). \end{array} \right.$$

In particular,

$$(\epsilon \Delta N_\epsilon, \epsilon \Delta \Phi_\epsilon) = (\sqrt{\epsilon}(\sqrt{\epsilon} \Delta N_\epsilon), \sqrt{\epsilon}(\sqrt{\epsilon} \Delta \Phi_\epsilon)) \rightharpoonup (0, 0) \text{ weakly in } L^2(0, T_f; L^2(\Omega)).$$

From Aubin-Lions compactness

$$\left\{ \begin{array}{ll} T_\epsilon \rightarrow T & \text{strong in } L^2(0, T_f; L^2(\Omega)) \cap C^0(0, T_f; (H^1(\Omega))'), \\ (N_\epsilon, \Phi_\epsilon) \rightarrow (N, \Phi) & \text{strong in } (C^0(0, T_f; L^2(\Omega)))^2. \end{array} \right. \quad (3.28)$$

Now, we will take limits in the nonlinear diffusion term in $L^2(0, T_f; L^2(\Omega))$. On the one hand, we have that $\kappa_1 P(\Phi_\epsilon, T_\epsilon) + \kappa_0$ is continuous in \mathbb{R}^2 and it is bounded in $L^\infty(0, T_f; L^\infty(\Omega))$ and for (3.28), we obtain that $(T_\epsilon, \Phi_\epsilon) \rightarrow (T, \Phi)$ a.e. in $(0, T_f) \times \Omega$. Hence, using dominated convergence Theorem

$$\left(\kappa_1 P\left((\Phi_\epsilon)_+^K, (T_\epsilon)_+^K\right) + \kappa_0 \right) \rightarrow \left(\kappa_1 P\left(\Phi_+^K, T_+^K\right) + \kappa_0 \right) \text{ in } L^p(0, T_f; L^p(\Omega)), \quad \forall p < \infty. \quad (3.29)$$

3. Theoretical and numerical analysis for a hybrid tumor model with nonlinear diffusion depending on vasculature

On the other hand, $\nabla T_\epsilon \rightharpoonup \nabla T$ weakly in $L^2(0, T_f; L^2(\Omega))$.

Hence, since $(\kappa_1 P((\Phi_\epsilon)_+^K, (T_\epsilon)_+^K) + \kappa_0) \nabla T_\epsilon$ is bounded in $L^2(0, T_f; L^2(\Omega))$, one has

$$(\kappa_1 P((\Phi_\epsilon)_+^K, (T_\epsilon)_+^K) + \kappa_0) \nabla T_\epsilon \rightharpoonup (\kappa_1 P(\Phi_+^K, T_+^K) + \kappa_0) \nabla T \text{ weakly in } L^2(0, T_f; L^2(\Omega)).$$

Finally, for all $\varphi \in L^2(0, T_f; H^1(\Omega))$ we conclude that

$$\begin{aligned} \int_0^{T_f} \int_\Omega ((T_\epsilon)_t, (N_\epsilon)_t, (\Phi_\epsilon)_t) \varphi \, dx \, dt &\rightarrow \int_0^{T_f} \int_\Omega (T_t, N_t, \Phi_t) \varphi \, dx \, dt, \\ \int_0^{T_f} \int_\Omega (\kappa_1 P((\Phi_\epsilon)_+^K, (T_\epsilon)_+^K) + \kappa_0) \nabla T_\epsilon \cdot \nabla \varphi \, dx \, dt &\rightarrow \\ \int_0^{T_f} \int_\Omega (\kappa_1 P(\Phi_+^K, T_+^K) + \kappa_0) \nabla T \cdot \nabla \varphi \, dx \, dt, \\ \int_0^{T_f} \int_\Omega (\sqrt{\epsilon}(\sqrt{\epsilon} \Delta N_\epsilon), \sqrt{\epsilon}(\sqrt{\epsilon} \Delta \Phi_\epsilon)) \varphi \, dx \, dt &\rightarrow (0, 0), \\ \int_0^{T_f} \int_\Omega f_i((T_\epsilon)_+, (N_\epsilon)_\epsilon, (\Phi_\epsilon)_\epsilon) \varphi \, dx \, dt &\rightarrow \int_0^{T_f} \int_\Omega f_i(T_+, N_+, \Phi_+) \varphi \, dx \, dt, \end{aligned}$$

para $i = 1, 2, 3$.

Taking limits as $\epsilon \rightarrow 0$ in (3.15), we deduce that (T, N, Φ) is a weak-strong solution of (3.8) (which is in addition a weak-strong solution of problem (3.1)-(3.3)) where the convergence for (3.3) is obtained thanks to (3.28). \square

3.3 Asymptotic behaviour

Once we have proved the existence of weak-strong solution of (3.1)-(3.3) for any finite time $T_f > 0$, we are going to study the asymptotic behaviour of the solution as $t \rightarrow \infty$. In order to obtain the equilibrium points, we solve the following nonlinear algebraic system

$$f_1(T, N, \Phi) = 0, \quad f_2(T, N, \Phi) = 0, \quad f_3(T, N, \Phi) = 0.$$

Following the same argument used in Section 2.3.1 of Chapter 2, the equilibria of (3.1) are

3. Theoretical and numerical analysis for a hybrid tumor model with nonlinear diffusion depending on vasculature

- $P_1 = \{(0, 0, 0)\}$.
 - $P_2 = \{(0, N, 0), \quad N > 0\}$.
 - $P_3 = \{(0, 0, \Phi), \quad \Phi > 0\}$.
- (3.30)

Remark 3.3. Observe that $P_1 \cup P_2 \cup P_3$ is a continuum of equilibrium points.

Remark 3.4. As we said in Remark 2.6 although we assume sometimes the hypothesis $N_0(x) > 0$ for $x \in \bar{\Omega}$ in the following results, this condition can be relaxed for $N(t_*, x) > 0$ for some $t_* \geq 0$ and for all $x \in \bar{\Omega}$.

Now, we present a result of pointwise convergence to zero of the vasculature.

Lemma 3.7. Given $\epsilon > 0$ and a solution (T, N, Φ) of (3.1)-(3.3), if there exists $\tilde{\Omega} \subset \Omega$ with $|\tilde{\Omega}| > 0$ such that $0 < \epsilon \leq N_0(x)$ a.e. $x \in \tilde{\Omega}$, one has $\Phi(t, x) \rightarrow 0$ when $t \rightarrow +\infty$ a.e. $x \in \tilde{\Omega}$.

The proof of this result is rather similar to Lemma 2.12 of Chapter 2 with the difference that due to the fact that $\Phi(t, x), N(t, x) \in L^\infty(0, T_f; H^1(\Omega))$, we prove Lemma 3.7 using a subdomain $\tilde{\Omega} \subset \Omega$ with positive measure instead of a pointwise argument for every $x \in \Omega$.

As consequence of Lemma 3.7 and that $t \mapsto N(t, \cdot)$ is increasing a.e. $x \in \Omega$, we deduce:

Corollary 3.2. The equilibria solution P_3 is unstable.

Now, we prove a comparison result that provides an uniform bound for the solution of a nonlinear diffusion equation which we will use later:

Lemma 3.8. Let $\Omega \subseteq \mathbb{R}^n$ a bounded set of class C^2 , and $0 < T_f < +\infty$. Given the following problems

$$\left\{ \begin{array}{l} T_t - \nabla(\nu(t, x, T) \cdot \nabla T) = f(t, x, T) \quad \text{in } (0, T_f) \times \Omega, \\ T(0, x) = T_0(x) \quad \text{in } \Omega, \\ \left. \frac{\partial T}{\partial n} \right|_{\partial\Omega} = 0 \quad \text{in } (0, T_f) \times \partial\Omega, \end{array} \right. \quad (3.31)$$

with $\nu(\cdot, \cdot, T) \in L^\infty(0, T_f; L^\infty(\Omega))$ for all $T \in \mathbb{R}$ a given non-negative function,

$$f(\cdot, \cdot, T) \in L^2(0, T_f; H^1(\Omega)) \quad \forall T \in \mathbb{R}$$

and

$$\left\{ \begin{array}{l} y_t = g(t, y) \quad \text{in } (0, T_{\max}), \\ y(0) = y_0 \end{array} \right. \quad (3.32)$$

3. Theoretical and numerical analysis for a hybrid tumor model with nonlinear diffusion depending on vasculature

with $0 < T_{\max} < +\infty$ and $g \in C^0([0, T_{\max}] \times \mathbb{R})$ and locally lipschitz with respect y . Suppose that (3.31) has a weak solution $T \in \mathcal{W}_2 \cap L^\infty(0, T_f; L^\infty(\Omega))$ in $(0, T_f) \times \Omega$, and (3.32) has an unique solution $y \in C^1([0, T_{\max}])$ in $[0, T_{\max}]$. If $T_0(x) \leq y_0$ a.e. $x \in \Omega$ and

$$f(t, x, p) \leq g(t, p), \quad \text{a.e. } (t, x) \in (0, T_*) \times \Omega, \quad \forall p \in \mathbb{R} \quad (3.33)$$

with $T_* = \min\{T_f, T_{\max}\}$. Then,

$$T(t, x) \leq y(t), \quad \text{a.e. } (t, x) \in (0, T_*) \times \Omega.$$

Proof. Let $T = T(t, x)$ a weak solution of (3.31) in $(0, T_f)$ and $y = y(t)$ the classical solution of (3.32) in $[0, T_{\max}]$ and we consider the problem which satisfies the difference $T - y$,

$$\begin{cases} (T - y)_t - \nabla \cdot (\nu(t, x, T) \nabla (T - y)) = f(t, x, T) - g(t, y) & \text{in } (0, T_*) \times \Omega, \\ T(0, x) - y(0) = T_0(x) - y_0 & \text{a.e. } x \in \Omega, \\ \left. \frac{\partial(T - y)}{\partial \mathbf{n}} \right|_{\partial \Omega} = 0 & \text{in } (0, T_*) \times \partial \Omega, \end{cases} \quad (3.34)$$

Multiplying the first equation of (3.34) by $(T - y)_+$ and integrating in Ω and using (3.33), we obtain that

$$\begin{aligned} \frac{1}{2} \frac{d}{dt} \int_{\Omega} (T - y)_+^2 dx + \int_{\Omega} \nu(t, x, T) |\nabla (T - y)_+|^2 dx &= \int_{\Omega} (f(t, x, T) - g(t, y)) (T - y)_+ dx \\ &\leq \int_{\Omega} (g(t, T) - g(t, y)) (T - y)_+ dx \leq L_{\tilde{K}} \int_{\Omega} (T - y)_+^2 dx \end{aligned}$$

since the graph of $T(t, x)$ and $y(t)$ belong to a compact set $\tilde{K} \subset \mathbb{R}$ because $T \in L^\infty(0, T_f; L^\infty(\Omega))$ and $y \in C^1([0, T_{\max}])$ and hence $L_{\tilde{K}}$ is a lipschitz constant of this compact set. Thus, we deduce

$$\|(T - y)_+(t)\|_{L^2(\Omega)}^2 \leq \|(T_0(x) - y_0)_+\|_{L^2(\Omega)}^2 e^{2L_{\tilde{K}}t} = 0,$$

hence, $T(t, x) \leq y(t)$ a.e. $(t, x) \in (0, T_*) \times \Omega$. □

Now, using Lemma 3.8, we are going to deduce the same results for the asymptotic behaviour of any solution (T, N, Φ) of (3.1)-(3.3) which we proved in Lemmas 2.13 and 2.15 of Chapter 2, where uniform convergence for (T, N, Φ) was obtained.

3. Theoretical and numerical analysis for a hybrid tumor model with nonlinear diffusion depending on vasculature

Lemma 3.9. *Given a solution (T, N, Φ) of (3.1)-(3.3) such that*

$$N_0(x) \geq N_0^{\min} > 0 \quad \text{a.e. } x \in \Omega$$

and assume that

$$\delta \geq \frac{\gamma}{K}. \quad (3.35)$$

Then,

$$0 \leq \Phi(t, x) \leq \|\Phi_0\|_{L^\infty(\Omega)} e^{-\beta_2 N_0^{\min} t}, \quad \text{a.e. } (t, x) \in (0, +\infty) \times \Omega. \quad (3.36)$$

In addition, it holds that if $\beta_1 \neq \beta_2$, then

$$0 \leq T(t, x) \leq \|T_0\|_{L^\infty(\Omega)} e^{-\beta_1 N_0^{\min} t} + \frac{\rho \|\Phi_0\|_{L^\infty(\Omega)}}{(\beta_1 - \beta_2) N_0^{\min}} \left(e^{-\beta_2 N_0^{\min} t} - e^{-\beta_1 N_0^{\min} t} \right), \quad (3.37)$$

a.e. $(t, x) \in (0, +\infty) \times \Omega$, whereas if $\beta_1 = \beta_2$, then

$$0 \leq T(t, x) \leq (\|T_0\|_{L^\infty(\Omega)} + \rho \|\Phi_0\|_{L^\infty(\Omega)} t) e^{-\beta_1 N_0^{\min} t}, \quad \text{a.e. } (t, x) \in (0, +\infty) \times \Omega. \quad (3.38)$$

Moreover, there exists $N_{\max} > \|N_0\|_{L^\infty(\Omega)}$ such that

$$N(t, x) \leq N_{\max}, \quad \text{a.e. } (t, x) \in (0, +\infty) \times \Omega.$$

Proof. To prove (3.36) we repeat the same argument for the exponential convergence of $\Phi(t, x)$ to zero in $L^\infty(0, T_f; L^\infty(\Omega))$ made in Lemma 2.13 of Chapter 2. To prove (3.37) and (3.38), we bound $f_1(T, N, \Phi)$ using (3.36) as follows

$$f_1(T, N, \Phi) \leq \rho \|\Phi_0\|_{L^\infty(\Omega)} e^{-\beta_2 N_0^{\min} t} - \beta_1 N_0^{\min} T,$$

and we apply Lemma 3.8 taking the following linear differential problem

$$\begin{cases} y_t = \rho \|\Phi_0\|_{L^\infty(\Omega)} e^{-\beta_2 N_0^{\min} t} - \beta_1 N_0^{\min} y & \text{in } (0, +\infty), \\ y(0) = \|T_0\|_{L^\infty(\Omega)}. \end{cases} \quad (3.39)$$

Solving (3.39) we obtain that if $\beta_1 \neq \beta_2$,

$$y(t) = \|T_0\|_{L^\infty(\Omega)} e^{-\beta_1 N_0^{\min} t} + \frac{\rho \|\Phi_0\|_{L^\infty(\Omega)}}{(\beta_1 - \beta_2) N_0^{\min}} \left(e^{-\beta_2 N_0^{\min} t} - e^{-\beta_1 N_0^{\min} t} \right), \quad \text{in } (0, +\infty),$$

and if $\beta_1 = \beta_2$,

$$y(t) = (\|T_0\|_{L^\infty(\Omega)} + \rho \|\Phi_0\|_{L^\infty(\Omega)} t) e^{-\beta_1 N_0^{\min} t}, \quad \text{in } (0, +\infty).$$

Hence, we obtain that

$$T(t, x) \leq y(t), \quad \text{a.e. } (t, x) \in (0, +\infty) \times \Omega.$$

Finally, we get the bound $N(t, x) \leq N_{\max}$ as in Lemma 2.13 of Chapter 2 using the upper uniform bounds obtained for $T(t, x)$ and $\Phi(t, x)$ previously in (3.36) and (3.37) or (3.38). \square

3. Theoretical and numerical analysis for a hybrid tumor model with nonlinear diffusion depending on vasculature

In the following result, we study the situation when $N_0(x)$ is close to K in the whole domain Ω .

Lemma 3.10. *Assuming $N_0(x) \geq K - \epsilon$ a.e. $x \in \Omega$ for ϵ small enough and a weak-strong solution (T, N, Φ) of (3.1)-(3.3), then,*

$$0 \leq T(t, x) \leq \|T_0\|_{L^\infty(\Omega)} e^{-\left(\beta_1(K-\epsilon) - \rho \frac{\epsilon}{K}\right)t}, \quad \text{a.e. } (t, x) \in (0, +\infty) \times \Omega, \quad (3.40)$$

and

$$0 \leq \Phi(t, x) \leq \|\Phi_0\|_{L^\infty(\Omega)} e^{-\left(\beta_2(K-\epsilon) - \gamma \frac{\epsilon}{K}\right)t}, \quad \text{a.e. } (t, x) \in (0, +\infty) \times \Omega, \quad (3.41)$$

In addition, if $\rho \frac{\epsilon}{K} - \beta_1(K - \epsilon) < 0$ and $\gamma \frac{\epsilon}{K} - \beta_2(K - \epsilon) < 0$ then, there exists $N_{\max} > \|N_0\|_{L^\infty(\Omega)}$ such that

$$N(t, x) \leq N_{\max}, \quad \text{a.e. } (t, x) \in (0, +\infty) \times \Omega. \quad (3.42)$$

Proof. Since N is increasing in time, we get

$$N(t, x) \geq N_0(x) > K - \epsilon \quad \text{a.e. } (t, x) \in (0, +\infty) \times \Omega.$$

Using now that $T, \Phi \geq 0$, and

$$1 - \frac{T + N + \Phi}{K} \leq 1 - \frac{N}{K} < 1 - \frac{K - \epsilon}{K} = \frac{\epsilon}{K}$$

therefore,

$$\frac{\partial T}{\partial t} - \nabla \cdot ((\kappa_1 P(\Phi, T) + \kappa_0) \nabla T) = f_1(T, N, \Phi) \leq \rho T \frac{\epsilon}{K} - \beta_1(K - \epsilon) T = \left(\rho \frac{\epsilon}{K} - \beta_1(K - \epsilon)\right) T.$$

Hence, we apply Lemma 3.8 with $y_0 = \|T_0\|_{L^\infty(\Omega)}$ and $g(t, y) = \left(\rho \frac{\epsilon}{K} - \beta_1(K - \epsilon)\right) y$ to obtain that

$$T(t, x) \leq y(t) = \|T_0\|_{L^\infty(\Omega)} e^{-\left(\beta_1(K-\epsilon) - \rho \frac{\epsilon}{K}\right)t}, \quad \text{a.e. } (t, x) \in (0, +\infty) \times \Omega.$$

Now we repeat the same argument made in Lemma 2.15 of Chapter 2 to prove the uniform exponential convergence of $\Phi(t, x)$ to zero in $L^\infty(0, T_f; L^\infty(\Omega))$ given in (3.41) and for the bound of $N(t, x)$ given in (3.42) using the upper uniform bounds (3.40) and (3.41) already proved for $T(t, x)$ and $\Phi(t, x)$. \square

Remark 3.5. *In Lemmas 3.9 and 3.10 using that $N(\cdot, x)$ is increasing in time, there exists $N_* \in L^\infty(\Omega)$ with $N_{\max} \geq N_* \geq N_0$ a.e. in Ω such that*

$$N(t, x) \rightarrow N_*(x) \quad \text{as } t \rightarrow +\infty, \quad \text{a.e. } x \in \Omega.$$

3. Theoretical and numerical analysis for a hybrid tumor model with nonlinear diffusion depending on vasculature

3.4 A FE numerical scheme

In this Section, we build an uncoupled and linear fully discrete scheme of (3.1)-(3.3) by means of an Implicit-Explicit (IMEX) Finite Difference in time approximation and P_1 continuous finite element with “mass-lumping” in space. This scheme will preserve the pointwise and energy estimates that appear in Lemmas 3.1 and 3.6 considering acute triangulations.

Now we introduce the hypotheses required along this Section.

- a) Let $0 < T_f < +\infty$ and a bounded set $\Omega \subseteq \mathbb{R}^2$ or \mathbb{R}^3 with polygonal or polyhedral lipschitz-continuous boundary. We consider the uniform time partition

$$(0, T_f] = \bigcup_{k=0}^{K_f-1} (t_k, t_{k+1}],$$

with $t_k = k dt$ where $K_f \in \mathbb{N}$ and $dt = \frac{T_f}{K_f}$ is the time step.

- b) Let $\{\mathcal{T}_h\}_{h>0}$ be a family of shape-regular, quasi-uniform triangulations of $\bar{\Omega}$ formed by acute N-simplexes (triangles in 2D and tetrahedral in 3D), such that

$$\bar{\Omega} = \bigcup_{\mathcal{K} \in \mathcal{T}_h} \mathcal{K},$$

where $h = \max_{\mathcal{K} \in \mathcal{T}_h} h_{\mathcal{K}}$, with $h_{\mathcal{K}}$ being the diameter of \mathcal{K} . Further, let $\mathcal{N}_h = \{a_i\}_{i \in I}$ be the set of all the nodes of \mathcal{T}_h .

- c) Conforming piecewise linear, finite element spaces associated to \mathcal{T}_h are assumed for approximating $H^1(\Omega)$:

$$N_h = \{n_h \in C^0(\bar{\Omega}) : n_h|_{\mathcal{K}} \in \mathcal{P}_1(\mathcal{K}) \quad \forall \mathcal{K} \in \mathcal{T}_h\}$$

whose Lagrange basis is denoted by $\{\varphi_a\}_{a \in \mathcal{N}_h}$.

Let $I_h : C^0(\bar{\Omega}) \rightarrow N_h$ be the nodal interpolation operator and consider the discrete inner product

$$(n_h, \bar{n}_h)_h = \int_{\Omega} I_h(n_h \cdot \bar{n}_h) = \sum_{a \in \mathcal{N}_h} n_h(a) \bar{n}_h(a) \int_{\Omega} \varphi_a, \quad \forall n_h, \bar{n}_h \in N_h$$

which induces the discrete norm $\|n_h\|_h = \sqrt{(n_h, n_h)_h}$ defined on N_h (that is equivalent to $L^2(\Omega)$ -norm).

3. Theoretical and numerical analysis for a hybrid tumor model with nonlinear diffusion depending on vasculature

Thus, in each time step, we consider the following linear uncoupled numerical scheme for the model (3.1): given $T_h^k, N_h^k, \Phi_h^k \in N_h$, find $T_h^{k+1}, N_h^{k+1}, \Phi_h^{k+1} \in N_h$ in a decoupled way (first T , then Φ and finally N) satisfying

$$\left(\delta_t T_h^{k+1}, v \right)_h + \left((\kappa_1 P_h^k + \kappa_0) \nabla T_h^{k+1}, \nabla v \right) = \left(\left(\widehat{f}_1 \right)_h^k, v \right)_h \quad (3.43)$$

$$\delta_t N_h^{k+1}(a) = \left(\widehat{f}_2 \right)_h^k(a) \quad (3.44)$$

$$\delta_t \Phi_h^{k+1}(a) = \left(\widehat{f}_3 \right)_h^k(a) \quad (3.45)$$

$\forall v \in N_h$ and $\forall a \in \mathcal{N}_h$. We have denoted

$$\delta_t T_h^{k+1} = \frac{T_h^{k+1} - T_h^k}{dt}$$

and similarly for $\delta_t N_h^{k+1}$ and $\delta_t \Phi_h^{k+1}$ and $P_h^k = P(\Phi_h^k, T_h^k)$. The approximation of the initial conditions are taken as

$$T_h^0 = I_h(T_0) \in N_h, \quad N_h^0 = I_h(N_0) \in N_h, \quad \Phi_h^0 = I_h(\Phi_0) \in N_h \quad (3.46)$$

where we consider for simplicity that $T_0, N_0, \Phi_0 \in C^0(\overline{\Omega})$.

Finally, the functions \widehat{f}_i for $i = 1, 2, 3$ which appear in (3.43), (3.44) and (3.45), have the following definitions:

$$\begin{aligned} \left(\widehat{f}_1 \right)_h^k &= \rho P_h^k \left[T_h^k \left(1 - \frac{T_h^{k+1}}{K} \right) - T_h^{k+1} \left(\frac{N_h^k + \Phi_h^k}{K} \right) \right] \\ &\quad - \alpha T_h^{k+1} \sqrt{1 - (P_h^k)^2} - \beta_1 N_h^k T_h^{k+1}, \end{aligned} \quad (3.47)$$

$$\left(\widehat{f}_2 \right)_h^k = \alpha T_h^{k+1} \sqrt{1 - (P_h^k)^2} \beta_1 N_h^k T_h^{k+1} + \delta T_h^{k+1} \Phi_h^{k+1} + \beta_2 N_h^k \Phi_h^{k+1}, \quad (3.48)$$

$$\begin{aligned} \left(\widehat{f}_3 \right)_h^k &= \gamma \frac{T_h^{k+1}}{K} \sqrt{1 - (P_h^k)^2} \left[\Phi_h^k \left(1 - \frac{\Phi_h^{k+1}}{K} \right) - \Phi_h^{k+1} \left(\frac{T_h^k + N_h^k}{K} \right) \right] \\ &\quad - \delta T_h^{k+1} \Phi_h^{k+1} - \beta_2 N_h^k \Phi_h^{k+1}. \end{aligned} \quad (3.49)$$

The discretization of (3.47)-(3.49) is based in two main ideas:

3. Theoretical and numerical analysis for a hybrid tumor model with nonlinear diffusion depending on vasculature

1. We take an approximation of the negative reaction terms in a linear semi-implicit form and an explicit approximation of the positive reaction terms.
2. The sum of non-logistic reaction terms of (3.47)-(3.49) cancels, as in the continuous case.

Remark 3.6. Observe that (3.44) and (3.45) can be rewritten in a variational sense as follows:

$$\left(\delta_t N_h^{k+1}, v_2\right)_h = \left(\left(\widehat{f}_2\right)_h^k, v_2\right)_h \quad (3.50)$$

$$\left(\delta_t \Phi_h^{k+1}, v_3\right)_h = \left(\left(\widehat{f}_3\right)_h^k, v_3\right)_h \quad (3.51)$$

$\forall v_i \in N_h$ for $i = 2, 3$.

3.4.1 A priori energy estimates

In this part, we are going to get a priori energy estimates for the fully discrete solution T_h^{k+1} , N_h^{k+1} and Φ_h^{k+1} of (3.43), (3.44) and (3.45) which are independent of (h, k) . The following two lemmas are based on the hypothesis of acute triangulations to get a discrete maximum principle, see [12].

Lemma 3.11 (Lower bounds; positivity). *Let $T_h^k, N_h^k, \Phi_h^k \in N_h$ such that $0 \leq T_h^k, N_h^k, \Phi_h^k$ in Ω . Then, $T_h^{k+1}, N_h^{k+1}, \Phi_h^{k+1} \geq 0$ in Ω .*

Proof. Let $I_h((T_h^{k+1})_-) \in N_h$ be defined as

$$I_h\left(\left(T_h^{k+1}\right)_-\right) = \sum_{a \in \mathcal{N}_h} \left(T_h^{k+1}(a)\right)_- \varphi_a,$$

where $\left(T_h^{k+1}(a)\right)_- = \min\{0, T_h^{k+1}(a)\}$. Analogously, one defines $I_h((T_h^{k+1})_+) \in N_h$ as

$$I_h\left(\left(T_h^{k+1}\right)_+\right) = \sum_{a \in \mathcal{N}_h} \left(T_h^{k+1}(a)\right)_+ \varphi_a,$$

where $\left(T_h^{k+1}(a)\right)_+ = \max\{0, T_h^{k+1}(a)\}$. Notice that $T_h^{k+1} = I_h((T_h^{k+1})_-) + I_h((T_h^{k+1})_+)$.

Choosing $v = I_h((T_h^{k+1})_-)$ in (3.43), it follows that

$$\frac{1}{dt} \left\| \left(T_h^{k+1}\right)_- \right\|_h^2 + \left((\kappa_1 P_h^k + \kappa_0) \nabla T_h^{k+1}, \nabla I_h\left(\left(T_h^{k+1}\right)_-\right) \right) \leq \left(\left(\widehat{f}_1\right)_h^k, \left(T_h^{k+1}\right)_- \right)_h, \quad (3.52)$$

3. Theoretical and numerical analysis for a hybrid tumor model with nonlinear diffusion depending on vasculature

where we have used in the left hand side that in every node $a \in \mathcal{N}_h$,

$$\delta_t T_h^{k+1}(a) \cdot \left(T_h^{k+1}(a) \right)_- = \frac{1}{dt} \left(\left| \left(T_h^{k+1}(a) \right)_- \right|^2 - T_h^k(a) \cdot \left(T_h^{k+1}(a) \right)_- \right) \geq \frac{1}{dt} \left(\left| \left(T_h^{k+1}(a) \right)_- \right|^2 \right)$$

using that $T_h^k(a) \geq 0$ and $\left(T_h^{k+1}(a) \right)_- \leq 0$. Now, we can make the following

$$\begin{aligned} & \left(\left(\kappa_1 P_h^k + \kappa_0 \right) \nabla T_h^{k+1}, \nabla I_h \left(\left(T_h^{k+1} \right)_- \right) \right) \\ &= \left(\left(\kappa_1 P_h^k + \kappa_0 \right) \nabla I_h \left(\left(T_h^{k+1} \right)_- \right), \nabla I_h \left(\left(T_h^{k+1} \right)_- \right) \right) \\ &+ \left(\left(\kappa_1 P_h^k + \kappa_0 \right) \nabla I_h \left(\left(T_h^{k+1} \right)_+ \right), \nabla I_h \left(\left(T_h^{k+1} \right)_- \right) \right) \\ &= \left\| \left(\kappa_1 P_h^k + \kappa_0 \right)^{1/2} \nabla I_h \left(\left(T_h^{k+1} \right)_- \right) \right\|_{L^2(\Omega)}^2 \\ &+ \sum_{a \neq \tilde{a} \in \mathcal{N}_h} \left(T_h^{k+1}(a) \right)_- \left(T_h^{k+1}(\tilde{a}) \right)_+ \left(\left(\kappa_1 P_h^k + \kappa_0 \right) \nabla \varphi_a, \nabla \varphi_{\tilde{a}} \right). \end{aligned}$$

Hence, using that $\left(T_h^{k+1}(a) \right)_- \left(T_h^{k+1}(\tilde{a}) \right)_+ \leq 0$ if $a \neq \tilde{a}$, $(\kappa_1 P(\Phi_h^k, T_h^k) + \kappa_0)$ is a nonnegative function and that

$$\nabla \varphi_a \cdot \nabla \varphi_{\tilde{a}} \leq 0 \quad \forall a \neq \tilde{a} \in \mathcal{N}_h$$

(owing to an acute triangulation is assumed), we deduce,

$$\left(\left(\kappa_1 P_h^k + \kappa_0 \right) \nabla T_h^{k+1}, \nabla I_h \left(\left(T_h^{k+1} \right)_- \right) \right) \geq \left\| \left(\kappa_1 P_h^k + \kappa_0 \right)^{1/2} \nabla I_h \left(\left(T_h^{k+1} \right)_- \right) \right\|_{L^2(\Omega)}^2. \quad (3.53)$$

Adding (3.53) in (3.52), it holds that

$$\frac{1}{dt} \left\| \left(T_h^{k+1} \right)_- \right\|_h^2 + \left\| \left(\kappa_1 P_h^k + \kappa_0 \right)^{1/2} \nabla I_h \left(\left(T_h^{k+1} \right)_- \right) \right\|_{L^2(\Omega)}^2 \leq \left(\left(\hat{f}_1 \right)_h^k, \left(T_h^{k+1} \right)_- \right)_h \leq 0. \quad (3.54)$$

For the last inequality above, we used that in every node $a \in \mathcal{N}_h$ we have, due to the form of $\left(\hat{f}_1 \right)_h^k$ given in (3.47), the following

$$\rho P_h^k(a) \left(T_h^k(a) \right) \left(T_h^{k+1}(a) \right)_- \leq 0$$

and

$$\begin{aligned} & - \left(\rho P_h^k(a) \left(\frac{T_h^k(a) + N_h^k(a) + \Phi_h^k(a)}{K} \right) + \alpha \sqrt{1 - (P_h^k(a))^2} \right. \\ & \left. + \beta_1 N_h^k(a) \right) \left(T_h^{k+1}(a) \right) \left(T_h^{k+1}(a) \right)_- \leq 0. \end{aligned}$$

3. Theoretical and numerical analysis for a hybrid tumor model with nonlinear diffusion depending on vasculature

Therefore, from (3.54), $(T_h^{k+1})_- \equiv 0$ and this implies $T_h^{k+1} \geq 0$ in Ω .

For (3.45), the same argument can be used and it is even easier. Thus, multiplying (3.45) by $(\Phi_h^{k+1}(a))_-$,

$$\frac{1}{dt} \left(\Phi_h^{k+1}(a) \right)_-^2 \leq (\hat{f}_3)_h^k(a) \left(\Phi_h^{k+1}(a) \right)_- \leq 0 \quad (3.55)$$

since in every node $a \in \mathcal{N}_h$ we have, due to the form of $(\hat{f}_3)_h^k$ given in (3.49), the following

$$\gamma \frac{T_h^{k+1}(a)}{K} \sqrt{1 - (P_h^k(a))^2} \left(\Phi_h^k(a) \right) \left(\Phi_h^{k+1}(a) \right)_- \leq 0$$

and

$$\begin{aligned} & - \left(\gamma \frac{T_h^{k+1}(a)}{K} \sqrt{1 - (P_h^k(a))^2} \left(\frac{T_h^k(a) + N_h^k(a) + \Phi_h^k(a)}{K} \right) + \delta T_h^{k+1}(a) \right. \\ & \quad \left. + \beta_2 N_h^k(a) \right) \left(\Phi_h^{k+1}(a) \right) \left(\Phi_h^{k+1}(a) \right)_- \leq 0. \end{aligned}$$

Therefore, from (3.55), $(\Phi_h^{k+1}(a))_- \equiv 0 \forall a \in \mathcal{N}_h$ and this implies $\Phi_h^{k+1} \geq 0$ in Ω .

Finally, for (3.44) it is easy to obtain that

$$\frac{1}{dt} \left(N_h^{k+1}(a) \right)_-^2 \leq (\hat{f}_2)_h^k(a) \left(N_h^{k+1}(a) \right)_- \leq 0$$

since $(\hat{f}_2)_h^k(a) \geq 0$ in every node $a \in \mathcal{N}_h$ due to the form of $(\hat{f}_2)_h^k$ given in (3.48). Hence, $(N_h^{k+1}(a))_- \equiv 0 \forall a \in \mathcal{N}_h$ and this implies $N_h^{k+1} \geq 0$ in Ω . □

Lemma 3.12 (Upper bounds). *Let $T_h^k, N_h^k, \Phi_h^k \in N_h$ such that $0 \leq T_h^k, \Phi_h^k \leq K$ and $0 \leq N_h^k$ in Ω . Then one has*

a) $T_h^{k+1}, \Phi_h^{k+1} \leq K$ in Ω .

b) $N_h^k \leq N_h^{k+1}$ in Ω .

c) $N_h^k \leq \tilde{C}(T_f)$ in Ω , for all $k = 1, \dots, K_f$, with \tilde{C} independent of (h, k) .

Proof. a) We argue in a similar fashion of Lemma 3.11. In this case, by writing (3.43) as

$$\left(\delta_t \left(T_h^{k+1} - K \right), v \right)_h + \left(\left(\kappa_1 P_h^k + \kappa_0 \right) \nabla \left(T_h^{k+1} - K \right), \nabla v \right) = \left(\left(\hat{f}_1 \right)_h^k, v \right)_h$$

3. Theoretical and numerical analysis for a hybrid tumor model with nonlinear diffusion depending on vasculature

and taking $v = I_h((T_h^{k+1} - K)_+)$, it follows that

$$\begin{aligned} \frac{1}{dt} \left\| \left(T_h^{k+1} - K \right)_+ \right\|_h^2 + \left\| \left(\kappa_1 P_h^k + \kappa_0 \right)^{1/2} \nabla I_h \left(\left(T_h^{k+1} - K \right)_+ \right) \right\|_{L^2(\Omega)}^2 \\ \leq \left(\left(\widehat{f}_1 \right)_h^k, \left(T_h^{k+1} - K \right)_+ \right)_h \leq 0 \end{aligned}$$

since in every node $a \in \mathcal{N}_h$ we have on one side that

$$\begin{aligned} \delta_t \left(\left(T_h^{k+1} - K \right) (a) \right) \cdot \left(\left(T_h^{k+1} - K \right) (a) \right)_+ &= \left| \left(\left(T_h^{k+1} - K \right) (a) \right)_+ \right|^2 \\ - \left(\left(T_h^k - K \right) (a) \right) \cdot \left(\left(T_h^{k+1} - K \right) (a) \right)_+ &\geq \left| \left(\left(T_h^{k+1} - K \right) (a) \right)_+ \right|^2 \end{aligned}$$

using that $\left(\left(T_h^k - K \right) (a) \right) \leq 0$ and $\left(\left(T_h^{k+1} - K \right) (a) \right)_+ \geq 0$. On other side, in every node $a \in \mathcal{N}_h$, due to the form of $\left(\widehat{f}_1 \right)_h^k$ given in (3.47), the following

$$\left(\rho P_h^k (a) T_h^k (a) \left(1 - \frac{T_h^{k+1} (a)}{K} \right) \right) \left(\left(T_h^{k+1} - K \right) (a) \right)_+ \leq 0$$

and

$$\begin{aligned} - \left(\rho P_h^k (a) \left(\frac{N_h^k (a) + \Phi_h^k (a)}{K} \right) + \alpha \sqrt{1 - (P_h^k (a))^2} \right. \\ \left. + \beta_1 N_h^k (a) \right) \left(T_h^{k+1} (a) \right) \left(\left(T_h^{k+1} - K \right) (a) \right)_+ \leq 0. \end{aligned}$$

Hence, $\left(T_h^{k+1} - K \right)_+ \equiv 0$ and this implies $T_h^{k+1} \leq K$ in Ω .

With a similar reasoning, now for (3.45), we get

$$\frac{1}{dt} \left(\left(\Phi_h^{k+1} - K \right) (a) \right)_+^2 \leq \left(\widehat{f}_3 \right)_h^k (a) \left(\Phi_h^{k+1} (a) - K \right)_+ \leq 0.$$

Hence, $\left(\Phi_h^{k+1} (a) - K \right)_+ \equiv 0 \forall a \in \mathcal{N}_h$ and this implies $\Phi_h^{k+1} \leq K$ in Ω .

b) Using that $T_h^k, T_h^{k+1}, \Phi_h^k, \Phi_h^{k+1}, N_h^k \geq 0$, we can estimate (3.44) as follows

$$\begin{aligned} \frac{N_h^{k+1} (a) - N_h^k (a)}{dt} &= \alpha T_h^{k+1} (a) \sqrt{1 - (P_h^k (a))^2} + \beta_1 N_h^k (a) T_h^{k+1} (a) \\ &\quad + \delta T_h^{k+1} (a) \Phi_h^{k+1} (a) + \beta_2 N_h^k (a) \Phi_h^{k+1} (a) \geq 0. \end{aligned} \tag{3.56}$$

Hence,

$$N_h^k (a) \leq N_h^{k+1} (a) \quad \forall k = 0, \dots, K_f - 1, \text{ in } \Omega.$$

3. Theoretical and numerical analysis for a hybrid tumor model with nonlinear diffusion depending on vasculature

c) Using that $0 \leq T_h^k, T_h^{k+1}, \Phi_h^k, \Phi_h^{k+1} \leq K$ in Ω and for all $k = 0, \dots, K_f$, we can bound (3.44) in the following way

$$\frac{N_h^{k+1}(a) - N_h^k(a)}{dt} \leq C_1 N_h^k(a) + C_2, \quad \text{in } \Omega.$$

Applying discrete Gronwall inequality pointwise for every $a \in \mathcal{N}_h$, it holds that $\forall k = 1, \dots, K_f$

$$N_h^k(a) \leq N_h^0(a) e^{C_1 k dt} + C_2 \frac{e^{C_1 k dt} - 1}{C_1} \leq C (\|N_h^0\|_{L^\infty(\Omega)}, T_f) = \tilde{C}(T_f). \quad (3.57)$$

Thus, we have deduced an exponential upper bound for N_h^k , with a similar expression that in the continuous estimate obtained in Lemma 3.1a), which depends on the initial data of necrosis and the final time T_f and is independent of dt and (h, k) . □

Moreover, some a priori energy estimates will be obtained. To get these estimates, we define the piecewise functions

$$T_h^{dt} = \begin{cases} T_h^{k+1} & \text{if } t \in (t_k, t_{k+1}], \\ T_h^0 & \text{if } t = 0, \end{cases}$$

and the same for N_h^{dt} and Φ_h^{dt} .

Lemma 3.13. *Given $T_h^k, N_h^k, \Phi_h^k \in N_h$ such that $0 \leq T_h^k, \Phi_h^k \leq K$ and $0 \leq N_h^k \leq \tilde{C}(T_f)$ in Ω with $\tilde{C}(T_f)$ the upper finite bound defined in (3.57), then*

$$\|T_h^{dt}\|_{L^2(0, T_f; H^1(\Omega))}^2 = dt \sum_{k=1}^{K_f} \|T_h^k\|_{H^1(\Omega)}^2 \leq C$$

with $C > 0$ independent of (h, dt) .

Proof. Take $v = T_h^{k+1}$ in (3.43) (using that

$$(a - b)a = \frac{1}{2} (a^2 - b^2 + (a - b)^2) \geq \frac{1}{2} (a^2 - b^2)$$

for all $a, b \in \mathbb{R}$) and estimating the right hand side, it holds that

$$\frac{1}{2} \frac{1}{dt} \left(\|T_h^{k+1}\|_h^2 - \|T_h^k\|_h^2 \right) + \int_{\Omega} (\kappa_1 P_h^k + \kappa_0) |\nabla T_h^{k+1}|^2 \leq \rho (T_h^k, T_h^{k+1})_h \leq \rho K^2 |\Omega|.$$

Applying Hölder and Young's inequalities for the last right term in every node $a \in \mathcal{N}_h$, and adding in all the time steps, we get the following energy estimate

3. Theoretical and numerical analysis for a hybrid tumor model with nonlinear diffusion depending on vasculature

$$\kappa_0 dt \sum_{k=0}^{K_f-1} \|\nabla T_h^{k+1}\|_{L^2(\Omega)} \leq \frac{1}{2} \|T_h^0\|_h^2 + T_f \rho K^2 |\Omega|.$$

hence the desired bound is deduced. \square

Before presenting the energy estimate for N_h^{dt} and Φ_h^{dt} in $L^\infty(0, T_f; H^1(\Omega))$ we define the Laplacian in a discrete way using the discrete L^2 product, that is $-\Delta_h n_h \in N_h$ such that $(-\Delta_h n_h, \bar{n}_h)_h = (\nabla n_h, \nabla \bar{n}_h)$, $\forall \bar{n}_h \in N_h$. Now, we show a result of discrete Laplacian which we will use later.

Lemma 3.14. *Given $-\Delta_h n_h \in N_h$, it holds that*

$$\|-\Delta_h n_h\|_{L^2(\Omega)} \leq C \frac{1}{h} \|n_h\|_{H^1(\Omega)} \quad \forall n_h \in N_h.$$

Proof. Choosing $-\Delta_h n_h \in N_h$ as test function in the definition of discrete Laplacian, we obtain that

$$\|-\Delta_h n_h\|_h^2 = (-\Delta_h n_h, -\Delta_h n_h)_h = (\nabla n_h, \nabla (-\Delta_h n_h)) \leq \|\nabla n_h\|_{L^2(\Omega)} \frac{1}{h} \|-\Delta_h n_h\|_{L^2(\Omega)}$$

where we have used the inverse inequality $\|\bar{n}_h\|_{H^1(\Omega)} \leq C \frac{1}{h} \|\bar{n}_h\|_{L^2(\Omega)} \quad \forall \bar{n}_h \in N_h$. On other hand, we have that $\|\cdot\|_h$ and $\|\cdot\|_{L^2(\Omega)}$ are equivalent norms, hence $\|-\Delta_h n_h\|_h^2 \geq C \|-\Delta_h n_h\|_{L^2(\Omega)}^2$.

Finally, we deduce

$$\|-\Delta_h n_h\|_{L^2(\Omega)} \leq C \frac{1}{h} \|\nabla n_h\|_{L^2(\Omega)}.$$

\square

Lemma 3.15. *Given $T_h^k, N_h^k, \Phi_h^k \in N_h$ such that $0 \leq T_h^k, \Phi_h^k \leq K$ and $0 \leq N_h^k \leq \tilde{C}(T_f)$ in Ω with $\tilde{C}(T_f)$ the upper finite bound defined in (3.57), then for small enough dt , one has*

$$\left\| N_h^{dt}, \Phi_h^{dt} \right\|_{L^\infty(0, T_f; H^1(\Omega))} \leq C$$

with $C > 0$, independent of (h, dt) .

Proof. We make the proof for N_h^{dt} since for Φ_h^{dt} is similar. By multiplying by $-\Delta_h N_h^{k+1}$ in (3.50), it holds that

$$\frac{1}{2} \frac{1}{dt} \left(\left\| \nabla N_h^{k+1} \right\|_h^2 - \left\| \nabla N_h^k \right\|_h^2 \right) \leq \left(\left(\widehat{f_2} \right)_h^k, -\Delta_h N_h^{k+1} \right)_h. \quad (3.58)$$

For the right hand side, we use an extension of the Scott-Zhang interpolation operator \mathcal{Q}_h from $L^2(\Omega)$ to N_h (see [29] Proposition 2.4) and the references therein) in the following way

3. Theoretical and numerical analysis for a hybrid tumor model with nonlinear diffusion depending on vasculature

$$\left(\widehat{f}_2, -\Delta_h N_h^{k+1}\right)_h = \left(\widehat{f}_2 - \mathcal{Q}_h(\widehat{f}_2), -\Delta_h N_h^{k+1}\right)_h + \left(\mathcal{Q}_h(\widehat{f}_2), -\Delta_h N_h^{k+1}\right)_h \quad (3.59)$$

where we denoted $\widehat{f}_2 = \left(\widehat{f}_2\right)_h^k$ in order to simplify the notation.

Now, we bound (3.59) using that $\|\widehat{f}_2 - \mathcal{Q}_h(\widehat{f}_2)\|_{L^2(\Omega)} \leq Ch\|\widehat{f}_2\|_{H^1(\Omega)}$, $\|\mathcal{Q}_h(\widehat{f}_2)\|_{H^1(\Omega)} \leq C\|\widehat{f}_2\|_{H^1(\Omega)}$ and Lemma 3.14 to obtain that

$$\begin{aligned} & \left(\widehat{f}_2 - \mathcal{Q}_h(\widehat{f}_2), -\Delta_h N_h^{k+1}\right)_h + \left(\mathcal{Q}_h(\widehat{f}_2), -\Delta_h N_h^{k+1}\right)_h \leq \left(\widehat{f}_2 - \mathcal{Q}_h(\widehat{f}_2), -\Delta_h N_h^{k+1}\right)_h \\ & + \left(\nabla \mathcal{Q}_h(\widehat{f}_2), \nabla N_h^{k+1}\right) \leq Ch \|\widehat{f}_2\|_{H^1(\Omega)} \frac{1}{h} \|\nabla N_h^{k+1}\|_{L^2(\Omega)} + C \|\widehat{f}_2\|_{H^1(\Omega)} \|\nabla N_h^{k+1}\|_{L^2(\Omega)} \\ & \leq C \|\widehat{f}_2\|_{H^1(\Omega)} \|\nabla N_h^{k+1}\|_{L^2(\Omega)}. \end{aligned}$$

In these circumstances, we can follow a similar argument to (3.26) in an discrete way

$$\begin{aligned} C \|\widehat{f}_2\|_{H^1(\Omega)} \|\nabla N_h^{k+1}\|_{L^2(\Omega)} & \leq C \left(1 + \|\nabla T_h^k, \nabla T_h^{k+1}, \nabla N_h^k, \nabla \Phi_h^k, \nabla \Phi_h^{k+1}\|_{L^2(\Omega)}\right) \|\nabla N_h^{k+1}\|_{L^2(\Omega)} \\ & \leq C \left(1 + \|\nabla T_h^k, \nabla T_h^{k+1}, \nabla N_h^k, \nabla N_h^{k+1}, \nabla \Phi_h^k, \nabla \Phi_h^{k+1}\|_{L^2(\Omega)}^2\right). \end{aligned}$$

Hence,

$$\frac{1}{2} \frac{1}{dt} \left(\|\nabla N_h^{k+1}\|_h^2 - \|\nabla N_h^k\|_h^2 \right) \leq C \left(1 + \|\nabla T_h^k, \nabla T_h^{k+1}, \nabla N_h^k, \nabla N_h^{k+1}, \nabla \Phi_h^k, \nabla \Phi_h^{k+1}\|_{L^2(\Omega)}^2\right). \quad (3.60)$$

We can obtain a similar expression for Φ_h^{dt}

$$\frac{1}{2} \frac{1}{dt} \left(\|\nabla \Phi_h^{k+1}\|_h^2 - \|\nabla \Phi_h^k\|_h^2 \right) \leq C \left(1 + \|\nabla T_h^k, \nabla T_h^{k+1}, \nabla N_h^k, \nabla \Phi_h^k, \nabla \Phi_h^{k+1}\|_{L^2(\Omega)}^2\right). \quad (3.61)$$

Adding (3.60) and (3.61), multiplying by $2 dt$ and adding with respect $k = 0, \dots, \tilde{k} - 1$ with $0 \leq \tilde{k} \leq K_f$, we have (using that $\|\cdot\|_h$ is an equivalent norm to L^2)

$$\|\nabla N_h^{\tilde{k}}, \nabla \Phi_h^{\tilde{k}}\|_{L^2(\Omega)}^2 \leq C \left(T_f + dt \sum_{k=0}^{\tilde{k}} \|\nabla T_h^k, \nabla N_h^k, \nabla \Phi_h^k\|_{L^2(\Omega)}^2 \right) + C \|\nabla N_h^0, \nabla \Phi_h^0\|_{L^2(\Omega)}^2. \quad (3.62)$$

3. Theoretical and numerical analysis for a hybrid tumor model with nonlinear diffusion depending on vasculature

We can apply discrete Gronwall Lemma for any dt small enough such that $C dt \leq \delta_0 < 1$, to obtain

$$\left\| \nabla N_h^{\tilde{k}}, \nabla \Phi_h^{\tilde{k}} \right\|_{L^2(\Omega)}^2 \leq \frac{C}{1 - \delta_0} \left(T_f + dt \sum_{k=0}^{K_f} \left\| \nabla T_h^k \right\|_{L^2(\Omega)}^2 + C \left\| \nabla N_h^0, \nabla \Phi_h^0 \right\|_{L^2(\Omega)}^2 \right) e^{\frac{C}{1 - \delta_0} T_f}.$$

Since ∇T_h^{dt} is bounded in $L^2(0, T_f; L^2(\Omega))$, we deduce,

$$\left(\nabla N_h^{dt}, \nabla \Phi_h^{dt} \right) \text{ is bounded in } L^\infty(0, T_f; L^2(\Omega)).$$

Hence,

$$\left(N_h^{dt}, \Phi_h^{dt} \right) \text{ is bounded in } L^\infty(0, T_f; H^1(\Omega)).$$

□

3.4.2 Numerical Simulations

The main goals of this Section consist of:

1. Validate numerically the properties of the scheme (3.43)-(3.45), namely, the pointwise and energy estimates.
2. Compare (3.43)-(3.45) with two simplifications schemes: The first one changing the time approximation for a completely explicit scheme and later changing the space approximation for the scheme (3.43)-(3.45) without “mass-lumping”.

We start computing the lower and upper bounds of T_h^{k+1} for these schemes. We consider $T_f = 1$, time step $dt = 10^{-2}$, mesh size $h = 0.025$ and the parameters are taken as:

Parameter	κ_1	κ_0	ρ	α	β_1	β_2	γ	δ	K
Value	$8 \cdot 10^{-5}$	$8 \cdot 10^{-5}$	1	0.8	0.8	0.8	0.008	0.8	1

Table 3.1: Parameter values.

We take the initial vasculature $\Phi_0(x) = 0.5$ and the initial conditions for the tumor and necrosis given in Figure 3.1:

3. Theoretical and numerical analysis for a hybrid tumor model with nonlinear diffusion depending on vasculature

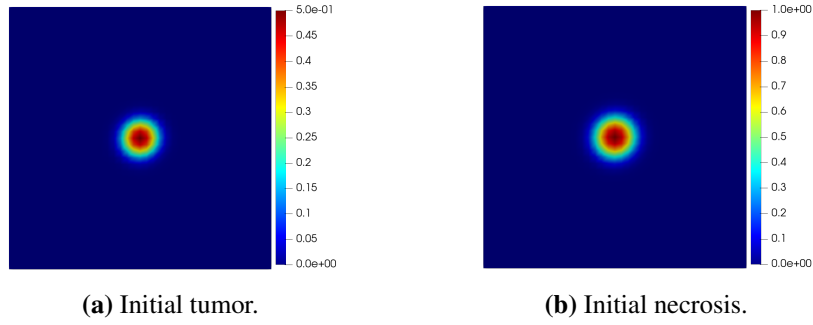


Figure 3.1: Initial tumor and necrosis.

We show in Figure 3.2 the minimum and maximum value of T_h^{k+1} in the first 10 time steps using IMEX and completely explicit scheme:

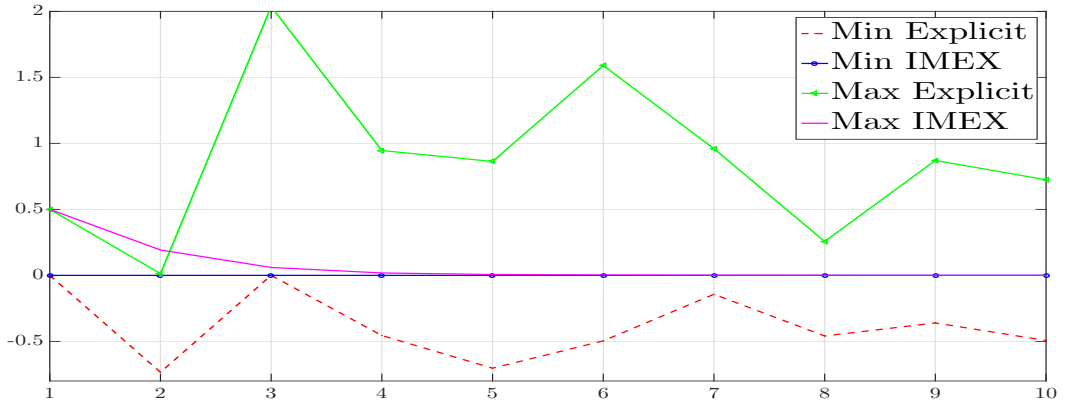


Figure 3.2: Pointwise estimate for T_h^{k+1} versus time using IMEX and completely explicit scheme.

We observe that lower and upper bounds are not satisfied for the completely explicit scheme while for IMEX scheme we get the pointwise estimates proved in Lemmas 3.11 and 3.12. Moreover, taking the mesh size h smaller, the completely explicit scheme has a similar behaviour. Hence, we can conclude that the explicit time approximation does not satisfy the maximum principle.

In our second numerical simulation, we compare graphically the lower bound of T_h^{k+1} for our scheme (3.43)-(3.45) and for the same scheme (3.43)-(3.45) but without “mass-lumping”. We consider $T_f = 1$, time step $dt = 10^{-2}$, $h = 0.1$ and the parameters are taken as:

3. Theoretical and numerical analysis for a hybrid tumor model with nonlinear diffusion depending on vasculature

Parameter	κ_1	κ_0	ρ	α	β_1	β_2	γ	δ	K
Value	$8 \cdot 10^{-4}$	$8 \cdot 10^{-4}$	1	0	0	0	0	0	1

Table 3.2: Parameter values.

We take again the initial vasculature $\Phi_0(x) = 0.5$ and the initial conditions for the tumor and necrosis given in Figure 3.1. We show in Figure 3.3 the minimum value of T_h^{k+1} in 40 time step using IMEX with “mass-lumping” and IMEX without “mass-lumping”:

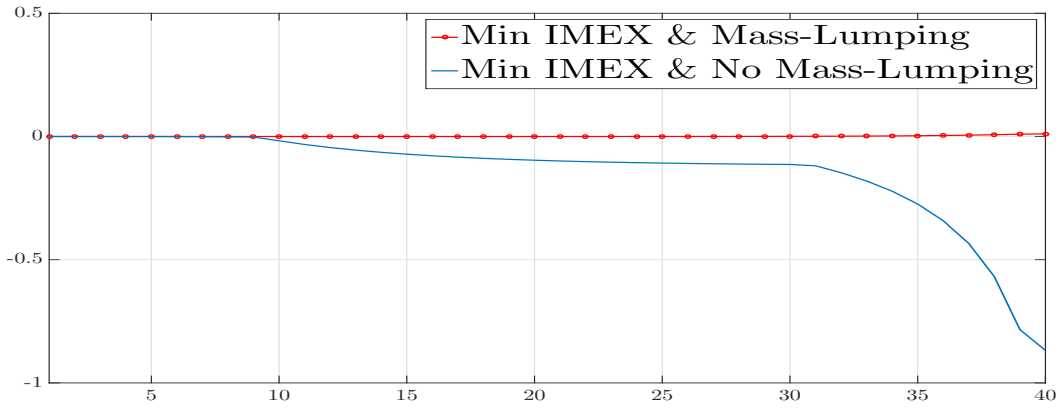


Figure 3.3: Minimum value of T_h^{k+1} using IMEX with “mass-lumping” and IMEX without “mass-lumping”.

We observe how positivity is not satisfied for IMEX without “mass-lumping” while it is conserved for IMEX with “mass-lumping”, in agreement with Lemma 3.11. Moreover, taking the time step dt smaller, we do not get positivity for scheme (3.43)-(3.45) without “mass-lumping”. Hence, we can conclude that the space approximation without “mass-lumping” does not satisfy positivity.

Thus, we have proved that the completely explicit scheme and the IMEX without “mass-lumping” do not satisfy positivity.

Finally, we are going to check the energy estimate of T_h^{k+1} obtained in Lemma 3.13 for our scheme (3.43)-(3.45) and for a completely explicit scheme and finite element with “mass-lumping”. Now, we consider $T_f = 0.01$, the mesh size $h = 0.025$, the same initial condition than in Figure 3.1) and the parameters are taken as:

3. Theoretical and numerical analysis for a hybrid tumor model with nonlinear diffusion depending on vasculature

Parameter	κ_1	κ_0	ρ	α	β_1	β_2	γ	δ	K
Value	$2.9 \cdot 10^{-7}$	$2.9 \cdot 10^{-7}$	1	0.0029	0.0029	0	0.0029	0.00029	1

Table 3.3: Parameter values.

We show in Figure 3.4 the value of $\|T_h^{dt}\|_{L^2(0,T_f;H^1(\Omega))}^2$ for the different dt obtained with

$$K_f = 10, 60, 110, 160, 210, 260, 310, 360, 410, 460, 510.$$

using the IMEX and completely explicit scheme.

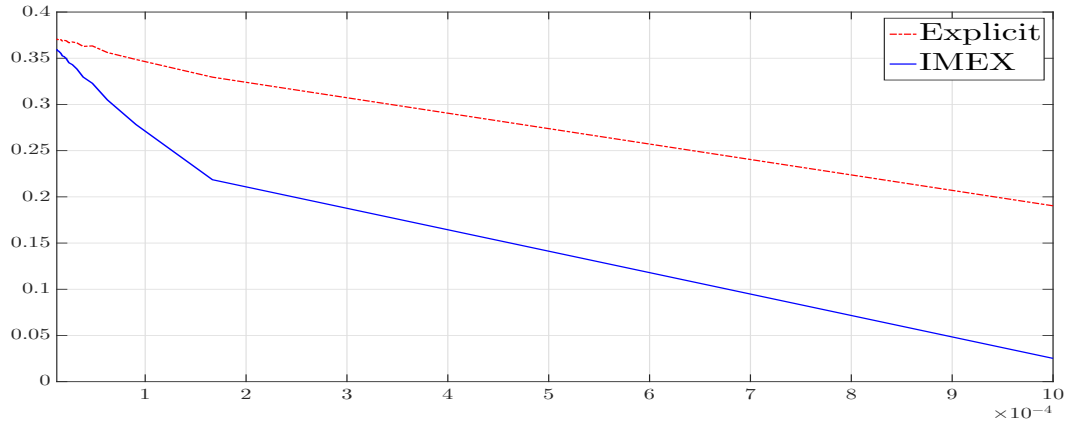


Figure 3.4: Value of $\|T_h^{dt}\|_{L^2(0,T_f;H^1(\Omega))}^2$ versus time using IMEX and completely explicit scheme.

We observe that the difference between the value of $\|T_h^{dt}\|_{L^2(0,T_f;H^1(\Omega))}^2$ using these two schemes increases as dt increases.

Remark 3.7. We have presented some numerical simulations in order to verify the analytical results of Section 3.4. In the following Chapter, we will explore the behaviour of the model depending on the parameters using appropriate numerical simulations. In particular, we will study different situations such as tumor growth with vasculature non-uniformly distributed. Moreover, in all the above simulations, the hypothesis (3.35) is satisfied and hence tumor, T , and vasculature, Φ , will vanish at infinity time. When the proliferating part of the tumor, T , goes to zero, only the necrotic part, N , remains. This situation represents that the tumor remains encapsulated, it could not longer grow.

Determining parameters giving different growths of a new Glioblastoma differential model

This Chapter is dedicated to the study of numerical simulations according to the different kind of GBM growth using the nonlinear diffusion model defined in Chapter [3](#)

The structure of the Chapter is the following: In Section [4.1](#), we present the model. In Section [4.2](#), an adimensionalization of the model is showed to reduce the number of parameters. Next, in Section [4.3](#), we make the study of the ring volume in relation to the parameters. Section [4.4](#) is devoted to study the regularity surface of the GBM with respect to the parameters. Finally, in Section [4.5](#), we discuss and summarize our results.

The results of this Chapter have been submitted to [\[23\]](#).

4. Determining parameters giving different growths of a new Glioblastoma differential model

4.1 The model

Here, we present the nonlinear diffusion model studied in Chapter 3:

$$\left\{ \begin{array}{l} \frac{\partial T}{\partial t} - \nabla \cdot ((\kappa_1 P(\Phi, T) + \kappa_0) \nabla T) = f_1(T, N, \Phi) \quad \text{in } (0, T_f] \times \Omega, \\ \frac{\partial N}{\partial t} = f_2(T, N, \Phi) \quad \text{in } (0, T_f] \times \Omega, \\ \frac{\partial \Phi}{\partial t} = f_3(T, N, \Phi) \quad \text{in } (0, T_f] \times \Omega, \end{array} \right. \quad (4.1)$$

with non-flux boundary condition

$$-(\kappa_1 P(\Phi, T) + \kappa_0) \nabla T \cdot n = 0 \quad (4.2)$$

where n is the outward unit normal vector to $\partial\Omega$, and initial conditions

$$T(0, \cdot) = T_0(x), \quad N(0, \cdot) = N_0(x), \quad \Phi(0, \cdot) = \Phi_0(x) \quad \text{in } \Omega. \quad (4.3)$$

The domain $\Omega \subset \mathbb{R}^2$ or \mathbb{R}^3 is bounded and regular and $T_f > 0$ is the final time. The nonlinear reactions terms of (4.1) are defined by

$$f_1(T, N, \Phi) := \underbrace{\rho T P(\Phi, T) \left(1 - \frac{T + N + \Phi}{K}\right)}_{\text{Tumor growth}} - \underbrace{\alpha T \sqrt{1 - P(\Phi, T)^2}}_{\text{Hypoxia}} - \underbrace{\beta_1 N T}_{\text{Tumor destruction by necrosis}}, \quad (4.4a)$$

$$f_2(T, N, \Phi) := \alpha T \sqrt{1 - P(\Phi, T)^2} + \beta_1 N T + \delta T \Phi + \beta_2 N \Phi, \quad (4.4b)$$

$$f_3(T, N, \Phi) := \underbrace{\gamma T \sqrt{1 - P(\Phi, T)^2} \frac{\Phi}{K} \left(1 - \frac{T + N + \Phi}{K}\right)}_{\text{Vasculature growth}} - \underbrace{\delta T \Phi}_{\text{Vascular destruction by tumor}} - \underbrace{\beta_2 N \Phi}_{\text{Vasculature destruction by necrosis}}. \quad (4.4c)$$

Here, factor $P(\Phi, T)$ will be a ratio between vasculature and tumor plus vasculature, and it is defined as follows

$$P(\Phi, T) = \frac{\Phi_+}{\left(\frac{\Phi_+ + K}{2}\right) + T_+}. \quad (4.5)$$

4. Determining parameters giving different growths of a new Glioblastoma differential model

Notice that the vasculature volume fraction $P(\Phi, T)$ is a continuous function in \mathbb{R}^2 , satisfying the pointwise estimates

$$0 \leq P(\Phi, T) \leq 1 \quad \forall (T, \Phi) \in [0, K] \times [0, K]$$

and $P(\Phi, T) = 0$ for $\Phi = 0$. On the other hand, the factor $\sqrt{1 - P(\Phi, T)^2}$ acting in the hypoxia term can be seen as a volume fraction measuring the lack of vasculature, and it has the same pointwise estimates that $P(\Phi, T)$.

As a reminder, the parameters in (4.1) have the following description:

Variable	Description	Value
κ_1	Anisotropic speed diffusion	cm^2/day
κ_0	Isotropic speed diffusion	cm^2/day
ρ	Tumor proliferation rate	day^{-1}
α	Hypoxic death rate by persistent anoxia	$cell/day$
β_1	Change rate from tumor to necrosis	day^{-1}
β_2	Change rate from vasculature to necrosis	day^{-1}
γ	Vasculature proliferation rate	day^{-1}
δ	Vasculature destruction by tumor action	day^{-1}
K	Carrying capacity	$cell/cm^3$

Table 4.1: Parameters.

In Chapter 3, problem (4.1)-(3.12) has been studied mathematically (from analysis to numerics). In addition, the numerical scheme, that we will use in this Chapter, has been presented in Chapter 3, proving that preserves the pointwise and energy estimates showed in Lemma 3.1

4.2 Adimensionalization

Before showing the numerical simulations related to the different GBM growths, we make a study about the parameters, simplifying and presenting only the simulations according to the relevant adimensional parameters.

The first study will depend on the carrying capacity, the parameter $K > 0$. We consider the change of variables

$$\tilde{T} = \frac{T}{K}, \quad \tilde{N} = \frac{N}{K} \quad \text{and} \quad \tilde{\Phi} = \frac{\Phi}{K}$$

4. Determining parameters giving different growths of a new Glioblastoma differential model

passing the normalized capacity to 1.

Since ρ corresponds to tumor proliferation rate and is related with the time while the diffusion parameter κ_0 is related to the spatial variable, we consider these parameters for the second adimensionalization as our point of study. Thus, we can make the following change of the independent variables:

$$\begin{cases} s = \rho t & \Rightarrow ds = \rho dt, \\ y = \sqrt{\frac{\rho}{\kappa_0}} x & \Rightarrow dy = \sqrt{\frac{\rho}{\kappa_0}} dx. \end{cases} \quad (4.6)$$

Applying these changes, our system (4.1) becomes to

$$\begin{cases} \frac{\partial \tilde{T}}{\partial s} - \nabla \cdot \left(\left(\frac{\kappa_1}{\kappa_0} P(\tilde{\Phi}, \tilde{T}) + 1 \right) \nabla \tilde{T} \right) = \tilde{f}_1(\tilde{T}, \tilde{N}, \tilde{\Phi}) \\ \frac{\partial \tilde{N}}{\partial s} = \tilde{f}_2(\tilde{T}, \tilde{N}, \tilde{\Phi}) \\ \frac{\partial \tilde{\Phi}}{\partial s} = \tilde{f}_3(\tilde{T}, \tilde{N}, \tilde{\Phi}) \end{cases} \quad (4.7)$$

where

$$\begin{cases} \tilde{f}_1(\tilde{T}, \tilde{N}, \tilde{\Phi}) = \tilde{T} P(\tilde{\Phi}, \tilde{T}) (1 - (\tilde{T} + \tilde{N} + \tilde{\Phi})) - \frac{\alpha}{\rho} \tilde{T} \sqrt{1 - P(\tilde{\Phi}, \tilde{T})^2} - K \frac{\beta_1}{\rho} \tilde{N} \tilde{T}, \\ \tilde{f}_2(\tilde{T}, \tilde{N}, \tilde{\Phi}) = \frac{\alpha}{\rho} \tilde{T} \sqrt{1 - P(\tilde{\Phi}, \tilde{T})^2} + K \frac{\beta_1}{\rho} \tilde{N} \tilde{T} + K \frac{\delta}{\rho} \tilde{T} \tilde{\Phi} + K \frac{\beta_2}{\rho} \tilde{N} \tilde{\Phi}, \\ \tilde{f}_3(\tilde{T}, \tilde{N}, \tilde{\Phi}) = \frac{\gamma}{\rho} \tilde{T} \sqrt{1 - P(\tilde{\Phi}, \tilde{T})^2} \tilde{\Phi} (1 - (\tilde{T} + \tilde{N} + \tilde{\Phi})) - K \frac{\delta}{\rho} \tilde{T} \tilde{\Phi} - K \frac{\beta_2}{\rho} \tilde{N} \tilde{\Phi}. \end{cases} \quad (4.8)$$

Hence, we can rewrite the rest of the dimensionless parameters as follows:

Dimensionless parameter	κ_1^*	α^*	β_1^*	β_2^*	γ^*	δ^*
Original parameter	$\frac{\kappa_1}{\kappa_0}$	$\frac{\alpha}{\rho}$	$K \frac{\beta_1}{\rho}$	$K \frac{\beta_2}{\rho}$	$\frac{\gamma}{\rho}$	$K \frac{\delta}{\rho}$

Table 4.2: Dimensionless parameters.

Thus, we have reduced our model in three parameters: κ_0 , ρ and K . Moreover, with this simplification, we could obtain the same conclusions depending on every parameter without the necessity

4. Determining parameters giving different growths of a new Glioblastoma differential model

to simulate the growth for different κ_0 and/or ρ since the increase or decrease of κ_0 and/or ρ will be understood as an increase or decrease of the other parameters.

Remark 4.1. *To simplify the notation, we consider along the Chapter: $s = t$, $y = x$, $\kappa_1^* = \kappa_1$, $\alpha^* = \alpha$, $\beta_i^* = \beta_i$ for $i = 1, 2$, $\gamma^* = \gamma$, $\delta^* = \delta$, $\tilde{T} = T$, $\tilde{N} = N$, $\tilde{\Phi} = \Phi$ and $\tilde{f}_i = f_i$ for $i = 1, 2, 3$.*

To get the numerical simulations we will work with an uncoupled and linear fully discrete scheme of (4.1)-(4.3) defined in (3.43)-(3.45) by means of an Implicit-Explicit (IMEX) Finite Difference in time approximation and P_1 continuous finite element with “mass-lumping” in space. The computational domain $\Omega = (-9, 9) \times (-9, 9)$ and the final time $T_f = 500$. Moreover, this scheme will preserve the pointwise and energy estimates. In the numerical setting, we construct a structured triangulation $\{\mathcal{T}_h\}_{h>0}$ of $\bar{\Omega}$ such that $\bar{\Omega} = \bigcup_{\mathcal{K} \in \mathcal{T}_h} \mathcal{K}$ with the partitioning the edges of the boundary of Ω into 45 subintervals, corresponding with the mesh size $h = 0.4$. Finally, the time step size is chosen as $dt = 10^{-3}$.

In all the simulations we consider necrosis zero initially and the initial tumor is given by Figure 4.1:

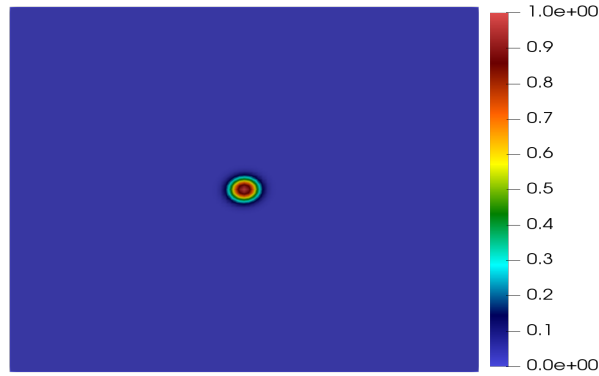


Figure 4.1: Initial tumor.

The initial condition for vasculature will change depending on the kind of tumor growth studied

4.3 Ring width

Based on the study [47], we know that tumors with a thick tumor ring have the worst prognosis, see Figure 1.2. Hence, in order to detect in our model which parameter/s could have more influence in the ring width, we will present numerical simulations according to quantify the tumor-ring with respect to the density of tumor and necrosis. For every simulation, we will change the value of one parameter and checking how the tumor growth changes. Moreover, along this Section, we take the initial vasculature

4. Determining parameters giving different growths of a new Glioblastoma differential model

defined uniformly in space.

Since we keep in mind tumor and necrosis, we move the parameters appearing in tumor and necrosis equations, these are, κ_1 , α and β_1 . In all the simulations the value of γ , δ and β_2 are fixed (see Table 4.3).

Variable	γ	δ	β_2
Value	0.255	2.55	2.55

Table 4.3: Fixed value parameters.

For the variable parameters, κ_1 , α and β_1 , we will take the following values (see Table 4.4).

Variable (Fixed value)	κ_1 (55)	α (45)	β_1 (27.5)
Ranges	[10, 100]	[10, 100]	[5, 50]

Table 4.4: Variable value parameters.

Finally, the chosen criterion in order to capture the prognosis of tumors will be through the total density of the tumor. That is, we will consider the tumor with more amount of density as the tumor with the worst prognosis.

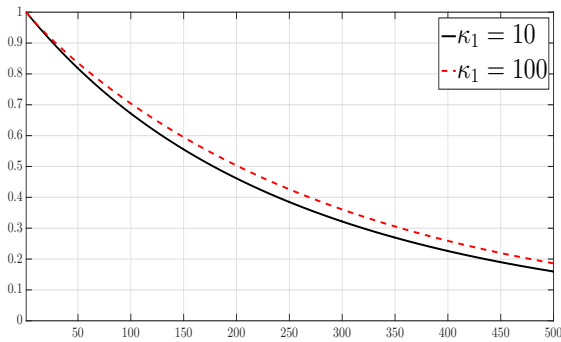
4.3.1 Tumor Ring quotient

To start with, we show the graphs according to the ratio between proliferative tumor density, $\int_{\Omega} T dx$ and total tumor density, $\int_{\Omega} (T + N) dx$, for the different values of κ_1 , α and β_1 taken in Table 4.4. For that, we have defined the following “ring quotient” (RQ) coefficient:

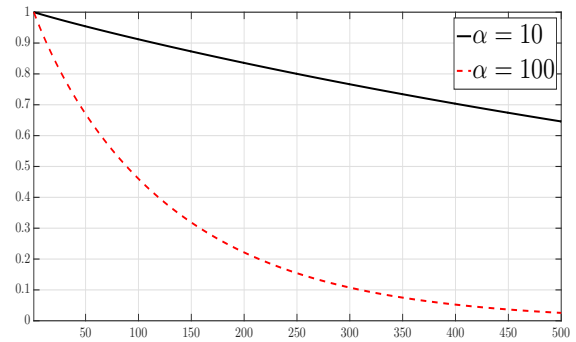
$$0 \leq \text{RQ} = \frac{\int_{\Omega} T dx}{\int_{\Omega} (T + N) dx} \leq 1. \quad (4.9)$$

Thus, we can conclude that if RQ is near to zero, tumor ring will be slim due to there exists a high density of necrosis whereas if RQ is close to one, tumor ring will be thick.

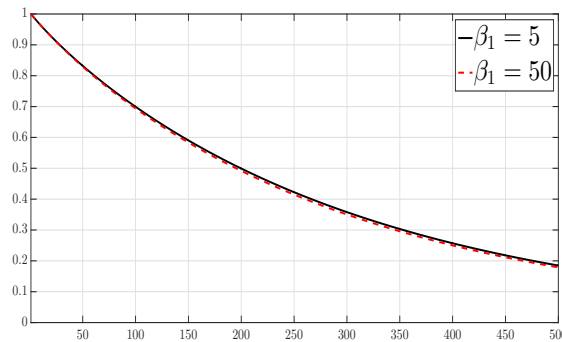
4. Determining parameters giving different growths of a new Glioblastoma differential model



(a) RQ versus time for κ_1 .



(b) RQ versus time for α .



(c) RQ versus time for β_1 .

Figure 4.2: RQ versus time for κ_1 , α and β_1 .

Since RQ measures the tumor rings, we see in Figs [4.2a](#) [4.2c](#) how the model captures three kinds of tumor ring changing mainly the parameters κ_1 , α or β_1 .

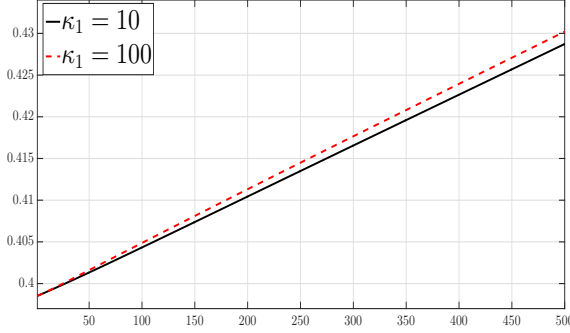
Comparing Figs [4.2a](#) [4.2c](#), we appreciate as the change in α has a greater influence in tumor rings than κ_1 and β . Hence, the best configurations to obtain a slim (resp. thick) ring would be choose a big (resp. small) α .

4.3.2 Density tumor growth

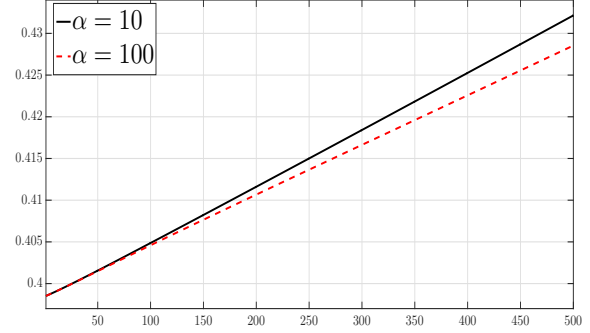
Now, we measure the amount of density of total tumor in order to obtain the different tumor growths related to different values of κ_1 , α and β .

4. Determining parameters giving different growths of a new Glioblastoma differential model

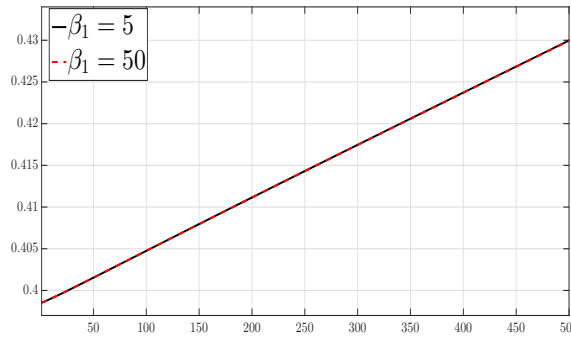
In Figure 4.3, we compare $\int_{\Omega} (T + N) dx$ for the different values of κ_1 , α and β_1 chosen in Table 4.4.



(a) $\int_{\Omega} (T + N) dx$ versus time for κ_1 .



(b) $\int_{\Omega} (T + N) dx$ versus time for α .



(c) $\int_{\Omega} (T + N) dx$ versus time for β_1 .

Figure 4.3: $\int_{\Omega} (T + N) dx$ versus time for κ_1 , α and β_1 .

We see in Figure 4.3 that the parameters κ_1 and α produce more variation than β_1 in the total tumor density.

With respect to α , see Figure 4.3b, we get the maximum density for $\alpha = 10$ due to low hypoxia allows a higher tumor growth than for high hypoxia. Thus, the minimum density is obtained for $\alpha = 100$. In the case of κ_1 , see Figure 4.3a, the difference between the two total densities is lower than for α . The maximum and minimum densities are achieved for $\kappa_1 = 100$ and $\kappa_1 = 10$, respectively.

4. Determining parameters giving different growths of a new Glioblastoma differential model

Furthermore, the highest density is obtained for $\alpha = 10$ while the density for $\alpha = 100$ and $\kappa_1 = 10$ are similar.

For the previous considerations, we can conclude that α is the most important parameter in relation to the tumor ring and α and κ_1 have more relevancy for total density in the tumor growth than β_1 .

4.4 Regularity surface

In this Section, we based on the study [49], which concludes that tumors with a high irregularity in their surface have the worst prognosis, see Figure 1.3.

We know that our model (4.7) can get different regularities for the tumor surfaces as we see in Figure 4.4, where we show in Figure 4.4a the tumor growth with the initial vasculature uniformly distributed in the space, similar to the previous Section, and in Figure 4.4b the tumor growth with the initial vasculature distributed in three zones with different concentrations of vasculature:

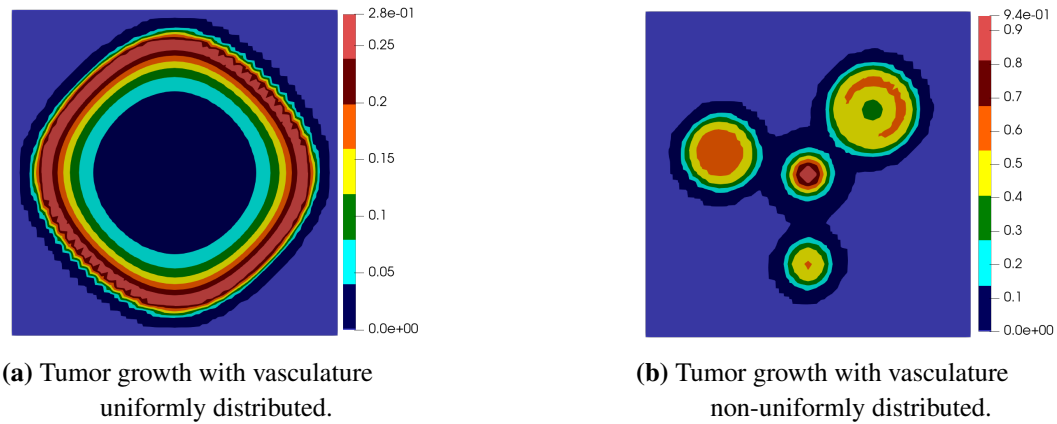


Figure 4.4: Tumor growth for different distributions of vasculature

Thus, we see as our model captures tumor growths with regular or irregular surface due to the speed of the tumor diffusion function of tumor depends on the vasculature. We remember that the adimension-alized diffusion term is defined by $\nabla \cdot ((\kappa_1 P(\Phi, T) + 1) \nabla T)$ with $\kappa_1 > 0$ and $P(\Phi, T)$ defined in (4.5). In particular, the parameter κ_1 regulates the influence of the vasculature spatial distribution in the regularity surface of the tumor.

4. Determining parameters giving different growths of a new Glioblastoma differential model

In order to detect which parameter could be more effective for the regularity surface of the tumor, we show some simulations moving the value of one parameter and checking how the tumor growth changes.

Since we focus our criteria on tumor and vasculature, we are going to move the parameters which appear in their equations, that is, κ_1 , α , β_1 , β_2 , γ and δ .

For these parameters we take the following values:

Variable (Fixed value)	κ_1 (55)	α (45)	β_1 (27.5)	β_2 (2.55)	γ (0.255)	δ (2.55)
Ranges	[10, 100]	[10, 100]	[5, 50]	[0.1, 5]	[0.01, 0.5]	[0.1, 5]

Table 4.5: Variable value parameters.

In the following simulations, the initial vasculature is distributed in various zones with different concentrations along the domain as we can see in Figure 4.5:

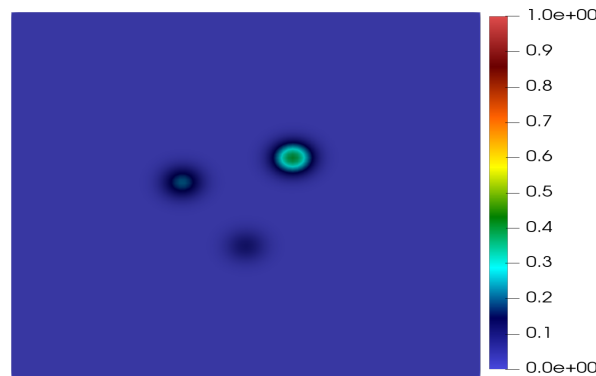


Figure 4.5: Initial vasculature.

We remember that initial tumor is defined as in Figure 4.1 and necrosis is initially zero.

4.4.1 Regularity Surface quotient

We start showing the simulations according to the following quotient between the area occupied by the total tumor (tumor and necrosis) and the area of a sphere whose radio is equal to the maximum radio of the tumor, that is the smallest sphere containing the tumor. Thus, we show this difference for the different values of κ_1 , α , β_1 , γ , δ and β_2 chosen in Table 4.5. For this, we have considered the following “surface

4. Determining parameters giving different growths of a new Glioblastoma differential model

quotient” (SQ) coefficient:

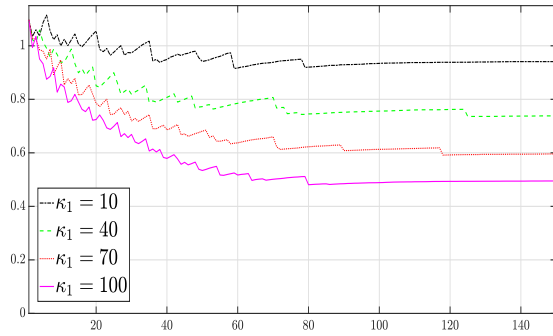
$$0 \leq \text{SQ} = \frac{\int_{\Omega} (T + N)_{\min} dx}{\pi \cdot (\mathbf{R}_{\max})^2} \leq 1 \quad (4.10)$$

where $(T + N)_{\min}$ and \mathbf{R}_{\max} are defined as follows:

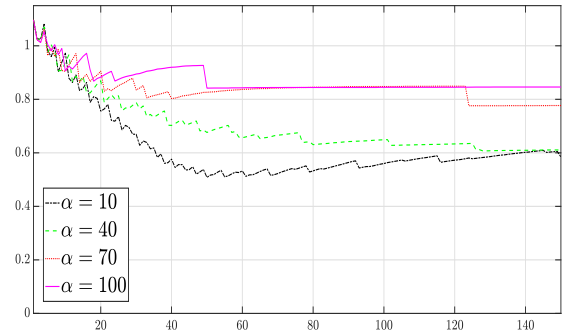
$$(T + N)_{\min} = \begin{cases} 1 & \text{if } T + N \geq 0.001, \\ 0 & \text{otherwise.} \end{cases} \quad (4.11)$$

$$\mathbf{R}_{\max} = \max \{ \text{radius of the subdomain where } (T + N)_{\min} = 1 \}. \quad (4.12)$$

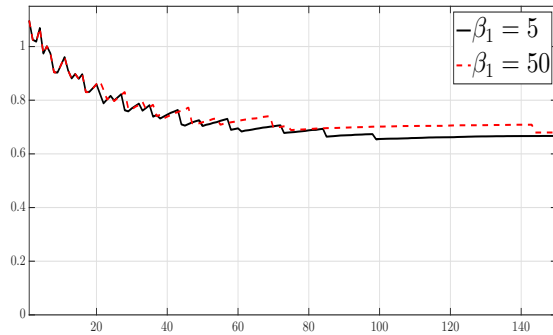
Thus, we could conclude that if SQ is near to zero, the surface will be irregular whereas if SQ is close to one, the surface will be regular.



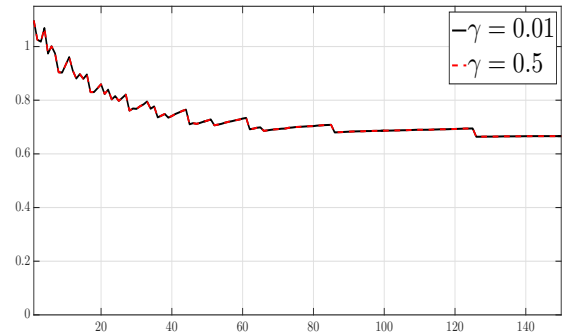
(a) SQ versus time for κ_1 .



(b) SQ versus time for α .

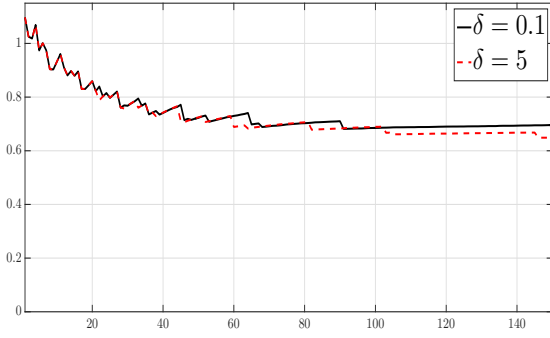


(c) SQ versus time for β_1 .

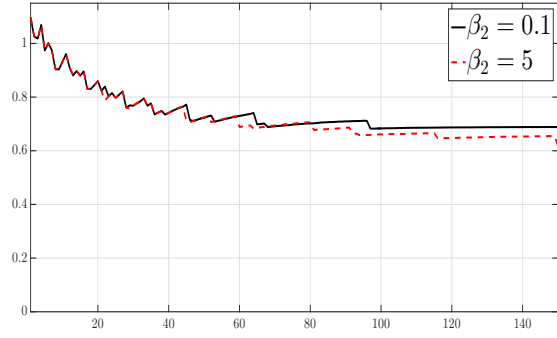


(d) SQ versus time for γ .

4. Determining parameters giving different growths of a new Glioblastoma differential model



(e) SQ versus time for δ .



(f) SQ versus time for β_2 .

Figure 4.6: SQ versus time for κ_1 , α , β_1 , γ , δ and β_2 .

Remark 4.2. Due to the size of mesh considered, at the beginning of the pictures given in Figure 4.6 the value of SQ is larger than 1 and it is observed oscillations in the graphs of SQ . Indeed, if we consider a mesh size smaller, these initial values of SQ and the oscillations can be corrected. However, it is not completely necessary the use of a mesh size smaller since we obtain the same behaviour (in average) for the mesh considered initially and we reduce the computational time.

We see in Figs 4.6a-4.6f how our model can differentiate two kinds of tumor growth changing mainly the parameters κ_1 and/or α , see Figs 4.6a and 4.6b, respectively while the variation in the parameters β_1 , γ , δ and β_2 do not change the irregularity of tumor growth as we see in Figs 4.6c-4.6f.

Once we have identified that the more important parameters for the regularity surface are κ_1 and α , we measure the area of total tumor for the different values of κ_1 and α taken in Figs 4.6a and 4.6b.

4.4.2 Area

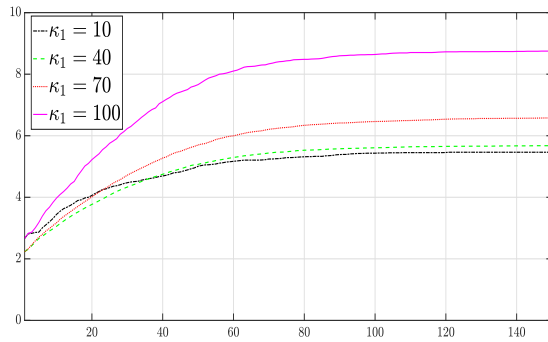
Here, we will compare the area occupied by total tumors for the different values of κ_1 and α . In order to measure this area, we consider:

$$\int_{\Omega} (T + N)_{\min} dx \quad (4.13)$$

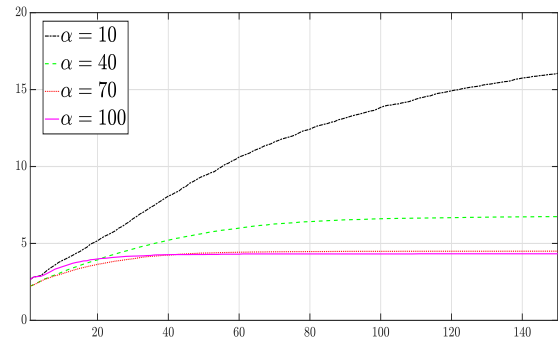
where $(T + N)_{\min}$ is defined in (4.11).

In the following graphs we show the area of total tumor (tumor and necrosis) for the different values of κ_1 and α chosen in Table 4.5.

4. Determining parameters giving different growths of a new Glioblastoma differential model



(a) Area of total tumor versus time for κ_1 .



(b) Area of total tumor time for α .

Figure 4.7: Area of total tumor versus time for κ_1 and α .

We see in Figure 4.7 how the largest area corresponds to $\alpha = 10$. For $\kappa_1 = 100$, we also obtain a high area due to the large value of anisotropic speed diffusion κ_1 . Finally, for $\kappa_1 = 10$ and $\alpha = 100$, total area has a similar variation due to the effect of low diffusion in the case of $\kappa_1 = 10$ and high tumor destruction for hypoxia in the case of $\alpha = 100$.

Thus, we deduce that the variation speed of total area is not constant for the different values of κ_1 and α considered in Figure 4.7. However, if we consider the "surface quotient" (SQ), we obtain a similar variation between the different values of κ_1 and α , see Figure 4.6. Hence, the factor which modifies this variation is the term \mathbf{R}_{\max} , defined by 4.12. Moreover, \mathbf{R}_{\max} will change more with the variation of α than for different values of κ_1 since the variation of SQ for κ_1 , Figure 4.6a, is bigger than for α , Figure 4.6b.

4.4.3 Tumor growth

In this part, we will show the tumor growth for $\kappa_1 = 100$ and $\alpha = 10$ in five time steps in order to see the spatial growth of tumor. The rest of parameters take the values showed in Table 4.5.

4. Determining parameters giving different growths of a new Glioblastoma differential model

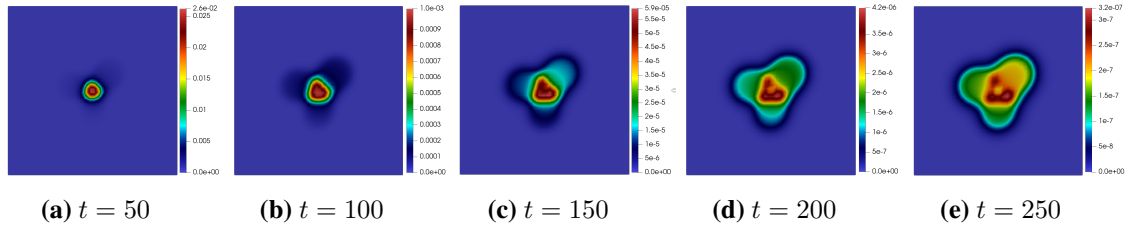


Figure 4.8: Irregular tumor growth for $\kappa_1 = 100$.

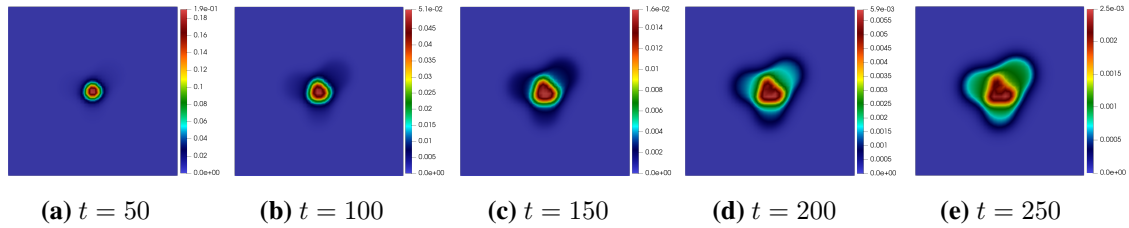


Figure 4.9: Tumor growth for $\alpha = 10$.

We observe a faster tumor growth for $\kappa_1 = 100$ than for $\alpha = 10$ in each time step. However, the amount of tumor for $\alpha = 10$ is higher than for $\kappa_1 = 100$. These results are in concordance with the obtained in Figs [4.6a](#) and [4.6b](#), where we see more irregularity for $\kappa_1 = 100$ than for $\alpha = 10$, and Figs [4.7a](#) and [4.7b](#), where the area for $\alpha = 10$ is higher than for $\kappa_1 = 100$. Furthermore, from Figure [4.8b](#), we observe that the maximum value of tumor is lower than the critical value of 0.001 given in [\(4.11\)](#) whereas in Figure [4.9](#) there are always zones where tumor achieves this critical value. Hence, it is normal that the area of total tumor for $\alpha = 10$ be higher than for $\kappa_1 = 100$.

Therefore, we can conclude that κ_1 and α are the parameters more relevant in the irregular surface of tumor and α is the most important parameter for total area in the tumor growth.

4.5 Discussion

In this Chapter, we have presented a differential system for modelling the GBM growth for which we capture two properties according this kind of brain tumor: the ring width and the regularity of the tumor surface.

In order to detect these phenomena, we have made a numerical study with respect to the parameters of the model. After the simulations and the results obtained, we have proved that the parameters more

4. Determining parameters giving different growths of a new Glioblastoma differential model

relevant according to the tumor growth are κ_1 and α .

For the tumor ring, where the vasculature is uniformly distributed, the results show that α is the most relevant parameter as we can observe in Figs [4.2a](#)-[4.2c](#). In the case of surface regularity, where the vasculature is non-uniformly distributed, the parameter which produce more irregularity in the tumor surface is κ_1 , see Figs [4.6a](#)-[4.6f](#).

However, for the total area in the surface regularity, the parameter α achieves the highest area for $\alpha = 10$. Furthermore, in Section [4.4.3](#), despite the areas for $\kappa_1 = 100$ and $\alpha = 10$ seem similar, the critical value from which the tumor is considered, defined in [\(4.11\)](#), occupies more space for $\alpha = 10$ than for κ_1 as we can see in Figs [4.9e](#) and [4.8e](#). Hence, we can conclude that not only is α the main parameter for the tumor ring, but also it can increase or decrease the amount of total area with higher influence than κ_1 .

Finally, we have reduced our study from 9 initial parameters to 2 essentials parameters which determine the both main issues of GBM; the different tumor rings and the regular or irregular tumor surface. We have showed that α is the most relevant parameter related to the density and area of tumor independently the distribution of the vasculature.

A priori estimates for a tumor chemotaxis model and for a numerical scheme

In this Chapter we analyse the chemotaxis model presented in the Introduction (1.1) for $\kappa_1 = 0$. Particularly,

$$\left\{ \begin{array}{l} \frac{\partial T}{\partial t} - \kappa_0 \Delta T + \kappa \nabla \cdot (T \nabla \Phi) = f_1(T, N, \Phi) \\ \frac{\partial N}{\partial t} = f_2(T, \Phi) \\ \frac{\partial \Phi}{\partial t} = f_3(T, N, \Phi) \end{array} \right. \quad (5.1)$$

endowed with non-flux boundary condition

$$(-\kappa_0 \nabla T + \kappa T \nabla \Phi) \cdot n = 0 \quad (5.2)$$

where n is the outward unit normal vector to $\partial\Omega$ and initial conditions

$$T(0, \cdot) = T_0, \quad N(0, \cdot) = N_0, \quad \Phi(0, \cdot) = \Phi_0 \quad \text{in } \Omega, \quad (5.3)$$

5. A priori estimates for a tumor chemotaxis model and for a numerical scheme

and where $\Omega \subset \mathbb{R}^3$ is a smooth bounded domain and $T_f > 0$ the final time. The nonlinear reactions functions $f_i : \mathbb{R}^3 \rightarrow \mathbb{R}$ for $i = 1, 2, 3$ of (5.1), have the following form

$$\begin{cases} f_1(T, N, \Phi) := \rho P(\Phi, T) T \left(1 - \frac{T + N + \Phi}{K}\right) - \alpha S(\Phi, T) T \\ f_2(T, N, \Phi) := \alpha S(\Phi, T) T + \delta Q(\Phi, T) \Phi \\ f_3(T, N, \Phi) := \gamma R(\Phi, T) \Phi \left(1 - \frac{T + N + \Phi}{K}\right) - \delta Q(\Phi, T) \Phi \end{cases} \quad (5.4)$$

where the $\rho, \alpha, \delta, \gamma, K > 0$ are defined in Table 1.1 and the dimensionless factors $P(\Phi, T)$, $S(\Phi, T)$, $R(\Phi, T)$ and $Q(\Phi, T)$ are generic factors satisfying the constraints (5.6)-(5.10).

In order to obtain some estimates of the solutions of (5.1)-(5.3) (see (5.13)), we define the following truncated system of (5.1):

$$\begin{cases} \frac{\partial T}{\partial t} - \kappa_0 \Delta T + \kappa \nabla \cdot (T_+ \nabla \Phi) = f_1(T_+, N_+, \Phi_+^K) \\ \frac{\partial N}{\partial t} = f_2(T_+, \Phi_+) \\ \frac{\partial \Phi}{\partial t} = f_3(T_+, N_+, \Phi_+^K) \end{cases} \quad (5.5)$$

subject to (5.2) and (5.3). We have denoted Φ_+^K , T_+ and N_+ as in (2.12).

The main contributions of this Chapter are the following:

Theorem 5.1 (A priori estimates). *Any regular enough solution (T, N, Φ) of (5.5)-(5.3) verifying (2.7), satisfies that:*

a)

$$0 \leq \Phi \leq K, \quad T \geq 0 \quad \text{and} \quad N \geq 0, \quad \text{a.e. in } (0, T_f) \times \Omega$$

and

$$T, N \text{ are bounded in } L^\infty(0, T_f; L^1(\Omega)).$$

b) Assume that there exists a constant $C_1 > 0$ such that

$$C_1 P(\Phi, T) \geq R(\Phi, T) \Phi \quad \forall 0 \leq \Phi \leq K, \text{ and } T \geq 0 \quad (5.6)$$

and

$$\rho \geq \frac{\kappa}{\kappa_0} \gamma C_1, \quad (5.7)$$

5. A priori estimates for a tumor chemotaxis model and for a numerical scheme

then

$$T, N \text{ are bounded in } L^\infty(0, T_f; L^\infty(\Omega)).$$

c) Assume (5.6)-(5.7) and that there exist constants $C_i > 0$ for $i = 2, 3, 4$ such that for all $0 \leq \Phi \leq K$ and $T \geq 0$,

$$\left| \frac{\partial(R(\Phi, T) \Phi)}{\partial \Phi} \right|, \left| \frac{\partial(R(\Phi, T) \Phi)}{\partial T} \right| \leq C_2, \quad (5.8)$$

$$\left| \frac{\partial(Q(\Phi, T) \Phi)}{\partial \Phi} \right|, \left| \frac{\partial(Q(\Phi, T) \Phi)}{\partial T} \right| \leq C_3 \quad (5.9)$$

and

$$\left| \frac{\partial(S(\Phi, T) T)}{\partial \Phi} \right|, \left| \frac{\partial(S(\Phi, T) T)}{\partial T} \right| \leq C_4, \quad (5.10)$$

then

$$\nabla N, \nabla \Phi \text{ are bounded in } L^\infty(0, T_f; L^2(\Omega)),$$

and

$$\nabla T \text{ is bounded in } L^2(0, T_f; L^2(\Omega)).$$

By Theorem 5.1 a), for any (T, N, Φ) solution of (5.5), we deduce that

$T_+ = T$, $N_+ = N$ and $\Phi_+^K = \Phi$ and then, $f_i(T_+, N_+, \Phi_+^K) = f_i(T, N, \Phi)$ for $i = 1, 3$ and $f_2(T_+, \Phi_+^K) = f_2(T, \Phi)$. Hence, we obtain the following crucial corollary:

Corollary 5.1. *If (T, N, Φ) is a solution of the truncated problem (5.5), then (T, N, Φ) is also a solution of (5.1)-(5.3) and (T, N, Φ) satisfies the estimates of Theorem 5.1*

Remark 5.1. *An example of dimensionless factors $P(\Phi, T)$, $S(\Phi, T)$, $R(\Phi, T)$ and $Q(\Phi, T)$ can be the following:*

$$\begin{aligned} P(\Phi, T) &= \frac{\Phi}{\Phi + T}, & S(\Phi, T) &= \frac{K - \Phi}{T + \Phi + K} \\ Q(\Phi, T) &= \frac{T}{\Phi + T}, & R(\Phi, T) &= \frac{T}{\frac{T^2}{K} + \Phi + K} \end{aligned} \quad (5.11)$$

Observe that the dimensionless factors $P(\Phi, T)$ and $R(\Phi, T)$ chosen in (5.11) satisfy the constraint imposed above in (5.6). Indeed,

$$\frac{R(\Phi, T) \Phi}{P(\Phi, T)} = \frac{T(\Phi + T)}{T^2/K + \Phi + K} \leq C_1$$

for some $C_1 > 0$.

In Section 5.2, we design a Finite Element numerical scheme, computing (Φ_k^h, T_k^h, N_k^h) as an approximation of $(\Phi(t_k, \cdot), T(t_k, \cdot), N(t_k, \cdot))$ where t_k is a partition of the time interval $(0, T_f)$ and h is the mesh size.

5. A priori estimates for a tumor chemotaxis model and for a numerical scheme

Theorem 5.2 (Discrete version of Theorem 5.1 a). *Scheme (5.43)-(5.49) has an unique solution satisfying the first pointwise estimates of Theorem 5.1 a), these are:*

$$0 \leq \Phi_h^k \leq K, \quad T_h^k \geq 0 \quad \text{and} \quad N_h^k \geq 0, \quad \text{in } \Omega. \quad (5.12)$$

The outline of the paper is as follows. In Section 5.1, we prove Theorem 5.1. In Section 5.2 we build a numerical scheme which preserves the a priori estimates of the continuous model given in Theorem 5.1 a). Finally, the more technical part of the proof of Theorem 5.1 b), obtained via an Alikakos' argument, is given in an Appendix.

The results of this Chapter have been submitted to [26].

5.1 A priori estimates of the solutions of (5.1)-(5.3)

5.1.1 Proof of Theorem 5.1 a)

Lemma 5.1. *Assuming the constraint (2.7) of initial data, any solution (T, N, Φ) of the truncated problem (5.5) satisfy the following pointwise estimates:*

$$0 \leq \Phi \leq K, \quad T \geq 0 \quad \text{and} \quad N \geq 0, \quad \text{a.e. in } (0, T_f) \times \Omega. \quad (5.13)$$

Proof. Let (T, N, Φ) be a solution of (5.5). Since one can rewrite $f_1(T_+, N_+, \Phi_+^K) = T_+ \tilde{f}_1(T_+, N_+, \Phi_+)$, multiplying the first equation of (5.5) by T_- and integrating in Ω , we get

$$\frac{1}{2} \frac{d}{dt} \int_{\Omega} (T_-)^2 dx + \kappa_0 \int_{\Omega} |\nabla T_-|^2 dx = \int_{\Omega} T_- T_+^K \tilde{f}_1(T_+, N_+, \Phi_+^K) dx = 0, \quad \text{a.e. in } (0, T_f).$$

Hence, since $T_-(0, x) = 0$, then $T_-(t, x) = 0$ a.e. $(t, x) \in (0, T_f) \times \Omega$. We repeat the same argument for the other two equations of (5.5) using now that

$$\Phi_- f_3(T_+, N_+, \Phi_+^K) = 0 \quad \text{and} \quad N_- f_2(T_+, \Phi_+) \leq 0.$$

To obtain the upper bound $\Phi \leq K$, we multiply the third equation of (5.5) by $(\Phi - K)_+$ and integrate in Ω ,

$$\frac{1}{2} \frac{d}{dt} \int_{\Omega} ((\Phi - K)_+)^2 dx = \int_{\Omega} f_3(T_+, N_+, \Phi_+^K) (\Phi - K)_+ dx, \quad \text{a.e. in } (0, T_f).$$

Since $f_3(T_+, N_+, \Phi_+^K) \leq \gamma \Phi_+^K (1 - \frac{\Phi_+^K}{K})$, then $f_3(T_+, N_+, \Phi_+^K) (\Phi - K)_+ \leq 0$. As $(\Phi(0, x) - K)_+ = 0$, then $(\Phi(t, x) - K)_+ = 0$ a.e. $(t, x) \in (0, T_f) \times \Omega$.

□

5. A priori estimates for a tumor chemotaxis model and for a numerical scheme

Lemma 5.2. *Under hypotheses of Lemma 5.1 any solution of (T, N, Φ) satisfies the estimates:*

$$\|T\|_{L^\infty(0, T_f; L^1(\Omega))} + \|\sqrt{P(\Phi, T)} T\|_{L^2(0, T_f; L^2(\Omega))} \leq C(\rho, K, |\Omega|, T_f), \quad (5.14)$$

$$\|N\|_{L^\infty(0, T_f; L^1(\Omega))} \leq C(\rho, \alpha, \delta, K, |\Omega|, T_f). \quad (5.15)$$

Proof. Let (T, N, Φ) be a solution of (5.5). Integrating in Ω the first equation of (5.5) and using that $P(\Phi, T), S(\Phi, T) \geq 0$, we obtain that

$$\begin{aligned} \frac{d}{dt} \int_{\Omega} T \, dx &= \int_{\Omega} \rho P(\Phi, T) T \, dx - \int_{\Omega} \rho P(\Phi, T) \frac{T^2}{K} \, dx - \int_{\Omega} \underbrace{\rho P(\Phi, T) T \frac{N + \Phi}{K}}_{\geq 0} \, dx \\ &\quad - \int_{\Omega} \underbrace{\alpha S(\Phi, T) T}_{\geq 0} \, dx \leq \int_{\Omega} \rho P(\Phi, T) T \, dx - \frac{1}{K} \int_{\Omega} \rho P(\Phi, T) T^2 \, dx. \end{aligned}$$

Thus,

$$\frac{d}{dt} \int_{\Omega} T \, dx + \frac{1}{K} \int_{\Omega} \rho P(\Phi, T) T^2 \, dx \leq \int_{\Omega} \rho P(\Phi, T) T \, dx.$$

Rewriting $P(\Phi, T) T = \sqrt{P(\Phi, T)} \sqrt{P(\Phi, T)} T$ and applying Young's inequality for the right side, we get,

$$\frac{d}{dt} \int_{\Omega} T \, dx + \frac{1}{K} \int_{\Omega} \rho P(\Phi, T) T^2 \, dx \leq \rho \left(\frac{1}{2K} \int_{\Omega} P(\Phi, T) T^2 \, dx + \frac{K}{2} \int_{\Omega} P(\Phi, T) \right).$$

Hence, using that $P(\Phi, T) \leq 1$, we conclude that

$$\frac{d}{dt} \int_{\Omega} T \, dx + \frac{\rho}{2K} \int_{\Omega} P(\Phi, T) T^2 \, dx \leq \frac{\rho K}{2} |\Omega|.$$

Integrating in $(0, t)$ for $0 < t \leq T_f$, we obtain that

$$\|T(t, \cdot)\|_{L^1(\Omega)} + \frac{\rho}{2K} \int_0^t \int_{\Omega} P(\Phi, T) T^2 \, dx \, dt \leq T_f \frac{\rho K}{2} |\Omega|, \quad \forall t \in (0, T_f)$$

whence we deduce (5.14).

To prove (5.15), we integrate the second equation of (5.5) in $\Omega \times (0, t)$, with $0 < t \leq T_f$,

$$\|N(t, \cdot)\|_{L^1(\Omega)} \leq \alpha \int_0^t \int_{\Omega} T \, dx \, dt + \delta \int_0^t \int_{\Omega} \Phi \, dx \, dt$$

where we have used (1.19). Thus, using that $\Phi \leq K$ and the bound obtained for T in (5.14), we get (5.15). □

5. A priori estimates for a tumor chemotaxis model and for a numerical scheme

5.1.2 Proof of Theorem 5.1 b)

In order to obtain the L^∞ estimate for T , firstly we make a change of variable such that we rewrite the diffusion term and chemotaxis term as an unique diffusion term depending on the new variable. In fact, we consider:

$$w = \log(T) - \chi \Phi \Leftrightarrow T = e^w e^{\chi \Phi} = e^{\chi \Phi} u \quad (5.16)$$

with $u = e^w$ and $\chi = \frac{\kappa}{\kappa_0}$.

Thus, the first equation of (5.1) changes to

$$(e^{\chi \Phi} u)_t - \kappa_0 \nabla \cdot (e^{\chi \Phi} \nabla u) = f_1(e^{\chi \Phi} u, N, \Phi) \quad (5.17)$$

and the boundary condition (5.2) to

$$\nabla u \cdot n = 0. \quad (5.18)$$

Lemma 5.3 (Proof of Theorem 5.1 b)). *Assume hypotheses on the factors (5.6) and on the parameters (5.7). Then, given any solution (T, N, Φ) of (5.5), it holds that u is bounded in $L^\infty(0, T_f; L^\infty(\Omega))$ and ∇u is bounded in $L^2(0, T_f; L^2(\Omega))$. Moreover, T and N are bounded in $L^\infty(0, T_f; L^\infty(\Omega))$.*

Proof. To obtain the L^∞ estimates for T and N , taking into account the L^∞ estimates for Φ , it suffices that u be L^∞ . The proof of u is based in L^p estimates with an Alikakos' argument. Let (T, N, Φ) be a solution of (5.5). We multiply (5.17) by u^{p-1} (for any $p \geq 2$), and analyse term by term:

- Time derivative term:

$$(e^{\chi \Phi} u)_t u^{p-1} = \chi \Phi_t e^{\chi \Phi} u^p + \frac{1}{p} e^{\chi \Phi} (u^p)_t \quad (5.19)$$

and the second term of the right side of (5.19) can be expressed as

$$\frac{1}{p} e^{\chi \Phi} (u^p)_t = \frac{1}{p} (e^{\chi \Phi} u^p)_t - \frac{\chi}{p} e^{\chi \Phi} u^p \Phi_t. \quad (5.20)$$

Hence, from (5.19) and (5.20),

$$(e^{\chi \Phi} u)_t u^{p-1} = \frac{1}{p} (e^{\chi \Phi} u^p)_t + \frac{p-1}{p} \chi \Phi_t e^{\chi \Phi} u^p. \quad (5.21)$$

- Nonlinear diffusion term:

$$\begin{aligned} -\kappa_0 \nabla \cdot (e^{\chi \Phi} \nabla u) u^{p-1} &= -\kappa_0 \nabla \cdot (e^{\chi \Phi} (\nabla u) u^{p-1}) + \kappa_0 e^{\chi \Phi} (p-1) u^{p-2} |\nabla u|^2 \\ &= -\kappa_0 \nabla \cdot (e^{\chi \Phi} (\nabla u) u^{p-1}) + \kappa_0 e^{\chi \Phi} (p-1) \frac{4}{p^2} |\nabla(u^{p/2})|^2. \end{aligned} \quad (5.22)$$

5. A priori estimates for a tumor chemotaxis model and for a numerical scheme

- Reaction term:

$$f_1(e^{\chi \Phi} u, N, \Phi) u^{p-1} = \rho P(\Phi, T) e^{\chi \Phi} u^p \left(1 - \frac{e^{\chi \Phi} u + N + \Phi}{K}\right) - \alpha S(\Phi, T) e^{\chi \Phi} u^p. \quad (5.23)$$

Rewriting in (5.21) the function Φ_t as $f_3(e^{\chi \Phi} u, N, \Phi)$ and adding (5.21), (5.22) and (5.23), we get:

$$\begin{aligned} & \frac{1}{p} (e^{\chi \Phi} u^p)_t - \kappa_0 \nabla \cdot (e^{\chi \Phi} (\nabla u) u^{p-1}) + \kappa_0 e^{\chi \Phi} (p-1) \frac{4}{p^2} |\nabla(u^{p/2})|^2 + \alpha S(\Phi, T) e^{\chi \Phi} u^p \\ & + \left(\rho P(\Phi, T) - \left(\frac{p-1}{p}\right) \chi \gamma R(\Phi, T) \Phi \right) e^{\chi \Phi} u^p \left(\frac{e^{\chi \Phi} u + N + \Phi}{K} \right) \\ & = \left(\rho P(\Phi, T) - \left(\frac{p-1}{p}\right) \chi \gamma R(\Phi, T) \Phi \right) e^{\chi \Phi} u^p + \frac{\chi}{p} e^{\chi \Phi} u^p \delta Q(\Phi, T) \Phi. \end{aligned} \quad (5.24)$$

Due to hypothesis (5.6) and (5.7), it is easy to see in (5.24) that,

$$\rho P(\Phi, T) - \left(\frac{p-1}{p}\right) \chi \gamma R(\Phi, T) \Phi \geq 0.$$

Using now that $0 \leq \Phi \leq K$, (1.19) and (5.7) we obtain that

$$\begin{aligned} & \frac{1}{p} (e^{\chi \Phi} u^p)_t - \kappa_0 \nabla \cdot (e^{\chi \Phi} (\nabla u) u^{p-1}) + \kappa_0 e^{\chi \Phi} (p-1) \frac{4}{p^2} |\nabla(u^{p/2})|^2 + \alpha S(\Phi, T) e^{\chi \Phi} u^p \\ & \leq C e^{\chi \Phi} u^p \end{aligned} \quad (5.25)$$

with $C > 0$. Integrating (5.25) in Ω , it holds that

$$\begin{aligned} & \frac{1}{p} \frac{d}{dt} \int_{\Omega} e^{\chi \Phi} u^p dx + \nu (p-1) \frac{4}{p^2} \int_{\Omega} e^{\chi \Phi} |\nabla(u^{p/2})|^2 dx + \alpha \int_{\Omega} S(\Phi, T) e^{\chi \Phi} u^p dx \\ & \leq C \int_{\Omega} e^{\chi \Phi} u^p dx. \end{aligned} \quad (5.26)$$

with $C > 0$ independent of p (along the proof, we will denote by C different constants independent of p).

Using the auxiliary variable $w = u^{p/2}$, we can rewrite (5.26) as follows

5. A priori estimates for a tumor chemotaxis model and for a numerical scheme

$$\frac{1}{p} \frac{d}{dt} \|e^{\frac{\chi\Phi}{2}} w\|_{L^2(\Omega)}^2 + 4 \kappa_0 \frac{(p-1)}{p^2} \|e^{\frac{\chi\Phi}{2}} \nabla w\|_{L^2(\Omega)}^2 \leq C \|e^{\frac{\chi\Phi}{2}} w\|_{L^2(\Omega)}^2. \quad (5.27)$$

Thus, applying Gronwall's lemma, we deduce for $p = 2$ that

$$\nabla u \text{ is bounded in } L^2(0, T_f; L^2(\Omega)).$$

Now, using the following equivalent norms with constants independent of p

$$\|z\|_{L^2(\Omega)}^2 \leq \|e^{\frac{\chi\Phi}{2}} z\|_{L^2(\Omega)}^2 \leq e^{\chi K} \|z\|_{L^2(\Omega)}^2, \quad (5.28)$$

multiplying (5.27) by p and using that $\frac{p-1}{p} \geq \frac{1}{2}$ for any $p \geq 2$, we obtain that

$$\frac{d}{dt} \|e^{\frac{\chi\Phi}{2}} w\|_{L^2(\Omega)}^2 + 2\nu \|\nabla w\|_{L^2(\Omega)}^2 \leq C p \|w\|_{L^2(\Omega)}^2. \quad (5.29)$$

We are going to apply the following Gagliardo-Nirenberg interpolation inequality ([27, Theorem 10.1])

$$\|w\|_{L^2(\Omega)}^2 \leq \varepsilon \|\nabla w\|_{L^2(\Omega)}^2 + C \left(\frac{1}{\varepsilon}\right)^{n/2} \|w\|_{L^1(\Omega)}^2 \quad (5.30)$$

with $\varepsilon > 0$ and n the dimension of Ω (in this case $n = 3$). Applying (5.30) for $\varepsilon = \frac{\nu}{C p}$ in the right hand side of (5.29), we deduce that

$$\frac{d}{dt} \|e^{\frac{\chi\Phi}{2}} w\|_{L^2(\Omega)}^2 + \kappa_0 \|\nabla w\|_{L^2(\Omega)}^2 \leq C p^2 \|w\|_{L^1(\Omega)}^2. \quad (5.31)$$

Using (5.30) in (5.31) but now for $\varepsilon = \nu$, it holds that

$$\frac{d}{dt} \|e^{\frac{\chi\Phi}{2}} w\|_{L^2(\Omega)}^2 + \|w\|_{L^2(\Omega)}^2 \leq C (p^2 + 1) \|w\|_{L^1(\Omega)}^2. \quad (5.32)$$

Finally, due to (5.28), we can deduce that

$$\frac{d}{dt} \|e^{\frac{\chi\Phi}{2}} w\|_{L^2(\Omega)}^2 + C_1 \|e^{\frac{\chi\Phi}{2}} w\|_{L^2(\Omega)}^2 \leq C (p^2 + 1) \|w\|_{L^1(\Omega)}^2. \quad (5.33)$$

where $C_1 = e^{-\chi K}$.

5. A priori estimates for a tumor chemotaxis model and for a numerical scheme

Hence, we obtain that

$$\begin{aligned}
 \max_{t \in (0, T_f)} \|u\|_{L^p(\Omega)}^p &\leq \|e^{\frac{\chi \Phi}{2}} w(t)\|_{L^2(\Omega)}^2 \leq e^{-C_1 t} C \|u_0\|_{L^\infty(\Omega)}^p \\
 + C(p^2 + 1) e^{-C_1 t} \int_0^t e^{C_1 s} \left(\int_{\Omega} u^{p/2} dx \right)^2 ds &\leq C \|u_0\|_{L^\infty(\Omega)}^p + C(p^2 + 1) \max_{t \in (0, T_f)} \|u\|_{L^{p/2}(\Omega)}^p \\
 &\leq C \max \left\{ (p^2 + 1) \max_{t \in (0, T_f)} \|u\|_{L^{p/2}(\Omega)}^p, \|u_0\|_{L^\infty(\Omega)}^p \right\}.
 \end{aligned} \tag{5.34}$$

Following a similar argument to used by Alikakos in [3] (see Appendix), we can obtain that

$$u \text{ is bounded in } L^\infty(0, T_f; L^\infty(\Omega)).$$

As consequence, T is bounded in $L^\infty(0, T_f; L^\infty(\Omega))$.

Since $N_t = f_2(T, \Phi)$ and T and Φ are bounded in $L^\infty(0, T_f; L^\infty(\Omega))$ we obtain that N is bounded in $L^\infty(0, T_f; L^\infty(\Omega))$. \square

5.1.3 Proof of Theorem 5.1 c)

Let (T, N, Φ) be a solution of (5.5). Taking gradient in the second and third equation of (5.5),

$$\begin{aligned}
 (\nabla \Phi)_t &= \gamma \left[\left(\frac{\partial(R(\Phi, T) \Phi)}{\partial \Phi} \nabla \Phi + \frac{\partial(R(\Phi, T) \Phi)}{\partial T} \nabla T \right) \left(1 - \frac{T + N + \Phi}{K} \right) \right. \\
 &\quad \left. - \frac{R(\Phi, T) \Phi}{K} (\nabla T + \nabla N + \nabla \Phi) \right] - \delta \left(\frac{\partial(Q(\Phi, T) \Phi)}{\partial \Phi} \nabla \Phi \right. \\
 &\quad \left. + \frac{\partial(Q(\Phi, T) \Phi)}{\partial T} \nabla T \right),
 \end{aligned} \tag{5.35}$$

$$\begin{aligned}
 (\nabla N)_t &= \alpha \left(\frac{\partial(S(\Phi, T) T)}{\partial \Phi} \nabla \Phi + \frac{\partial(S(\Phi, T) T)}{\partial T} \nabla T \right) \\
 &\quad + \delta \left(\frac{\partial(Q(\Phi, T) \Phi)}{\partial \Phi} \nabla \Phi + \frac{\partial(Q(\Phi, T) \Phi)}{\partial T} \nabla T \right).
 \end{aligned} \tag{5.36}$$

Using the change of variable $T = e^{\chi \Phi} u$ as in Lemma 5.3, we deduce that

$$\nabla T = \chi e^{\chi \Phi} u \nabla \Phi + e^{\chi \Phi} \nabla u = \chi T \nabla \Phi + e^{\chi \Phi} \nabla u \tag{5.37}$$

5. A priori estimates for a tumor chemotaxis model and for a numerical scheme

and we know from Lemma 5.3 that ∇u is bounded in $L^2(0, T_f; L^2(\Omega))$. Taking into account that T and Φ are bounded in $L^\infty(0, T_f; L^\infty(\Omega))$, it holds that

$$|\nabla T| \leq C (|\nabla \Phi| + |\nabla u|).$$

Thus, rewriting (5.35) and (5.36) in terms of ∇u , multiplying (5.35) and (5.36) by $\nabla \Phi$ and ∇N respectively and integrating in Ω , we deduce

$$\frac{1}{2} \frac{d}{dt} \|\nabla \Phi\|_{L^2(\Omega)}^2 \leq C_1 \|\nabla \Phi\|_{L^2(\Omega)}^2 + C_2 \int_{\Omega} |\nabla u| |\nabla \Phi| dx + C_3 \int_{\Omega} |\nabla N| |\nabla \Phi| dx, \quad (5.38)$$

and

$$\frac{1}{2} \frac{d}{dt} \|\nabla N\|_{L^2(\Omega)}^2 \leq C_4 \int_{\Omega} |\nabla \Phi| |\nabla N| dx + C_5 \int_{\Omega} |\nabla u| |\nabla N| dx, \quad (5.39)$$

with $C_i > 0$ for $i = 1, \dots, 5$. In (5.38) and (5.39) we have applied the inequality for

$$\int_{\Omega} v |\nabla u| |\nabla \Phi| dx \leq \|v\|_{L^\infty(\Omega)} \int_{\Omega} |\nabla u| |\nabla \Phi| dx$$

with $v = T, N, \Phi$ since T, N and Φ are bounded in $L^\infty(0, T_f; L^\infty(\Omega))$.

Using now Cauchy-Schwarz and Young's inequalities in (5.38) and (5.39) and adding them, it holds that

$$\frac{1}{2} \frac{d}{dt} \left(\|\nabla \Phi\|_{L^2(\Omega)}^2 + \|\nabla N\|_{L^2(\Omega)}^2 \right) \leq \widehat{C}_1 \left(\|\nabla \Phi\|_{L^2(\Omega)}^2 + \|\nabla N\|_{L^2(\Omega)}^2 \right) + \widehat{C}_2 \|\nabla u\|_{L^2(\Omega)}^2, \quad (5.40)$$

with $\widehat{C}_i > 0$ for $i = 1, 2$. Since ∇u is bounded in $L^2(0, T_f; L^2(\Omega))$, applying Gronwall's Lemma, it holds that

$$\nabla N \text{ and } \nabla \Phi \text{ are bounded in } L^\infty(0, T_f; L^2(\Omega)).$$

Finally, using (5.37) in (5.35) and (5.36), we obtain that

$$(\nabla N)_t \text{ and } (\nabla \Phi)_t \text{ are bounded in } L^2(0, T_f; L^2(\Omega)).$$

Corollary 5.2. ∇T is bonded in $L^2(0, T_f; L^2(\Omega))$.

5.2 A FE numerical scheme

In this Section, we are going to design an uncoupled and linear fully discrete scheme to approach (5.1)-(5.3) by means of an Implicit-Explicit (IMEX) Finite Difference in time and P_1 continuous finite element with “mass-lumping” in space discretization. This scheme will preserve the pointwise estimates that appear in Lemma 5.1 considering acute triangulations.

Now we introduce the hypotheses required along this Section.

- a) Let $0 < T_f < +\infty$. We consider the uniform time partition

$$(0, T_f] = \bigcup_{k=0}^{K_f-1} (t_k, t_{k+1}],$$

with $t_k = k dt$ where $K_f \in \mathbb{N}$ and $dt = \frac{T_f}{K_f}$ is the time step. Let $\Omega \subseteq \mathbb{R}^2$ or \mathbb{R}^3 a bounded domain with polygonal or polyhedral lipschitz-continuous boundary.

- b) Let $\{\mathcal{T}_h\}_{h>0}$ be a family of shape-regular, quasi-uniform triangulations of $\bar{\Omega}$ formed by acute N-simplexes (triangles in 2D and tetrahedral in 3D with all angles lower than $\pi/2$), such that

$$\bar{\Omega} = \bigcup_{\mathcal{K} \in \mathcal{T}_h} \mathcal{K},$$

where $h = \max_{\mathcal{K} \in \mathcal{T}_h} h_{\mathcal{K}}$, with $h_{\mathcal{K}}$ being the diameter of \mathcal{K} . We denote $\mathcal{N}_h = \{a_i\}_{i \in I}$ the set of all the nodes of \mathcal{T}_h .

- c) Conforming piecewise linear, finite element spaces associated to \mathcal{T}_h are assumed for approximating $H^1(\Omega)$:

$$N_h = \{n_h \in C^0(\bar{\Omega}) : n_h|_{\mathcal{K}} \in \mathcal{P}_1(\mathcal{K}), \forall \mathcal{K} \in \mathcal{T}_h\}$$

and its Lagrange basis is denoted by $\{\varphi_a\}_{a \in \mathcal{N}_h}$.

Let $I_h : C^0(\bar{\Omega}) \rightarrow N_h$ be the nodal interpolation operator and consider the discrete inner product

$$(n_h, \bar{n}_h)_h = \int_{\Omega} I_h(n_h \cdot \bar{n}_h) = \sum_{a \in \mathcal{N}_h} n_h(a) \bar{n}_h(a) \int_{\Omega} \varphi_a, \quad \forall n_h, \bar{n}_h \in N_h$$

which induces the discrete norm $\|n_h\|_h = \sqrt{(n_h, n_h)_h}$ defined on N_h (that is equivalent to $L^2(\Omega)$ -norm).

5. A priori estimates for a tumor chemotaxis model and for a numerical scheme

Before building the numerical scheme, we will transform the first equation of (5.1) into a non-linear diffusion equation throughout the variable change of variable $T = u e^{\chi \Phi}$ as in Lemma 5.3. Therefore, the first equation of (5.1) changes to:

$$e^{\chi \Phi} u_t - \kappa_0 \nabla \cdot (e^{\chi \Phi} \nabla u) = \widehat{f}_1(u, N, \Phi) \quad (5.41)$$

where

$$\begin{aligned} \widehat{f}_1(u, N, \Phi) = & T \left[\rho P(\Phi, T) + \chi \Phi \left(\gamma R(\Phi, T) \left(\frac{T + N + \Phi}{K} \right) + \delta Q(\Phi, T) \right) \right] \\ & - T \left[\rho P(\Phi, T) \left(\frac{T + N + \Phi}{K} \right) + \alpha S(\Phi, T) + \chi \gamma R(\Phi, T) \Phi \right] \end{aligned} \quad (5.42)$$

with $T = e^{\chi \Phi} u$.

Thus, we consider the following linear uncoupled numerical scheme for the model (5.41) jointly with (5.1)_b and (5.1)_c: given $u_h^k, N_h^k, \Phi_h^k \in N_h$, find $u_h^{k+1}, N_h^{k+1}, \Phi_h^{k+1} \in N_h$ in a decoupled way (first Φ , then u and finally N) satisfying

$$\left(e^{\chi \Phi_h^k} \delta_t u_h^{k+1}, v \right)_h + \nu \left(e^{\chi \Phi_h^k} \nabla u_h^{k+1}, \nabla v \right) = \left(\left(\widehat{f}_1 \right)_h^k, v \right)_h, \quad \forall v \in N_h, \quad (5.43)$$

$$\delta_t N_h^{k+1}(a) = \left(\widehat{f}_2 \right)_h^k(a), \quad \forall a \in N_h, \quad (5.44)$$

$$\delta_t \Phi_h^{k+1}(a) = \left(\widehat{f}_3 \right)_h^k(a) \quad \forall a \in N_h. \quad (5.45)$$

We have denoted

$$\delta_t u_h^{k+1} = \frac{u_h^{k+1} - u_h^k}{dt}$$

and similarly for $\delta_t N_h^{k+1}$ and $\delta_t \Phi_h^{k+1}$. The approximation of the initial conditions are taken as

$$u_h^0 = I_h(u_0) \in N_h, \quad N_h^0 = I_h(N_0) \in N_h, \quad \Phi_h^0 = I_h(\Phi_0) \in N_h \quad (5.46)$$

where we consider for simplicity that $T_0, N_0, \Phi_0 \in C^0(\overline{\Omega})$ with $u_0 = e^{-\chi \Phi_0} T_0$.

Finally, the functions $\left(\widehat{f}_i \right)_h^k$ for $i = 1, 2, 3$ which appear in (5.43), (5.44) and (5.45), have the following definitions:

5. A priori estimates for a tumor chemotaxis model and for a numerical scheme

$$\begin{aligned} (\widehat{f}_1)_h^k &= T_h^k \left(\rho P_h^k + \chi \Phi_h^k \left(\gamma R_h^k \left(\frac{T_h^k + N_h^k + \Phi_h^k}{K} \right) + \delta Q_h^k \right) \right) \\ &\quad - T_h^{k+1} \left(\rho P_h^k \left(\frac{T_h^k + N_h^k + \Phi_h^k}{K} \right) + \alpha S_h^k + \chi \gamma R_h^k \Phi_h^k \right), \end{aligned} \quad (5.47)$$

$$(\widehat{f}_2)_h^k = \alpha S_h^k T_h^{k+1} + \delta Q_h^k \Phi_h^{k+1}, \quad (5.48)$$

$$(\widehat{f}_3)_h^k = \gamma R_h^k \Phi_h^k \left(1 - \frac{\Phi_h^{k+1}}{K} \right) - \Phi_h^{k+1} \left(\gamma R_h^k \frac{T_h^k + N_h^k}{K} + \delta Q_h^k \Phi_h^{k+1} \right). \quad (5.49)$$

The functions P_h^k , S_h^k , R_h^k and Q_h^k in (5.47)-(5.49), are the corresponding dimensionless factors $P(\Phi_h^k, T_h^k)$, $S(\Phi_h^k, T_h^k)$, $R(\Phi_h^k, T_h^k)$ and $Q(\Phi_h^k, T_h^k)$ defined in (??) with $T_h^k = e^{\chi \Phi_h^k} u_h^k$ and $T_h^{k+1} = e^{\chi \Phi_h^{k+1}} u_h^{k+1}$.

Remark 5.2. *There exists an unique solution of scheme (5.43)-(5.49) because:*

1. $\Phi_h^{k+1}(a)$ can be computed directly from (5.45).
2. There exists an unique u_h^{k+1} solution of (5.43) by Lax-Milgran.
3. $N_h^{k+1}(a)$ can be computed directly from (5.44).

5.2.1 Proof of Theorem 5.2

In this part, we are going to get a priori energy estimates for the fully discrete solution u_h^{k+1} , N_h^{k+1} and Φ_h^{k+1} (and hence, for T_h^{k+1}) of (5.43), (5.44) and (5.45) which are independent of (h, k) .

The following result is based on the hypothesis of acute triangulations to get a discrete maximum principle, see [12]. In fact, we arrive at discrete version of Lemma 5.1.

Lemma 5.4 (Proof of Theorem 5.2). *Let u_h^k , N_h^k , $\Phi_h^k \in N_h$ with $T_h^k = e^{\chi \Phi_h^k} u_h^k$ such that $0 \leq u_h^k$, N_h^k , Φ_h^k in Ω (in particular $T_h^k \geq 0$ in Ω). Then, $0 \leq \Phi_h^{k+1} \leq K$ and u_h^{k+1} , $N_h^{k+1} \geq 0$ in Ω (and also $T_h^{k+1} \geq 0$).*

Proof. • Step 1. $\Phi_h^{k+1} \geq 0$.

Multiplying (5.45) by $(\Phi_h^{k+1}(a))_-$ and using that $\Phi_h^k(a) \geq 0$, it holds that:

$$\frac{1}{dt} \left(\Phi_h^{k+1}(a) \right)_-^2 \leq (\widehat{f}_3)_h^k(a) \left(\Phi_h^{k+1}(a) \right)_-. \quad (5.50)$$

5. A priori estimates for a tumor chemotaxis model and for a numerical scheme

Indeed, using the form of $(\widehat{f_3})_h^k$ given in (5.49), the following estimates hold

$$\gamma R_h^k(a) \left(\Phi_h^k(a) \right) \left(\Phi_h^{k+1}(a) \right)_- \leq 0$$

and

$$- \left(\gamma R_h^k(a) \left(\frac{T_h^k(a) + N_h^k(a) + \Phi_h^k(a)}{K} \right) + \delta Q_h^k(a) \right) \left(\Phi_h^{k+1}(a) \right) \left(\Phi_h^{k+1}(a) \right)_- \leq 0.$$

Adding the last two inequalities, one has

$$\left(\widehat{f_3} \right)_h^k(a) \left(\Phi_h^{k+1}(a) \right)_- \leq 0. \quad (5.51)$$

Therefore, from (5.50) and (5.51), $\left(\Phi_h^{k+1}(a) \right)_- \equiv 0 \forall a \in \mathcal{N}_h$ and this implies $\Phi_h^{k+1} \geq 0$ in Ω .

- Step 2. $\Phi_h^{k+1} \leq K$.

Multiplying (5.45) by $\left(\left(\Phi_h^{k+1} - K \right)(a) \right)_+$, it holds that

$$\frac{1}{dt} \left(\left(\Phi_h^{k+1} - K \right)(a) \right)_+^2 \leq \left(\widehat{f_3} \right)_h^k(a) \left(\Phi_h^{k+1}(a) - K \right)_+ \quad (5.52)$$

On the other hand, since in every node $a \in \mathcal{N}$, due to the form of $(\widehat{f_3})_h^k$ given in (5.49) the following estimates hold

$$\left(\gamma R_h^k(a) \Phi_h^k(a) \left(1 - \frac{\Phi_h^{k+1}(a)}{K} \right) \right) \left(\Phi_h^{k+1}(a) - K \right)_+ \leq 0$$

and

$$- \left(\gamma R_h^k(a) \left(\frac{T_h^k(a) + N_h^k(a)}{K} \right) + \delta Q_h^k(a) \right) \left(\Phi_h^{k+1}(a) \right) \left(\Phi_h^{k+1}(a) - K \right)_+ \leq 0.$$

Thus, adding the last two inequalities, we obtain that

$$\left(\widehat{f_3} \right)_h^k(a) \left(\Phi_h^{k+1}(a) - K \right)_+ \leq 0. \quad (5.53)$$

Therefore, from (5.52) and (5.53), $\left(\Phi_h^{k+1}(a) - K \right)_+ \equiv 0 \forall a \in \mathcal{N}_h$ and this implies $\Phi_h^{k+1} \leq K$ in Ω .

5. A priori estimates for a tumor chemotaxis model and for a numerical scheme

- Step 3. $u_h^{k+1} \geq 0$.

Let $I_h((u_h^{k+1})_-) \in N_h$ be defined as

$$I_h\left(\left(u_h^{k+1}\right)_-\right) = \sum_{a \in \mathcal{N}_h} \left(u_h^{k+1}(a)\right)_- \varphi_a,$$

where $\left(u_h^{k+1}(a)\right)_- = \min\{0, u_h^{k+1}(a)\}$. Analogously, one defines $I_h((u_h^{k+1})_+) \in N_h$ as

$$I_h\left(\left(u_h^{k+1}\right)_+\right) = \sum_{a \in \mathcal{N}_h} \left(u_h^{k+1}(a)\right)_+ \varphi_a,$$

where $\left(u_h^{k+1}(a)\right)_+ = \max\{0, u_h^{k+1}(a)\}$. Notice that $u_h^{k+1} = I_h((u_h^{k+1})_-) + I_h((u_h^{k+1})_+)$.

Choosing $v = I_h((u_h^{k+1}(a))_-)$ in [\(5.43\)](#), it follows that,

$$\begin{aligned} \frac{1}{dt} \left\| \left(u_h^{k+1}\right)_- \right\|_h^2 + \nu \left(\left(e^{\chi \Phi_h^k}\right) \nabla u_h^{k+1}, \nabla I_h\left(\left(u_h^{k+1}\right)_-\right) \right) &\leq \\ &\leq \left(\widehat{f}_1\left(u_h^k, u_h^{k+1}, N_h^k, \Phi_h^k\right), \left(u_h^{k+1}\right)_- \right)_h, \end{aligned} \tag{5.54}$$

where we have used in the left hand side that

$$\frac{1}{dt} \left\| \left(u_h^{k+1}\right)_- \right\|_h^2 \leq \frac{1}{dt} \left\| \left(e^{\frac{\chi \Phi_h^k}{2}}\right) \left(u_h^{k+1}\right)_- \right\|_h^2$$

and that in every node $a \in \mathcal{N}_h$,

$$\begin{aligned} \delta_t u_h^{k+1}(a) \cdot \left(u_h^{k+1}(a)\right)_- &= \frac{1}{dt} \left(\left| \left(u_h^{k+1}(a)\right)_- \right|^2 - u_h^k(a) \cdot \left(u_h^{k+1}(a)\right)_- \right) \geq \\ &\geq \frac{1}{dt} \left(\left| \left(u_h^{k+1}(a)\right)_- \right|^2 \right) \end{aligned}$$

using that $e^{\chi \Phi_h^k(a)} > 0$, $u_h^k(a) \geq 0$ and $\left(u_h^{k+1}(a)\right)_- \leq 0$. On the other hand, we can make the following decomposition in the diffusion term

$$\begin{aligned} \left(\left(e^{\chi \Phi_h^k}\right) \nabla u_h^{k+1}, \nabla I_h\left(\left(u_h^{k+1}\right)_-\right) \right) &= \left(\left(e^{\chi \Phi_h^k}\right) \nabla I_h\left(\left(u_h^{k+1}\right)_-\right), \nabla I_h\left(\left(u_h^{k+1}\right)_-\right) \right) \\ + \left(\left(e^{\chi \Phi_h^k}\right) \nabla I_h\left(\left(u_h^{k+1}\right)_+\right), \nabla I_h\left(\left(u_h^{k+1}\right)_-\right) \right) &= \left\| \left(e^{\chi \Phi_h^k}\right)^{1/2} \nabla I_h\left(\left(u_h^{k+1}\right)_-\right) \right\|_{L^2(\Omega)}^2 \end{aligned}$$

5. A priori estimates for a tumor chemotaxis model and for a numerical scheme

$$+ \sum_{a \neq \tilde{a} \in \mathcal{N}_h} \left(u_h^{k+1}(a) \right)_- \left(u_h^{k+1}(\tilde{a}) \right)_+ \left(\left(e^{\chi \Phi_h^k} \right) \nabla \varphi_a, \nabla \varphi_{\tilde{a}} \right).$$

Hence, using that $\left(u_h^{k+1}(a) \right)_- \left(u_h^{k+1}(\tilde{a}) \right)_+ \leq 0$ if $a \neq \tilde{a}$, $e^{\chi \Phi_h^k(a)}$ is a positive function and that

$$\nabla \varphi_a \cdot \nabla \varphi_{\tilde{a}} \leq 0 \quad \forall a \neq \tilde{a} \in \mathcal{N}_h$$

(owing to the hypothesis of acute triangulation), we deduce,

$$\left(\left(e^{\chi \Phi_h^k} \right) \nabla u_h^{k+1}, \nabla I_h \left(\left(u_h^{k+1} \right)_- \right) \right) \geq \left\| \left(e^{\chi \Phi_h^k} \right)^{1/2} \nabla I_h \left(\left(u_h^{k+1} \right)_- \right) \right\|_{L^2(\Omega)}^2. \quad (5.55)$$

Adding (5.55) in (5.54), it holds that

$$\frac{1}{dt} \left\| \left(u_h^{k+1} \right)_- \right\|_h^2 + \nu \left\| \left(e^{\chi \Phi_h^k} \right)^{1/2} \nabla I_h \left(\left(u_h^{k+1} \right)_- \right) \right\|_{L^2(\Omega)}^2 \leq \left(\left(\widehat{f}_1 \right)_h^k, \left(u_h^{k+1} \right)_- \right)_h. \quad (5.56)$$

On the other hand, by using that in every node $a \in \mathcal{N}_h$, due to the form of $\left(\widehat{f}_1 \right)_h^k$ given in (5.47), the following estimates hold

$$\begin{aligned} & \left(\rho P_h^k(a) + \chi \Phi_h^k(a) \left(\gamma R_h^k(a) \left(\frac{T_h^k(a) + N_h^k(a) + \Phi_h^k(a)}{K} \right) + \delta Q_h^k(a) \right) \right) \\ & \quad \cdot \left(T_h^k(a) \right) \left(u_h^{k+1}(a) \right)_- \leq 0 \end{aligned}$$

and

$$\begin{aligned} & - \left(\rho P_h^k(a) \left(\frac{T_h^k(a) + N_h^k(a) + \Phi_h^k(a)}{K} \right) + \alpha S_h^k(a) + \chi \gamma R_h^k(a) \Phi_h^k(a) \right) \\ & \quad \cdot \left(T_h^{k+1}(a) \right) \left(u_h^{k+1}(a) \right)_- \leq 0 \end{aligned}$$

owing to $\left(T_h^{k+1}(a) \right) \left(u_h^{k+1}(a) \right)_- = \left(\left(u_h^{k+1}(a) \right)_- \right)^2 e^{\chi \Phi_h^{k+1}(a)} \geq 0$.

Then, adding the last two inequalities, we obtain that

$$\left(\left(\widehat{f}_1 \right)_h^k, \left(u_h^{k+1} \right)_- \right)_h \leq 0 \quad (5.57)$$

Therefore, from (5.56) and (5.57), $\left(u_h^{k+1} \right)_- \equiv 0$ and this implies $u_h^{k+1} \geq 0$ in Ω . As we recover T_h^{k+1} from u_h^{k+1} and Φ_h^{k+1} as $T_h^{k+1} = e^{\chi \Phi_h^{k+1}} u_h^{k+1}$, we have in particular that $T_h^{k+1} \geq 0$ in Ω .

5. A priori estimates for a tumor chemotaxis model and for a numerical scheme

- Step 4. $N_h^{k+1} \geq 0$

Finally, for (5.44) it is easy to obtain that

$$\frac{1}{dt} \left(N_h^{k+1}(a) \right)_-^2 \leq \left(\widehat{f}_2 \right)_h^k(a) \left(N_h^{k+1}(a) \right)_-. \quad (5.58)$$

In addition, $\left(\widehat{f}_2 \right)_h^k(a) \geq 0$ in every node $a \in \mathcal{N}_h$ due to the form of $\left(\widehat{f}_2 \right)_h^k$ given in (5.48). Hence,

$$\left(\widehat{f}_2 \right)_h^k(a) \left(N_h^{k+1}(a) \right)_- \leq 0. \quad (5.59)$$

Thus, from (5.58) and (5.59), $\left(N_h^{k+1}(a) \right)_- \equiv 0 \forall a \in \mathcal{N}_h$ and this implies $N_h^{k+1} \geq 0$ in Ω . □

5.3 Appendix

In this Appendix, we will prove an Alikakos recursive L^∞ estimate.

Following the proof of Lemma 5.3, we obtain in (5.34) that

$$\max_{t \in (0, T_f)} \|u\|_{L^p(\Omega)}^p \leq \widetilde{C} \max \left\{ (p^2 + 1) \max_{t \in (0, T_f)} \|u\|_{L^{p/2}(\Omega)}^p, \|u_0\|_{L^\infty(\Omega)}^p \right\}. \quad (5.60)$$

In [3], the authors obtained an estimate starting from an estimate like (5.60) but with power p instead of p^2 . Taking in (5.60) $p = 2^k$ for all $k \geq 1$, it holds that,

$$\begin{aligned} \max_{t \in (0, T_f)} \int_{\Omega} u^{2^k} dx &\leq C \max \left\{ \left(2^{2^k} + 1 \right) \max_{t \in (0, T_f)} \left(\int_{\Omega} u^{2^{k-1}} dx \right)^2, \|u_0\|_{L^\infty(\Omega)}^{2^k} \right\} \\ &\leq C C^2 \max \left\{ \left(2^{2^k} + 1 \right) \left[\max \left\{ \left(2^{2^{k-1}} + 1 \right) \max_{t \in (0, T_f)} \left(\int_{\Omega} u^{2^{k-2}} dx \right)^2 \right\} \right] \right\}, \end{aligned}$$

5. A priori estimates for a tumor chemotaxis model and for a numerical scheme

$$\begin{aligned}
& \left. \left. \|u_0\|_{L^\infty(\Omega)}^{2^{k-1}} \right\} \right]^2, \|u_0\|_{L^\infty(\Omega)}^{2^k} \left. \right\} \\
& \leq C C^2 C^{2^2} \max \left\{ (2^{2^k} + 1) (2^{2^{(k-1)}} + 1)^2 \left(\max_{t \in (0, T_f)} \int_\Omega u^{2^{k-3}} dx \right)^{2^2}, \right. \\
& \quad \left. (2^{2^k} + 1) \|u_0\|_{L^\infty(\Omega)}^{2^k} \right\} \\
& \leq C C^2 C^{2^2} C^{2^3} \max \left\{ (2^{2^k} + 1) (2^{2^{(k-1)}} + 1)^2 (2^{2^{(k-2)}} + 1)^{2^3} \max_{t \in (0, T_f)} \left(\int_\Omega u^{2^{k-3}} dx \right)^{2^3}, \right. \\
& \quad \left. (2^{2^k} + 1) (2^{2^{(k-1)}} + 1)^2 \|u_0\|_{L^\infty(\Omega)}^{2^k} \right\} \leq \dots \leq \\
& \leq \left(C (2^{2^k} + 1) \right) \left(C (2^{2^{(k-1)}} + 1) \right)^2 \left(C (2^{2^{(k-2)}} + 1) \right)^{2^2} \dots \left(C (2^2 + 1) \right)^{2^{k-1}} \tilde{K}^{2^k}. \tag{5.61}
\end{aligned}$$

where \tilde{K} is the constant that dominates $\|u\|_{L^1(\Omega)}$ for all time, since $u \in L^\infty(0, T_f; L^1(\Omega))$ (using Lemma 5.2 taking into account that $\|u_0\|_{L^\infty(\Omega)}$ and the hypothesis (2.7)). Thus, from (5.61)

$$\max_{t \in (0, T_f)} \int_\Omega u^{2^k} dx \leq (a 2^{2^k}) (a 2^{2^{(k-1)}})^2 (a 2^{2^{(k-2)}})^{2^2} (a 2^{2^{(k-3)}})^{2^3} \dots (a 2^2)^{2^{k-1}} \tilde{K}^{2^k}. \tag{5.62}$$

for a certain $a \geq 3C$ since $C(2^{2^{(k-j)}} + 1) \leq a 2^{2^k}$ if $a \geq 3C$ for all $j = 0, \dots, k-1$. Thus, we can express (5.62) as

$$\max_{t \in (0, T_f)} \int_\Omega u^{2^k} dx \leq a^{\sum_{j=0}^{k-1} 2^j} 2^{2 \sum_{j=0}^{k-1} (k-j) 2^j} \tilde{K}^{2^k} = a^{2^k - 1} 2^{(-k-6+2^{k+1})} \tilde{K}^{2^k}. \tag{5.63}$$

Taking the limit as $k \rightarrow +\infty$ of the $1/2^k$ power of both sides of (5.63) we obtain

$$\max_{t \in (0, T_f)} \|u\|_{L^\infty(\Omega)} \leq \lim_{k \rightarrow +\infty} \left(a^{\frac{2^k - 1}{2^k}} 2^{\frac{(-k-6+2^{k+1})}{2^k}} \tilde{K} \right) = a 2^2 \tilde{K}. \tag{5.64}$$

Hence,

$$u \in L^\infty(0, +\infty; L^\infty(\Omega)).$$

Numerical Simulations of a Glioblastoma PDE-ODE system with chemotaxis

In this Chapter, our propose is to use the PDE-ODE chemotactic model defined in Chapter 5 in order to check if we can capture the same phenomena about the GBM growth that in Chapter 4 and compare the results obtained here with the conclusions of Chapter 4.

Thus, the structure of this Chapter is as follows. First, In Section 6.1, we present the model. Next, in Section 6.2, we make a dimensionless study of the model. Finally, Section 6.3 is dedicated to show the different behaviour of the ring width and the regularity surface simulations with respect to the dimensionless parameters in Section 6.3.1 and 6.3.2, respectively.

The results of this Chapter have been submitted to [26].

6.1 Model

The chemotactic PDE-ODE model to be used in this Chapter, and studied in Chapter 5, is given by the equations

6. Numerical Simulations of a Glioblastoma PDE-ODE system with chemotaxis

$$\left\{ \begin{array}{l} \frac{\partial T}{\partial t} - \underbrace{\kappa_0 \Delta T}_{\text{Diffusion}} + \underbrace{\kappa \nabla \cdot (T \nabla \Phi)}_{\text{Chemotaxis}} = f_1(T, N, \Phi) \\ \frac{\partial N}{\partial t} = f_2(T, \Phi) \\ \frac{\partial \Phi}{\partial t} = f_3(T, N, \Phi) \end{array} \right. \quad (6.1)$$

endowed with non-flux boundary condition

$$(-\kappa_0 \nabla T + \kappa T \nabla \Phi) \cdot n = 0 \quad (6.2)$$

where n is the outward unit normal vector to $\partial\Omega$ and initial conditions

$$T(0, \cdot) = T_0, \quad N(0, \cdot) = N_0, \quad \Phi(0, \cdot) = \Phi_0 \quad \text{in } \Omega. \quad (6.3)$$

Here $\Omega \subset \mathbb{R}^2$ or \mathbb{R}^3 is a smooth bounded domain and $T_f > 0$ the final time.

The nonlinear functions $f_i : \mathbb{R}^3 \rightarrow \mathbb{R}$ for $i = 1, 2, 3$ denote the reaction functions and they have the following form

$$f_1(T, N, \Phi) := \underbrace{\rho P(\Phi, T) T \left(1 - \frac{T + N + \Phi}{K}\right)}_{\text{Tumor growth}} - \underbrace{\alpha S(\Phi, T) T}_{\text{Hypoxia}} \quad (6.4a)$$

$$f_2(T, N, \Phi) := \alpha S(\Phi, T) T + \delta Q(\Phi, T) \Phi \quad (6.4b)$$

$$f_3(T, N, \Phi) := \underbrace{\gamma R(\Phi, T) \Phi \left(1 - \frac{T + N + \Phi}{K}\right)}_{\text{Vasculature growth}} - \underbrace{\delta Q(\Phi, T) \Phi}_{\text{Vascular destruction by the tumor}} \quad (6.4c)$$

where

$$P(\Phi, T) = \frac{\Phi}{\Phi + T}, \quad (6.5)$$

$$S(\Phi, T) = \frac{K - \Phi}{T + (\Phi + K)}, \quad (6.6)$$

$$R(\Phi, T) = \frac{T}{\frac{T^2}{K} + \frac{\Phi + K}{2}} \quad (6.7)$$

6. Numerical Simulations of a Glioblastoma PDE-ODE system with chemotaxis

and

$$Q(\Phi, T) = \frac{T}{\Phi + T} \quad (6.8)$$

Moreover, notice that

$$0 \leq P(\Phi, T), S(\Phi, T), Q(\Phi, T), R(\Phi, T) \leq 1 \quad \forall (T, \Phi) \in \mathbb{R}^2. \quad (6.9)$$

We have considered in (6.4a) that the velocity of the tumor growth is proportional to $P(\Phi, T)$ since vasculature supplies nutrients and oxygenation to cells. Furthermore, tumor cells are destructed by the lack of vasculature in the hypoxia death rate of tumor cells, which is modelled by the factor $S(\Phi, T)$. From equation (6.4c), we also put a logistic growth term since vasculature needs space to growth. However, in the speed of the vasculature growth the presence of tumor through the factor $R(\Phi, T)$ shows that there will not be growth of vasculature in absence of tumor or in circumstance where tumor achieves a high value. Furthermore, a destruction of vasculature by tumor is considered with the factor $Q(\Phi, T)$.

For the convenience of the reader, we remember the description of the parameters of (6.1):

Variable	Description	Value
κ_0	Speed diffusion	$\frac{\text{cm}^2}{\text{sec}}$
κ	Speed chemotaxis	$\frac{\text{sec} \cdot \text{density}}{\text{cm}^2}$
ρ	Tumor proliferation rate	day^{-1}
α	Hypoxic death rate	day^{-1}
γ	Vasculature proliferation rate	day^{-1}
δ	Vasculature destruction by tumor	day^{-1}
K	Carrying capacity	cell/cm^3

Table 6.1: Parameters.

6.2 Adimensionalization

Here, we simplify the number of the parameters of (6.1) and present the simulations according to the dimensionless parameters.

We start studying the carrying capacity parameter $K > 0$. We consider the change of variables

$$\tilde{T} = \frac{T}{K}, \quad \tilde{N} = \frac{N}{K} \quad \text{and} \quad \tilde{\Phi} = \frac{\Phi}{K}$$

6. Numerical Simulations of a Glioblastoma PDE-ODE system with chemotaxis

passing the normalized capacity equal to 1.

Now, we consider the diffusion parameter κ_0 and the tumor proliferation parameter ρ since we know that ρ is related to the time variable while κ_0 is related to the spatial variable. Thus, we can make the following change of the independent variables:

$$\begin{cases} s = \rho t & \Rightarrow ds = \rho dt, \\ y = \sqrt{\frac{\rho}{\kappa_0}} x & \Rightarrow dy = \sqrt{\frac{\rho}{\kappa_0}} dx. \end{cases} \quad (6.10)$$

Applying these changes in the system (6.1), it holds that

$$\begin{cases} \frac{\partial \tilde{T}}{\partial s} - \Delta \tilde{T} + K \frac{\kappa}{\kappa_0} \nabla \cdot (\tilde{T} \nabla \tilde{\Phi}) & = \tilde{f}_1(\tilde{T}, \tilde{N}, \tilde{\Phi}) \\ \frac{\partial \tilde{N}}{\partial s} & = \tilde{f}_2(\tilde{u}, \tilde{\Phi}) \\ \frac{\partial \tilde{\Phi}}{\partial s} & = \tilde{f}_3(\tilde{u}, \tilde{N}, \tilde{\Phi}) \end{cases} \quad (6.11)$$

where

$$\begin{cases} \tilde{f}_1(\tilde{T}, \tilde{N}, \tilde{\Phi}) & = P(\tilde{\Phi}, \tilde{T}) \tilde{T} (1 - (\tilde{T} + \tilde{N} + \tilde{\Phi})) - \frac{\alpha}{\rho} S(\tilde{\Phi}, \tilde{T}) \tilde{T}, \\ \tilde{f}_2(\tilde{T}, \tilde{\Phi}) & = \frac{\alpha}{\rho} S(\tilde{\Phi}, \tilde{T}) \tilde{T} + \frac{\delta}{\rho} Q(\tilde{\Phi}, \tilde{T}) \tilde{\Phi}, \\ \tilde{f}_3(\tilde{T}, \tilde{N}, \tilde{\Phi}) & = \frac{\gamma}{\rho} R(\tilde{\Phi}, \tilde{T}) \tilde{\Phi} (1 - (\tilde{T} + \tilde{N} + \tilde{\Phi})) - \frac{\delta}{\rho} Q(\tilde{\Phi}, \tilde{T}) \tilde{\Phi}. \end{cases} \quad (6.12)$$

Hence, we obtain the following dimensionless parameters:

Dimensionless parameter	κ^*	α^*	γ^*	δ^*
Original parameter	$K \frac{\kappa}{\kappa_0}$	$\frac{\alpha}{\rho}$	$\frac{\gamma}{\rho}$	$\frac{\delta}{\rho}$

Table 6.2: Dimensionless parameters.

Thus, we have reduced our model in three parameters: ρ , κ_0 and K .

Remark 6.1. To simplify the notation, we consider along the Chapter: $s = t$, $y = x$, $\kappa^* = \kappa$, $\alpha^* = \alpha$, $\gamma^* = \gamma$, $\delta^* = \delta$, $\tilde{T} = T$, $\tilde{N} = N$, $\tilde{\Phi} = \Phi$ and $\tilde{f}_i = f_i$ for $i = 1, 2, 3$.

6. Numerical Simulations of a Glioblastoma PDE-ODE system with chemotaxis

Finally, the adimensionalized system is the following:

$$\left\{ \begin{array}{l} \frac{\partial T}{\partial t} - \Delta T + \kappa \nabla \cdot (T \nabla \Phi) = P(\Phi, T) T (1 - (T + N + \Phi)) - \alpha S(\Phi, T) T, \\ \frac{\partial N}{\partial t} = \alpha S(\Phi, T) T + \delta Q(\Phi, T) \Phi, \\ \frac{\partial \Phi}{\partial t} = \gamma R(\Phi, T) \tilde{\Phi} (1 - (T + N + \Phi)) - \delta Q(\Phi, T) \Phi. \end{array} \right. \quad (6.13)$$

6.3 Numerical Simulations

In this Section, we will show some numerical simulations in order to detect which parameters of (6.13) are more important in the behaviour ring width between tumor and necrosis and the regular or irregular growth of the surface of a GBM.

To get the numerical simulations we will use with the uncoupled and linear fully discrete scheme defined in (5.43)-(5.45) by means of an Implicit-Explicit (IMEX) Finite Difference in time approximation and P_1 continuous finite element with “mass-lumping” in space.

We will use the computational domain, $\Omega = (-9, 9) \times (-9, 9)$, the final time, $T_f = 500$, the structured triangulation, $\{\mathcal{T}_h\}_{h>0}$ of $\bar{\Omega}$ such that $\bar{\Omega} = \bigcup_{\mathcal{K} \in \mathcal{T}_h} \mathcal{K}$, partitioning the edges of $\partial\Omega$ into 45 subintervals, corresponding with the mesh size $h = 0.4$ and the time step, $dt = 10^{-3}$.

We consider along the simulations necrosis zero initially and initial tumor given by Figure 4.1. For the vasculature, we will take again different initial conditions depending on the kind of tumor growth considered.

6.3.1 Ring width

The first tumor growth considered, is related to the tumor ring. For that, we will contrast our results with an experimental study made in [47] where they show the following graph:

6. Numerical Simulations of a Glioblastoma PDE-ODE system with chemotaxis

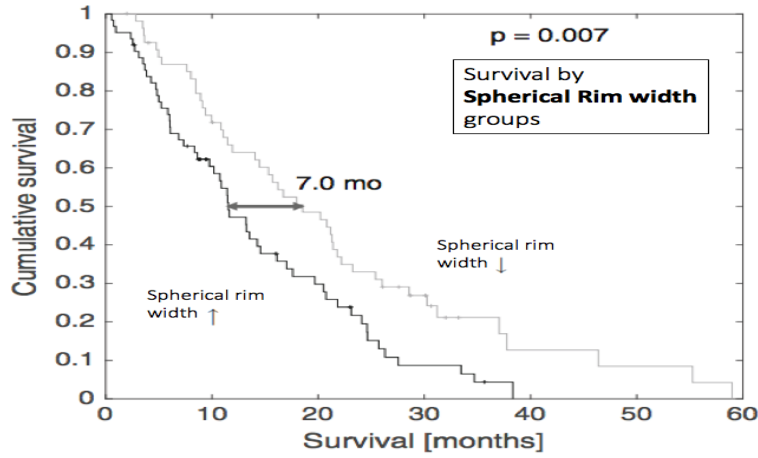


Figure 6.1: Survival vs the ring width of GBM.

Figure 6.1 determines that tumors with slim ring have better prognostic than tumors with thick ring.

Here, we present some numerical simulations according to the tumor-ring. For this, we will compare the density of tumor with respect to the density of tumor and necrosis. In every simulation, we will change the value of one parameter and testing how the tumor growth changes.

Since the subjects of study are tumor and necrosis, we change the parameters of the tumor and necrosis equations, these are, κ and α . Then, in all the simulations the value of γ and δ are fixed (see Table 6.3).

Variable	γ	δ
Value	0.255	2.55

Table 6.3: Fixed value parameters.

For κ and α , we will take either $\kappa = 5$ and $\alpha \in [10, 100]$ or $\kappa \in [1, 10]$ and $\alpha = 45$ (see Table 6.4).

Variable (Fixed value)	κ (5)	α (45)
Ranges	[1, 10]	[10, 100]

Table 6.4: Variable value parameters.

Moreover, we take the initial vasculature defined uniformly in space.

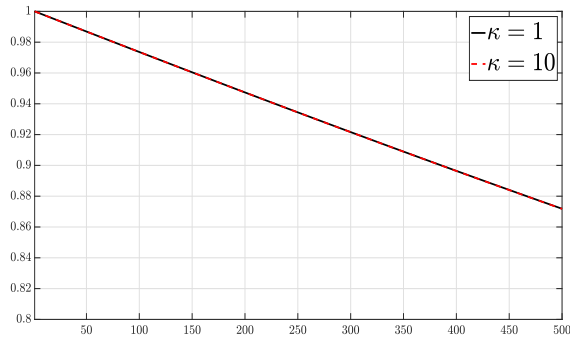
6. Numerical Simulations of a Glioblastoma PDE-ODE system with chemotaxis

6.3.1.1 Tumor Ring quotient

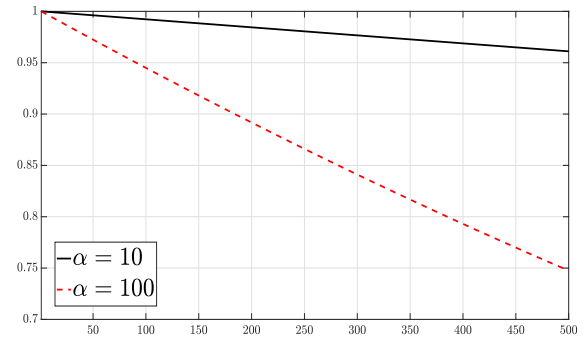
We will start studying the ratio between proliferative tumor density, $\int_{\Omega} T \, dx$ and total tumor density, $\int_{\Omega} (T + N) \, dx$ and we consider the different values of κ and α given in Table 6.4. In fact, we compute the following “ring quotient” (RQ) coefficient:

$$0 \leq \text{RQ} = \frac{\int_{\Omega} T \, dx}{\int_{\Omega} (T + N) \, dx} \leq 1. \quad (6.14)$$

Thus, if RQ is near to zero, there exists a high density of necrosis (which implies slim tumor ring) whereas if RQ is close to one, there is not enough necrosis in comparison with proliferative tumor density (which implies thick tumor ring).



(a) RQ versus time for κ .



(b) RQ versus time for α .

Figure 6.2: RQ versus time for κ and α .

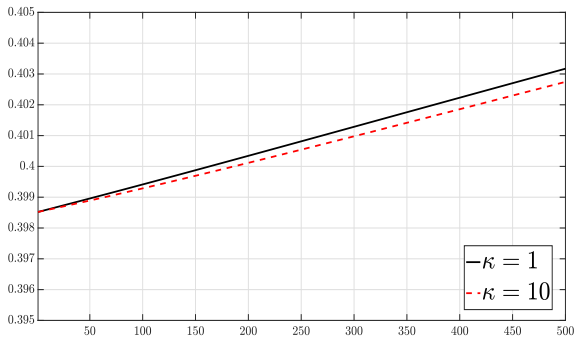
We can see in Figure 6.2 how the model captures two kinds of tumor ring changing the parameter α and the tumor rings for different κ do not change. This means that a change of the rate of tumor destruction for hypoxia produces much difference in the tumor rings.

Hence, the best configurations to obtain a slim (resp. thick) ring would be choose a big (resp. small) α .

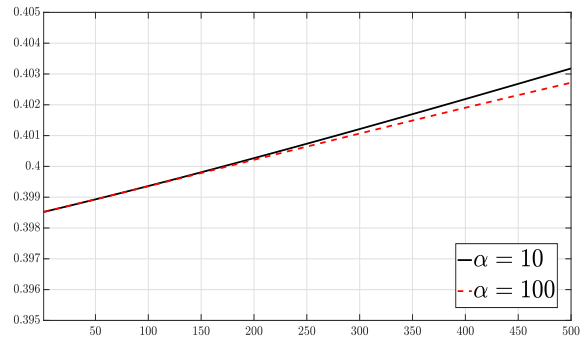
6.3.1.2 Density tumor growth

In Figure 6.3, we compute the total tumor $\int_{\Omega} (T + N) \, dx$ for the values of κ and α given in Table 6.4.

6. Numerical Simulations of a Glioblastoma PDE-ODE system with chemotaxis



(a) $\int_{\Omega} (T + N) dx$ versus time for κ .



(b) $\int_{\Omega} (T + N) dx$ versus time for α .

Figure 6.3: $\int_{\Omega} (T + N) dx$ versus time for κ and α .

We can see in Figure [6.3](#) how the variation in the parameters κ and α produces changes in the total tumor density. In fact, the total tumor decreases with respect to κ and α .

Therefore, we conclude that α is the most important parameter in order to change the tumor ring and both κ and α have relevancy to change the total density in the tumor growth.

6.3.2 Regularity surface

The second tumor growth correspond to the regularity surface. Now, we will base our results on the study published in [\[49\]](#) where appears the following survival curve:

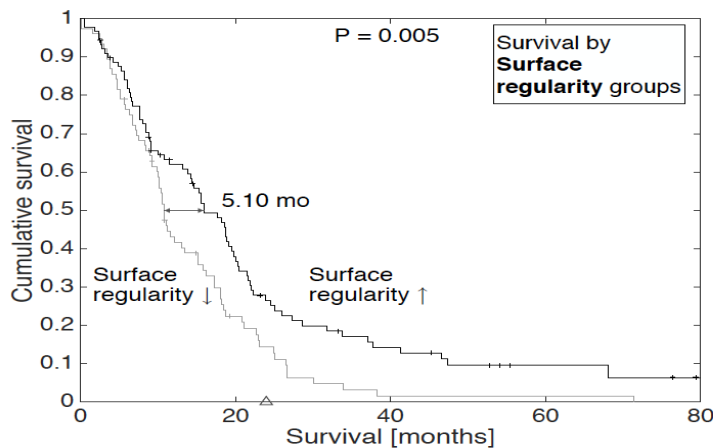


Figure 6.4: Survival vs the regularity surface of GBM.

6. Numerical Simulations of a Glioblastoma PDE-ODE system with chemotaxis

From Figure 6.4, the authors conclude that tumors with a regular surface have better prognosis than tumors with irregular surface.

Thus, we will test if our model (6.13) can develop different regularities for the tumor surfaces. For that, we simulate the tumor growth with the initial tumor defined in Figure 4.1, necrosis zero and the vasculature distributed in different zones as in Figure 4.5

Thus, the question is if the chemotaxis term (of tumor going to the vasculature) implies tumor growth with regular or irregular surface. We remember that the chemotaxis term in (6.13) is defined by $\kappa \nabla \cdot (T \nabla \Phi)$ with $\kappa > 0$.

Now, we want to detect which parameter is more relevant changing the regularity of the tumor surface, showing some simulations in which we move the value of one of them and observe how the tumor changes. For this, it is important the interaction between tumor and vasculature. Then, we will move the parameters which appear in tumor and vasculature equations, κ , α , γ and δ .

For these parameters we take the values of Table 6.5 (each parameter will change its value in the range, jointly the other parameters take fixed values):

Variable (Fixed value)	κ (5)	α (45)	γ (0.255)	δ (2.55)
Ranges	[1, 10]	[10, 100]	[0.01, 0.5]	[0.1, 5]

Table 6.5: Variable value parameters.

6.3.2.1 Regularity Surface quotient

The pictures of Figure 6.5 show the quotient between the area occupied by the total tumor (tumor and necrosis) and the area of ratio the smallest circle containing the tumor. Thus, we present these computations for the different values of κ , α , γ and δ chosen in Table 6.5. In fact, we compute the following “surface quotient” (SQ) coefficient:

$$0 \leq \text{SQ} = \frac{\int_{\Omega} (T + N)_{\min} dx}{\pi \cdot (\mathbf{R}_{\max})^2} \leq 1 \quad (6.15)$$

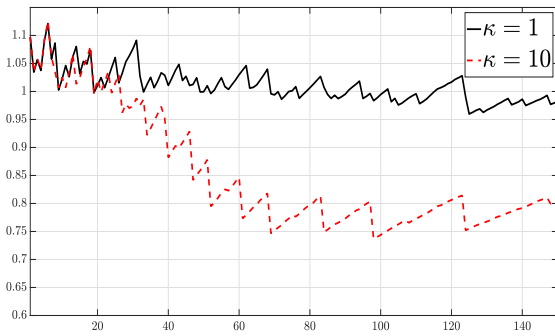
6. Numerical Simulations of a Glioblastoma PDE-ODE system with chemotaxis

where $(T + N)_{\min}$ and \mathbf{R}_{\max} are defined as follows:

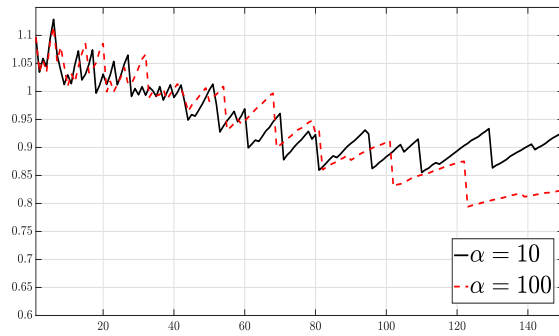
$$(T + N)_{\min} = \begin{cases} 1 & \text{if } T + N \geq 0.001, \\ 0 & \text{otherwise.} \end{cases} \quad (6.16)$$

$$\mathbf{R}_{\max} = \max \{ \text{ratio of the subdomain where } (T + N)_{\min} = 1 \}. \quad (6.17)$$

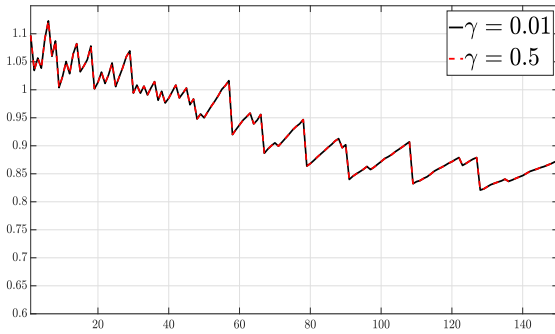
Thus, we will deduce that if SQ is near to zero, tumor will have an irregular surface whereas if SQ is close to one, tumor will have a regular surface.



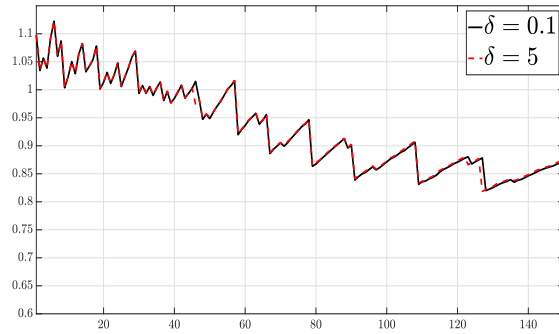
(a) SQ versus time for κ .



(b) SQ versus time for α .



(c) SQ versus time for γ .



(d) SQ versus time for δ .

Figure 6.5: SQ versus time for κ , α , γ and δ .

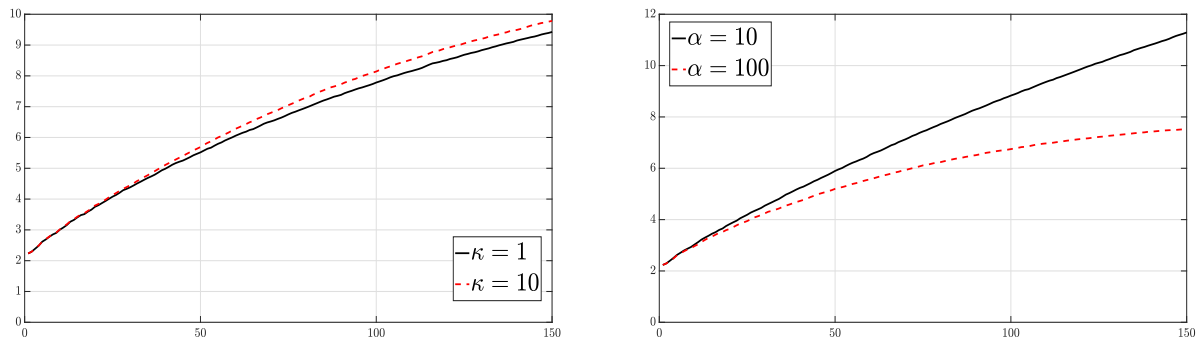
Remark 6.2. As in Chapter 4 the size of mesh considered produces at the beginning of the simulation the value of SQ is larger than 1 and the oscillations observed in the graphs of SQ. Considering a mesh size smaller, these numerical instabilities can be reduced. However, we think that the use of a mesh size smaller is not necessary since we capture the same mean behaviour that for the mesh considered initially and with this mesh, we reduce the computational time.

6. Numerical Simulations of a Glioblastoma PDE-ODE system with chemotaxis

We see in Figs [6.5a](#)-[6.5d](#) how our model differentiates two kinds of tumor growth changing the parameter κ , see Figure [6.5a](#), and with lower variation for α , see Figure [6.5b](#). On the other hand, we do not appreciate changes in the variation of parameters γ and δ for the irregularity of tumor growth as we see in Figs [6.5c](#)-[6.5d](#).

6.3.2.2 Area

Once we have identified that the more important parameters for the regularity surface are firstly κ and later α , we measure the area of total tumor for these parameters as in Table [6.5](#):



(a) Area of total tumor versus time for κ .

(b) Area of total tumor time for α .

Figure 6.6: Area of total tumor versus time for κ and α .

We see in Figure [6.6](#) how the largest area corresponds to $\alpha = 10$ and the smallest area holds for $\alpha = 100$. In the case of variation of κ , Figure [6.6a](#), a similar influence in the total tumor area for $\kappa = 1$ and $\kappa = 10$ is observed.

Thus, we have obtained a higher variation of total area for the different values of α than for κ , see Figure [6.6](#). Nevertheless, in the simulation of the “surface quotient” (SQ), we obtained more variation between the different values of κ than for the different values of α , see Figure [6.5](#). Hence, the factor which modifies this change is \mathbf{R}_{\max} , defined by [6.17](#). In fact, \mathbf{R}_{\max} will change more with the variation of κ than for the variation of α .

6.3.2.3 Tumor growth

Here, we examine the tumor growth for $\kappa = 10$ in five times step in order to see the variation in space of tumor. For this growth, the rest of parameters take the fixed values showed in Table [6.5](#).

6. Numerical Simulations of a Glioblastoma PDE-ODE system with chemotaxis

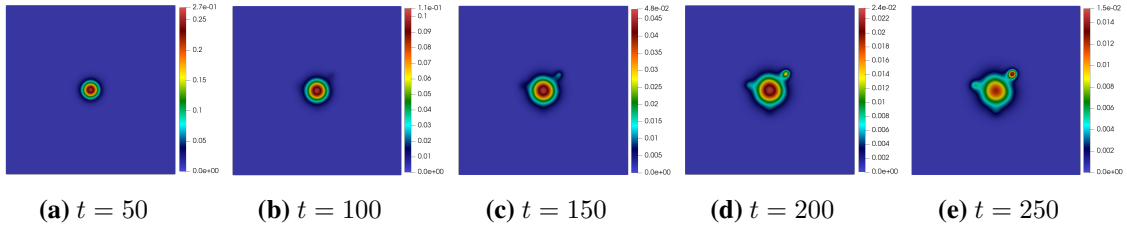


Figure 6.7: Irregular tumor growth for $\kappa = 10$.

We observe an irregular tumor growth for $\kappa = 10$ when time increases. These results are in concordance with Figure [6.5a](#), where we observed a great irregularity for $\kappa = 10$ and with Figure [6.6a](#), where the area of the tumor for $\kappa = 10$ is increasing.

Finally, we conclude that κ is the more relevant parameter in the irregular surface of tumor and α is the most important parameter for total area in the tumor growth.

6.3.3 Discussion

Summarizing the results obtained with respect to the ring width and the regularity surface for the chemotactic and dimensionless system [\(6.13\)](#) related to GBM growth model, we deduce that this model can capture these two properties varying some parameters. Moreover, we have proved that the parameters more relevant according to the tumor growth are κ and α .

For the tumor ring, where the vasculature is uniformly distributed, the results show that the hypoxia parameter α is the most relevant parameter as we can observe in Figs [6.2a](#)-[6.2b](#).

In the case of regularity surface, where the vasculature is non-uniformly distributed, the parameter which produces more irregularity in the tumor surface is the chemotaxis parameter κ , see Figs [6.5a](#)-[6.5a](#).

Finally, after the reduction of our model [\(6.1\)](#) from 7 initial parameters to 2 (κ and α) which capture the different behaviour of tumor growth, we conclude that hypoxia parameter α is the main parameter for the tumor ring and area of tumor and κ is the most influential parameter for the regularity surface.

Bibliography

- [1] S. Abrol, A. Kotrotsou, A. Salem, P. O. Zinn and R. R. Colen, Radiomic phenotyping in brain cancer to unravel hidden information in medical images, *Top in Magn Reson Imaging* **26** (2017) 43–53.
- [2] J. C. L. Alfonso, K. Talkenberger, M. Seifert, B. Klink, A. Hawkins-Daarud, K. R. Swanson, H. Hatzikirou and A. Deutsch, The biology and mathematical modelling of glioma invasion: a review, *J. R. Soc. Interface.* **14** (2017) 20170490.
- [3] N. D. Alikakos, An application of the invariance principle to reaction-diffusion equations, *J. Differential Equations.* **33** (1979) 201–225.
- [4] H. Amann, Highly degenerate quasilinear parabolic systems, *Ann. Scuola Norm. Sup. Pisa Cl. Sci. Ser. 4*, **18** (1991) 135–166.
- [5] H. Amann, Nonhomogeneous linear and quasilinear elliptic and parabolic boundary value problems, Schmeisser, Hans-Jürgen and Triebel, Hans (Eds.), *Function Spaces, Differential Operators and Nonlinear Analysis*, Vieweg+Teubner verlag, wiesbaden, (1993) 9–126.
- [6] A. R. A. Anderson and M. A. J. Chaplain, Continuous and discrete mathematical models of tumor-induced angiogenesis, *Bull. Math. Biol.* **60** (1998) 857–899.
- [7] A. Baldock, R. Rockne, A. Boone, M. Neal, C. Bridge, L. Guyman, M. Mrugala, J. Rockhill, K. Swanson, A. Trister, A. Hawkins-Daarud and D. Corwin, From patient-specific mathematical neuro-oncology to precision medicine, *Front. Oncol.* **3** (2013) 62.
- [8] A. L. Baldock, S. Ahn, R. Rockne, S. Johnston, M. Neal, D. Corwin, K. Clark-Swanson, G. Sterin, A. D. Trister, H. Malone, V. Ebiana, A. M. Sonabend, M. Mrugala, J. K. Rockhill, D. L. Silbergeld, A. Lai, T. Cloughesy, G. M. McKhann, II, J. N. Bruce, R. C. Rostomily, P. Canoll and K. R.

Bibliography

Swanson, Patient-specific metrics of invasiveness reveal significant prognostic benefit of resection in a predictable subset of Gliomas, *PLOS ONE* **9** (2014) 1–10.

- [9] V. Bitsouni, M. A. J. Chaplain and R. Eftimie, Mathematical modelling of cancer invasion: the multiple roles of TGF- β pathway on tumour proliferation and cell adhesion, *Math. Models Methods Appl. Sci.* **27** (2017) 1929–1962.
- [10] R. S. Cantrell and C. Cosner, *Spatial ecology via reaction-diffusion equations.*, Wiley series in mathematical and computational biology (Chichester, West Sussex, England ; Hoboken, NJ : J. Wiley, 2003).
- [11] M. A. J. Chaplain, Mathematical modelling of angiogenesis, *Neuro-Oncol.* **50** (2000) 37–51.
- [12] P. Ciarlet and P.-A. Raviart, Maximum principle and uniform convergence for the finite element method, *Comput. Methods Appl. Mech. Engrg.* **2** (1973) 17–31.
- [13] E. A. Coddington and N. Levinson, *Theory of ordinary differential equations* (McGraw-Hill Book Company, Inc., New York-Toronto-London, 1955).
- [14] L. Corrias, B. Perthame and H. Zaag, Global solutions of some chemotaxis and angiogenesis systems in high space dimensions, *Math. Models Methods. Appl. Sci.* **72** (2004) 1–28.
- [15] E. Cruz, M. Negreanu and J. I. Tello, Asymptotic behavior and global existence of solutions to a two-species chemotaxis system with two chemicals, *Z. Angew. Math. Phys.* **69** (2018) 20.
- [16] A. L. de Araujo and P. M. de Magalhães, Existence of solutions and optimal control for a model of tissue invasion by solid tumours, *J. Math. Anal. Appl.* **421** (2015) 842–877.
- [17] J. Deuel and P. Hess, Nonlinear parabolic boundary value problems with upper and lower solutions, *Israel J. Math.* **29** (1978) 92–104.
- [18] B. M. Ellingson, Radiogenomics and imaging phenotypes in Glioblastoma: novel observations and correlation with molecular characteristics, *Curr. Neurol. Neurosci. Rep.* **15**.
- [19] C. M. Elliott and A. M. Stuart, The global dynamics of discrete semilinear parabolic equations, *SIAM J. Numer. Anal.* **30** (1993) 1622–1663.
- [20] L. C. Evans, *Partial differential equations*, volume 19 (American Mathematical Society, 1998).

- [21] I. Faragó, J. Karátson and S. Korotov, Discrete maximum principles for nonlinear parabolic PDE systems, *IMA J. Numer. Anal.* **32** (2012) 1541–1573.
- [22] E. Feireisl and A. Novotny, *Singular limits in thermodynamics of viscous fluids* (Advances in Mathematical Fluid Mechanics, 2009).
- [23] A. Fernández-Romero, F. Guillén-González and A. Suárez, Determining parameters giving different growths of a new Glioblastoma differential model, 2021, submitted, <https://arxiv.org/abs/2104.04560>.
- [24] A. Fernández-Romero, F. Guillén-González and A. Suárez, Theoretical analysis for a PDE-ODE system related to a Glioblastoma tumor with vasculature, *Z. Angew. Math. Phys.* **72** (2021) 97.
- [25] A. Fernández-Romero, F. Guillén-González and A. Suárez, Theoretical and numerical analysis for a hybrid tumor model with diffusion depending on vasculature, *J. Math. Anal. Appl.* **503** (2021) 125325.
- [26] A. Fernández-Romero, F. Guillén-González and A. Suárez, A Glioblastoma PDE-ODE model including chemotaxis and vasculature, 2021, submitted.
- [27] A. Friedman, *Partial differential equations* (Holt, Reinhart and Winston, New York, 1969).
- [28] R. J. Gillies, P. E. Kinahan and H. Hricak, Radiomics: images are more than pictures, they are data, *Radiology* **278** (2016) 563–577.
- [29] F. Guillén-González and J. Gutiérrez-Santacreu, From a cell model with active motion to a Hele-Shaw-like system: a numerical approach, *Numer. Math.* **143** (2019) 107–137.
- [30] R. L. Klank, S. S. Rosenfeld and D. J. Odde, A brownian dynamics tumor progression simulator with application to Glioblastoma, *Converg. Sci. Phys. Oncol.* **4** (2018) 16.
- [31] A. Kubo and J. I. Tello, Mathematical analysis of a model of chemotaxis with competition terms, *Differ. Integral Equ.* **29** (2016) 441–454.
- [32] J. Li and Z. Wang, Convergence to traveling waves of a singular PDE-ODE hybrid chemotaxis system in the half space, *J. Differential Equations.* **268** (2020) 6940–6970.
- [33] J. L. Lions, *Quelques méthodes de résolution des problèmes aux limites non linéaires* (Durnod, 1969).

Bibliography

- [34] Y. Lou, Y. Tao and M. Winkler, Approaching the ideal free distribution in two-species competition models with fitness-dependent dispersal, *SIAM J. Math. Anal.* **46** (2014) 1228–1262.
- [35] A. Marciniak-Czochra and M. Ptashnyk, Boundedness of solutions of a haptotaxis model, *Math. Models Methods. Appl. Sci.* **20** (2010) 449–476.
- [36] A. Martínez-González, M. Durán-Prado, G. F. Calvo, F. J. Alcaín, L. A. Pérez-Romasanta and V. M. Pérez-García, Combined therapies of antithrombotics and antioxidants delay in silico brain tumour progression, *Math. Med. Biol.* **32** (2015) 239–262.
- [37] A. Martínez-González, G. F. Calvo, L. A. Pérez-Romasanta and V. M. Pérez-García, Hypoxic cell waves around necrotic cores in Glioblastoma: a biomathematical model and its therapeutic implications, *Bull. Math. Biol.* **74** (2012) 2875–2896.
- [38] D. Molina, J. Pérez-Beteta, A. Martínez-González, J. M. Sepúlveda, S. Peralta, M. J. Gil-Gil, G. Reynes, A. Herrero, R. D. L. Peñas, R. Luque, J. Capellades, C. Balaña and V. M. Pérez-García, Geometrical measures obtained from pretreatment postcontrast T1 weighted MRIs predict survival benefits from bevacizumab in Glioblastoma patients, *PLOS ONE* **11** (2016) 1–16.
- [39] D. Molina-García, L. Vera-Ramírez, J. Pérez-Beteta, E. Arana and V. M. Pérez-García, Prognostic models based on imaging findings in Glioblastoma: Human versus machine, *Sci. Rep.* **9** (2019) 5982.
- [40] S. Narang, M. Lehrer, D. Yang, J. Lee and A. Rao, Radiomics in Glioblastoma: current status, challenges and potential opportunities, *Transl. Cancer Res.* **5** (2016) 383–397.
- [41] M. Negreanu and J. I. Tello, On a parabolic-ODE system of chemotaxis, *Discrete Contin. Dyn. Syst. Ser. S* **13** (2020) 279–292.
- [42] Y.-Y. Nie and V. Thomée, A lumped mass finite-element method with quadrature for a non-linear parabolic problem, *IMA J. Numer. Anal.* **5** (1985) 371–396.
- [43] Q. T. Ostrom, H. Gittleman, P. Liao, C. Rouse, Y. Chen, J. Dowling, Y. Wolinsky, C. Kruchko and J. Barnholtz-Sloan, CBTRUS statistical report: primary brain and central nervous system tumors diagnosed in the united states in 2007-2011, *Neuro-Oncol.* **16** (2014) iv1–iv63.
- [44] P. Y. H. Pang and Y. Wang, Global boundedness of solutions to a chemotaxis–haptotaxis model with tissue remodeling, *Math. Models Methods Appl. Sci.* **28** (2018) 2211–2235.

- [45] M. Protopapa, A. Zygogianni, G. Stamatakos, C. Antypas, C. Armpilia, N. Uzunoglu and V. Kouloulis, Clinical implications of in silico mathematical modeling for Glioblastoma: a critical review, *J. Neuro-Oncology*. **136** (2018) 1–11.
- [46] J. Pérez-Beteta, J. Belmonte-Beitia and V. M. Pérez-García, Tumor width on T1-weighted MRI images of Glioblastoma as a prognostic biomarker: a mathematical model, *Math. Model. Nat. Phenom.* **15** (2020) 10.
- [47] J. Pérez-Beteta, A. Martínez-González, D. Molina, M. Amo-Salas, B. Luque, E. Arregui, M. Calvo, J. M. Borrás, C. López, M. Claramonte, J. A. Barcia, L. Iglesias, J. Avecillas, D. Albillo, M. Navarro, J. M. Villanueva, J. C. Paniagua, J. Martino, C. Velásquez, B. Asenjo, M. Benavides, I. Herruzo, M. del Carmen Delgado, A. del Valle, A. Falkov, P. Schucht, E. Arana, L. Pérez-Romasanta and V. M. Pérez-García, Glioblastoma: does the pre-treatment geometry matter? A postcontrast T1 MRI-based study, *Eur. Radiol.* **27** (2016) 1096–1104.
- [48] J. Pérez-Beteta, D. Molina-García, A. Martínez-González, A. Henares-Molina, M. Amo-Salas, B. Luque, E. Arregui, M. Calvo, J. M. Borrás, J. Martino, C. Velásquez, B. Meléndez-Asensio, Á. R. de Lope, R. Moreno, J. A. Barcia, B. Asenjo, M. Benavides, I. Herruzo, P. C. Lara, R. Cabrera, D. Albillo, M. Navarro, L. A. Pérez-Romasanta, A. Revert, E. Arana and V. M. Pérez-García, Morphological MRI-based features provide pretreatment survival prediction in Glioblastoma, *Eur. Radiol.* **29** (2019) 1968–1977.
- [49] J. Pérez-Beteta, D. Molina-García, J. A. Ortiz-Alhambra, A. Fernández-Romero, B. Luque, E. Arregui, M. Calvo, J. M. Borrás, B. Melédez, Á. Rodríguez de Lope, R. Moreno de la Presa, L. Iglesias Bayo, J. A. Barcia, J. Martino, C. Velásquez, B. Asenjo, M. Benavides, I. Herruzo, A. Revert, E. Arana and V. M. Pérez-García, Tumor surface regularity at MR imaging predicts survival and response to Surgery in patients with Glioblastoma, *Radiology*. **288** (2018) 218–225.
- [50] F. Rothe, *Global solutions of reaction-diffusion systems. Lecture notes in mathematics, vol. 1072* (Springer-Verlag, Berlin (West)-Heidelberg-New York-Tokyo, 1984).
- [51] J. Simon, Compact sets in the space $L^p(0, T, B)$, *Ann. Mat. Pura Appl.* **146** (1987) 65–96.
- [52] B. D. Sleeman and H. A. Levine, A system of reaction diffusion equations arising in the theory of reinforced random walks, *SIAM J. Appl. Math.* **57** (1997) 683–730.
- [53] A. Stevens, The derivation of chemotaxis equations as limit dynamics of moderately interacting stochastic many-particle systems, *SIAM J. Appl. Math.* **61** (2000) 183–212.

Bibliography

- [54] A. Stevens and H. G. Othmer, Aggregation, blowup, and collapse: The ABC's of taxis in reinforced random walks, *SIAM J. Appl. Math.* **57** (1997) 1044–1081.
- [55] Y. Tao and C. Cui, A density-dependent chemotaxis-haptotaxis system modeling cancer invasion, *J. Math. Ana. Appl.* **367** (2010) 612–624.
- [56] Y. Tao and M. Wang, A combined chemotaxis-haptotaxis system: The role of logistic source, *SIAM J. Appl. Math.* **41** (2009) 1533–1558.
- [57] Y. Tao and M. Winkler, A chemotaxis-haptotaxis model: The roles of nonlinear diffusion and logistic source, *SIAM J. Appl. Math.* **43** (2012) 685–704.
- [58] J. I. Tello and D. Wrzosek, Inter-species competition and chemorepulsion, *J. Math. Anal. Appl.* **459** (2018) 1233–1250.
- [59] V. Thomée, On positivity preservation in some finite element methods for the heat equation, *Int. J. Num. Math. Appl.* (2015) 13–24.
- [60] V. Thomée and L. B. Wahlbin, On the existence of maximum principles in parabolic finite element equations, *Math. Comput.* **77** (2008) 11–19.
- [61] J. Unkelbach, B. H. Menze, E. Konukoglu, F. Dittmann, M. Le, N. Ayache and H. A. Shih, Radiotherapy planning for Glioblastoma based on a tumor growth model: improving target volume delineation, *Phys. Med. Biol.* **59** (2014) 747–770.
- [62] M. Winkler and Y. Lou, Advantage and disadvantage of dispersal in two-species competition models, *CSIAM Trans. Appl. Math.* **1** (2020) 86–103.